Microwave-assisted low temperature steam reforming of methanol for hydrogen production

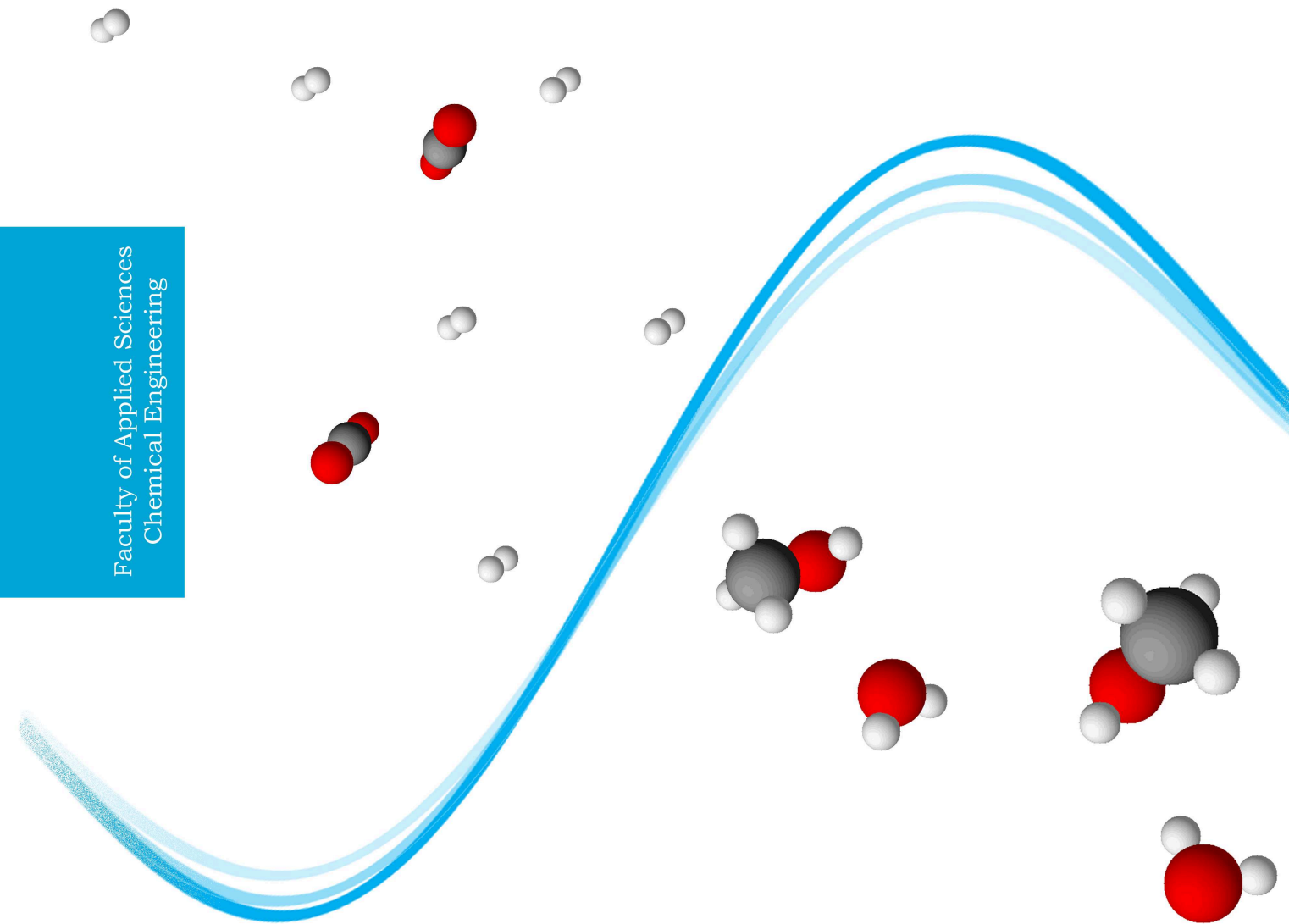## Master Thesis

Marloes Reus

Student number: 1148885
Report number: 2399

Department: Process & Energy, Faculty 3mE
Section: Intensified Reaction & Separation Systems

Graduation Committee:
        T. Durka, MSc.
        Dr. G. Mul
        Prof. dr. ir. A.I. Stankiewicz
        Dr. G. Stefanidis

Faculty of Applied Sciences
Chemical Engineering

Marloes Reus
May 2010

TUDelft
Delft
University of
Technology

Challenge the future

Preface

"It is an experience common to all scientists to find that, once you think every possible thing has gone wrong, something else goes wrong"

From: Capt. Edward A. Murphy

After slightly more than eight months of work in the laboratory hall of Process & Energy this master thesis is written. The choice to do this project about microwave influence on reactions, which I made after 7 years of studying Chemical Engineering at DelftChemTech, was mostly influenced by the fact that it would involve practical work in a relatively new and exciting field of process intensification. What I didn't know at the time was that the practical work would turn out to be more demanding than I thought; A lot of unexpected problems arose, which were actually fun to solve, looking back on it. However when I thought everything was fixed, something would yet again break down, and cause even more trouble. Nonetheless I had a great time working on the project.

Working at P&E – or API, as it used to be called – has been a very nice experience from the first day and onwards. I shared my office with Reina van Houten, who worked at a project very similar to my own, so we could work together at a part of the literature study, and of course ask each other for advice. Since the students offices were all located in the 'kop van de hal', there was a low threshold for a quick talk and coffee breaks with our fellow students. Even though I spent most of my time around the setup, I felt that this personal atmosphere was making me feel right at home.

Being around the experimental setup for the better part of each day didn't mean I was very solitary. Next to his fellow PhD-students Ernesto Altman Restrepo and Magdalena Komorowska, who were at times available for a nice conversation, my direct supervisor, PhD-student Tomasz Durka, was around for the better part of the day to help with the experiments, for which at times more than 2 hands were needed. Also he was available for discussion about the research plans and relieved me from my watch to take some small breaks every day. I am also very grateful for him tirelessly answering all my questions – which were many – and for stimulating me to write this thesis in the short time that remained after the experiments were finished.

All in all this project has been a great learning experience and a lot of fun, and I hope that this trend will continue in my future work.

Marloes Reus
April 2010, Den Haag, Netherlands

Summary

Due to the depleting fossil fuel reserves and the growing awareness of the environmental issues the search for alternative, renewable energy sources is stimulated. The aim of this study is to investigate the microwave effect on heterogeneous reactions, specifically the steam reforming of methanol. The steam reforming of methanol is already a well known process, however environmental awareness drives the intensification of processes and methanol steam reforming is no exception. The performance of reactions carried out under conductive and microwave heating are compared. The performance was evaluated in terms of the methanol conversion and the yields of H_2, CO_2 and CO. The parameters of influence were: steam-carbon (S/C) ratio (1:1, 1:1.5 and 1:2), temperature (130^oC-210^oC), and gas hourly space velocity (GHSV) ($37,000 - 120,000$ [h^{-1}]). Special attention was paid to the temperature mapping of the catalytic bed.

The microwave assisted reactions showed a significant increase in conversion and product yields opposed to reactions carried out under conductive heating. This is attributed to the existence of temperature gradients on the micro scale, between the catalyst and the bulk. The origin of these micro gradients (hot spot formation or selective heating of the catalyst material) was not established. Moreover large temperature gradients were observed on the macro scale. These gradients were mapped and taken into consideration. The influence of the varied parameters on the conversion of methanol was significant as well. An increase in conversion was observed for increased temperature and S/C ratio, and for decreased GHSV.

The results were finally combined in a qualitative assessment. From this qualitative evaluation it was clear that the reaction itself is very promising, however the energy demand of the total systems, including controls, may determine whether the technique is applicable for on demand hydrogen delivery systems.

For general information on the characteristics of microwave irradiation, the steam reforming of methanol, and the application of microwaves on heterogeneous reactions literature is consulted, of which an overview is given in this report. The experiments and the results are presented and finally discussed. At last, the conclusions and the recommendations for further research are given.

Table of Contents

1. Introduction

For some decades it has been known that the fossil fuel reserves, which we sorely depend upon for energy and chemicals production, are depleting. The extensive use of these resources gives rise to increased air pollution and has impact on the growing greenhouse gas effect. Awareness of these issues has stimulated the search for alternative, renewable energy sources.

One of the potential green energy sources is bio ethanol which has already been used successfully as an alternative fuel in automotive applications. An alternative approach is using alcohols as a source of hydrogen for fuel cell applications. The efficiency of hydrogen fuel cells is relatively high compared to that of spark ignition (SI) engines; tank-to-wheel efficiencies of up to 44% can be reached in fuel cells, compared to 22% in SI engines [1]. Although hydrogen has a very high energy density by mass, storage and refueling is an outstanding problem due to the low energy density by volume and the high volatility, respectively [2]. Bio-fuels like ethanol and methanol, on the other hand, have no storage and refueling issues; the current systems do not have to be adapted for use of these fuels, however purification of bio ethanol is a high energy demanding process and moreover, the corrosive properties of ethanol induce difficulties in automotive applications. Additionally the shortcoming of using bio-fuels lies in the efficiency of the engine, which is limited by the Carnot cycle efficiency and rarely reaches 15% [1]. A possible alternative would be to combine easy handling, transportation and storing properties of bio ethanol with the high efficiency of a fuel cell. In situ steam reforming of bio-fuels will yield hydrogen for a fuel cell, while the storage and refueling of the bio-fuel is safe and quick.

Both methanol and ethanol can be reformed to hydrogen using steam. However, since methanol has no C-C bond, the reforming can take place at a lower temperature range than ethanol and fewer by-products are expected. For purpose of this study, the reaction of steam reforming of methanol has been chosen as one of the possible routes for hydrogen production.

The steam reforming of methanol is a well known industrial process and conversions up to 100% can be achieved at relatively low temperatures (300^0C) [3]. However increased awareness of environmental aspects enforces intensification and improvement of even so well developed processes. In the last two decades the application of microwave energy has been intensively investigated as a potential way to enhance chemical reactions; numerous articles are published which report improved reaction outcomes under microwave irradiation [4 – 6].

Following the general trends in intensification of reactions by microwave irradiation combined with production of hydrogen from bio alcohols for automotive application, this study is focused on investigation of the microwave effect on heterogeneous reactions, and in particular that of the steam reforming of methanol. The performance of the reactions carried out under conductive heating is compared with the performance of microwave-assisted reactions. The comparison is performed with variation of the following parameters: steam-carbon (S/C) ratio (1:1, 1:1.5 and 1:2), temperature (130^oC-210^oC), and gas hourly space velocity (GHSV) (37k-120k [1/h]).

2. Microwave Theory

General information about microwaves is provided in order to gain insight in the effect of microwaves on different materials, and of how the microwaves can be applied in chemical processes. Thereto the characteristics of microwaves and the material properties governing the absorbance are discussed, together with the different types of microwave applicators.

2.1 History

The development of microwaves finds its origin in the research of radio waves. In 1888 the existence of electromagnetic waves was proven by Heinrich Hertz, who had built a device that could both generate and detect radio waves (see figure 1). Hertz discovered that these waves were reflected off metals, but transmitted through other materials [8]. This discovery led to rapid development of radio wave technology during World War II. The need to locate enemy forces led to the development of RADAR (Radio Detection and Ranging) devices, which make use of fixed frequency radio waves [9]. During a radar related research project, it was accidentally discovered by dr. Percy LeBaron Spencer that microwaves could cook food. Further investigation showed that

Figure 1. Hertz' radiator and resonator for creating and detecting radio waves [7]

the heating of beverages was much quicker with microwaves compared to conventional heating methods. The first commercial microwave oven for home use was a fact in 1954 [10]. In the same period investigation of microwave energy for industrial application started, and still today many new applications are discovered [9].
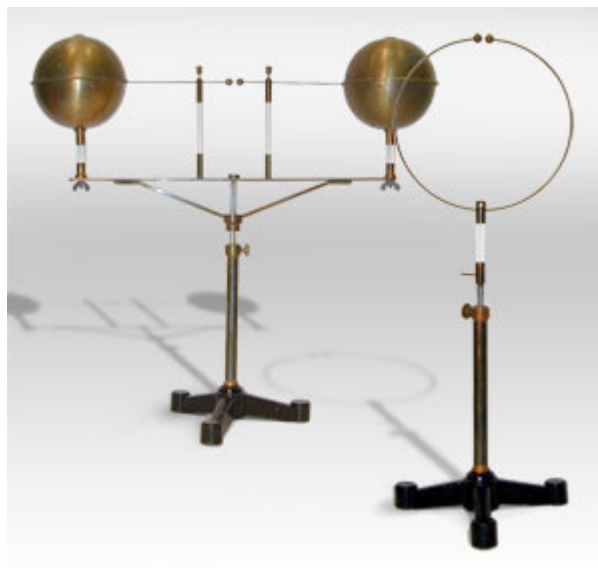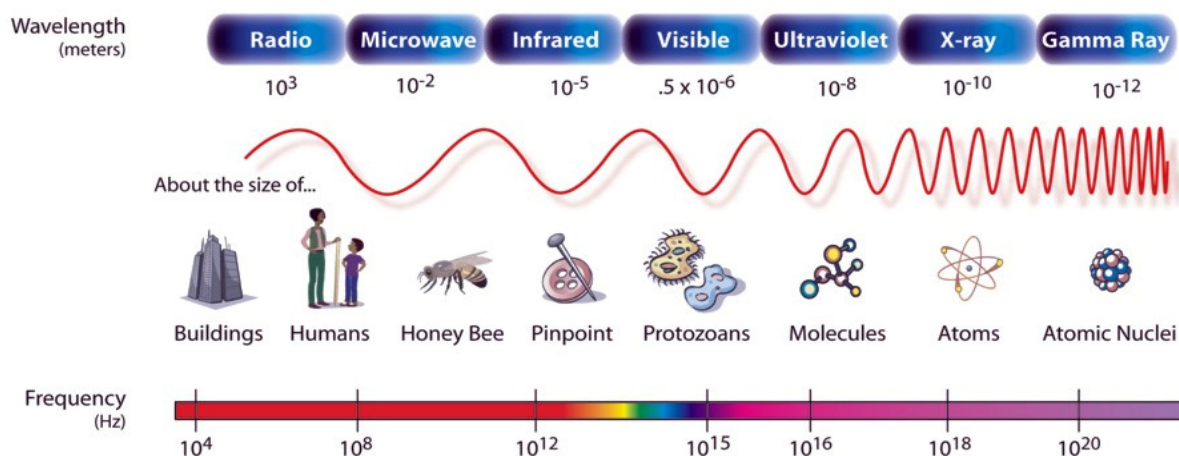

Figure 2. The electromagnetic spectrum

2.2 Characteristics

Microwaves are a form of electromagnetic waves which are located between radio waves and infrared radiation (see figure 2). Microwaves consist of electric and magnetic waves which are oriented perpendicular to each other and oscillate in phase to the wave propagation (see figure 3). Microwaves wavelengths range from 1 mm to 1 m with corresponding frequencies in the range from 300 to 300,000 megahertz (MHz) [11]. This is only a small range of the entire electromagnetic spectrum. Microwaves, similar to visible light, which is also a form of electromagnetic radiation, propagate with the speed of light and carry energy as well as light does. The energy of a certain electromagnetic wave is dependent on the wavelength.
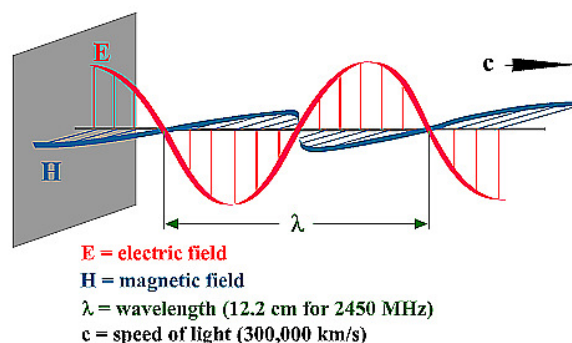

E = electric field
H = magnetic field
λ = wavelength (12.2 cm for 2450 MHz)
c = speed of light (300,000 km/s)

Figure 3. schematic of a microwave, in which E is the electric field, H is the magnetic field, λ is wavelength and c is the speed of light [12]

The relation between the energy of a photon and the wavelength is described by equation (2.1):

$$E = \frac{hc}{\lambda}$$

(2.1)

In which E is the energy of the photon, h is Planck's constant, c is the speed of light and λ is the wavelength. The energy of microwave photons (0.124 meV for $\lambda = 10^4$ µm), is relatively low compared to that of photons of UV-light (3.1 eV for λ = 0.4 µm). Whereas the photons of UV-light carry enough energy to cleave molecular bonds, the energy of microwave photons is by far too low to affect molecular structures. The specific frequency range of microwaves however, has a range in which molecular rotation is influenced, creating the opportunity to heat substances [9].

2.2.1 Heating of substances

In chemical processes traditionally conductive heating is applied to provide energy for the reaction. Drawbacks of this type of heating are that heating depends on the heat conductivity of the vessel materials, making the response time of a conductively heated system very slow. This means temperature gradients are unavoidable, with higher temperatures near the heat source (figure 4 (l)). Dependent on the size of the system and the conductivity of the materials, it can take a long time before a homogeneous temperature is achieved. Because reaction rates have Arrhenius like behavior (2.2), differences in temperature lead to differences in reaction rate. Moreover the cooling of a conductively heated mixture requires for the heating source to be physically removed or cooled down. This process is also very slow, which makes thermal control of a reaction system problematic.

$$k = A \cdot exp[-E_A/RT]$$

(2.2)

In liquid phases microwave heating eliminates most of these drawbacks. Due to the direct coupling of the microwaves with molecules, microwave heating is a very fast process. Since all molecules of the same species are evenly affected by the microwaves, temperature gradients are reduced in a microwave heated mixture (figure 4 (r)), though localized superheating takes place by the rapid heating of certain types of molecules [9].
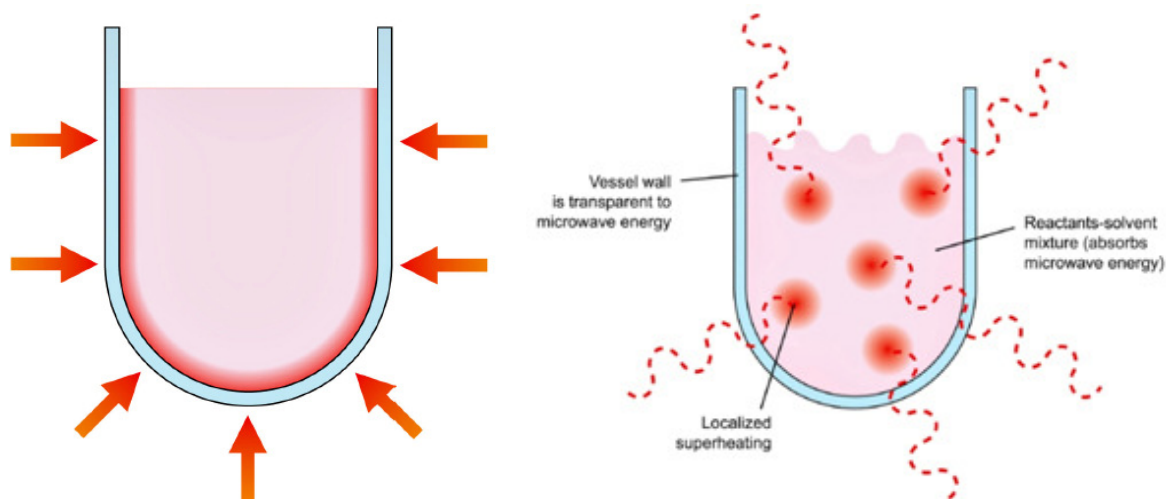
Figure 4. Conductive heating with temperature gradient near the external heating source (l) and microwave heating with direct coupling of microwaves with molecules [12]

Another advantage of the direct coupling is that microwave heating is an "instant-on/instant-off" application, meaning that when microwave power is reduced only latent heat remains. This significantly enhances thermal control of the process. However microwaves cannot heat all substances equally well. As with light, some materials reflect microwaves (conductors), while others are transparent (insulators) to microwaves or absorb them (dielectric lossy materials), as is illustrated in figure 5 [11].

Figure 5. Interaction of microwaves with (A) conductive, (B) insulating and (C) absorbing material [11]

There are two main mechanisms for microwave heating; dipole rotation and ionic conduction. In case of dipole rotation a polar molecule rotates around its axis to align itself with the rapidly changing electric field, which causes internal frictions. This mechanism is responsible for the rapid heating of substances. The coupling efficiency of the substance with the microwaves depends on the polarity of the molecules and the ability to align rapidly with the electric field. Ionic conduction can occur when free ionic species are present in the substance. Similar to the dipole molecules, these ionic species try to orient themselves to the electric field. In case of ionic conduction, the previously described superheating, which is illustrated in figure 4 can be achieved [9].

The extent to which a material can absorb energy from microwaves depends on the complex permittivity ε^*[-] (2.3) and permeability μ^*[-] (2.4), both of which are described by a real part and an imaginary part:

$$\varepsilon^* = \varepsilon' - i\varepsilon'' = \varepsilon_0(\varepsilon'_r - i\varepsilon''_{eff}) \tag{2.3}$$

$$\mu^* = \mu' - i\mu'' \tag{2.4}$$

The real part of the complex permittivity (ε') is a measure of the transparency of the material to microwaves, and the imaginary part (ε'') represents the ability of the material to dissipate the energy provided by microwaves. The permeability represents the interactions with the magnetic part of the microwave, the real part (μ') represents the amount of magnetic energy stored in the material and the imaginary part (μ'') determines the ability to convert magnetic energy into thermal energy [11]. Since from these equations it is not directly clear whether a material is a good absorber, the loss tangent is introduced, which is the ratio of the imaginary part over the real part of equations (2.5) and (2.6):

$$\tan \delta \ = \ \frac{\varepsilon''}{\varepsilon'} \tag{2.5}$$

$$\tan \delta_\mu = \frac{\mu''}{\mu'} \tag{2.6}$$

Equations (2.5) and (2.6) yield single numbers for the microwave characteristics of non-magnetic materials and magnetic lossy materials respectively. Since most materials in heterogeneous reactions are non-magnetic, the magnetic loss tangent is usually neglected. When ε' has a high value, microwaves have only a small penetration depth in the material. A large value for ε'' means that the substance is susceptible for microwave absorption. This means that for effective heating by microwaves the loss tangent should have a high value. The real and imaginary parts of the permittivity are the dielectric constant and the dielectric loss factor respectively. These properties are dependent on the frequency of the microwaves and temperature. In table 1 values of ε', ε'' and tan δ are presented for common and relevant materials.

Table 1. Dielectric constant (ε'), loss factor (ε''), and loss tangent (tan δ) of common materials at room temperature [11, 13]

Material	Dielectric constant	Dielectric loss	Loss tangent	Frequency
Vacuum (free space)	1	0	0	
Air	1.0006	0	0	
Water	80.4	9.89	0.123	2.45 GHz
Methanol	32.6	21.48	0.659	2.45 GHz
Ethanol	24.3	22.86	0.941	2.45 GHz
Glass (Pyrex)	4.82	0.026	0.0054	3 GHz
Glass (Quartz)	3.8	$2.28 \cdot 10^{-4}$	$6.00 \cdot 10^{-5}$	3 GHz
Neoprene rubber	4	$1.36 \cdot 10^{-1}$	$3.40 \cdot 10^{-2}$	3 GHz
Styrofoam	1.03	$1.00 \cdot 10^{-4}$	$1.00 \cdot 10^{-4}$	3 GHz
PTFE	2.08	0.0008	0.0004	10 GHz
Titanium oxide	50	0.25	0.005	
Zinc oxide	3	3	1	
Aluminum oxide	9	0.0063	0.0007	
Copper (II) oxide	18.1 [14]			

From table 1 it is seen that water is a good microwave absorber but alcohols have even better characteristics. The contrary, glass and polymeric species have very low loss tangents and dielectric constants, which means that when used as constructive material for a reactor only very little power will be lost through the wall. Regarding metal oxides, some are hardly expected to heat by microwave irradiation, like aluminum and titanium oxide, while zinc oxide is a very good absorber.

However more parameters influence the efficiency of microwave heating than the dielectric properties and the frequency of the electric field. The dielectric constant gives an indication of the transparency of material to the microwaves, however for better understanding and clear comparison of different materials the parameter called 'penetration depth' was introduced. Penetration depth describes the distance within the material which can be penetrated by microwaves with energy decay less than e^{-1} (~37%) of the original values on the surface. For materials where the loss tangent is smaller than unity, the penetration depth can be described by equation (2.7):

$$\boldsymbol{D_p} \, [\boldsymbol{m}] = \frac{\lambda}{2\pi} \cdot \sqrt{\frac{\varepsilon'}{\varepsilon''}} \qquad\qquad (2.7)$$

For metals, known to be good reflectors, the penetration depth is very small (for copper D_p = 1.3 μm at 2.45 GHz [15]); only surface heating can occur, but the bulk remains unchanged. However metal powders can absorb microwave radiation and can be heated very efficiently. It is proposed that this is due to reduced conductivity for particles smaller than 5 μm [11].

2.3 Microwave applicators

For the application of microwaves in chemical synthesis two types of microwave ovens exist; the multimode microwave (figure 6 (l)), useful because of its large capacity, and the single mode microwave (figure 6 (r)), where the microwave pattern is well defined and the concentration of the microwaves provides more effective heating for samples. The multimode microwave applicator finds its origin in the domestic microwave ovens, where large cavities were necessary for the heating of meals. These microwave ovens were the first to be used in laboratories, even though they were not designed for this application. Because this oven is capable of producing multiple modes of microwaves (typically 20 – 30), the modes interact with each other inside the cavity, resulting in hot and cold spots. The heating is therefore not homogeneous, unless rotation of the sample(s) through the cavity and/or efficient stirring is applied. This inhomogeneous heating resulted in the fact that experiments lacked reproducibility [9]. Moreover, even though the multimode microwave generates high power (~1000 W), due to the large cavity the power density is relatively low (0,025 – 0,040 W/ml).

In order to improve the energy distribution in the cavity of microwave ovens, and thereby facilitating the reproducibility of experiments, single-mode microwaves were developed. In contrast to the multimode instrument, this equipment generates lower amounts of power (~300 W) [9]. The small volume of the cavity the causes that power density is higher (0,90 W/ml) than that in multimode microwaves.
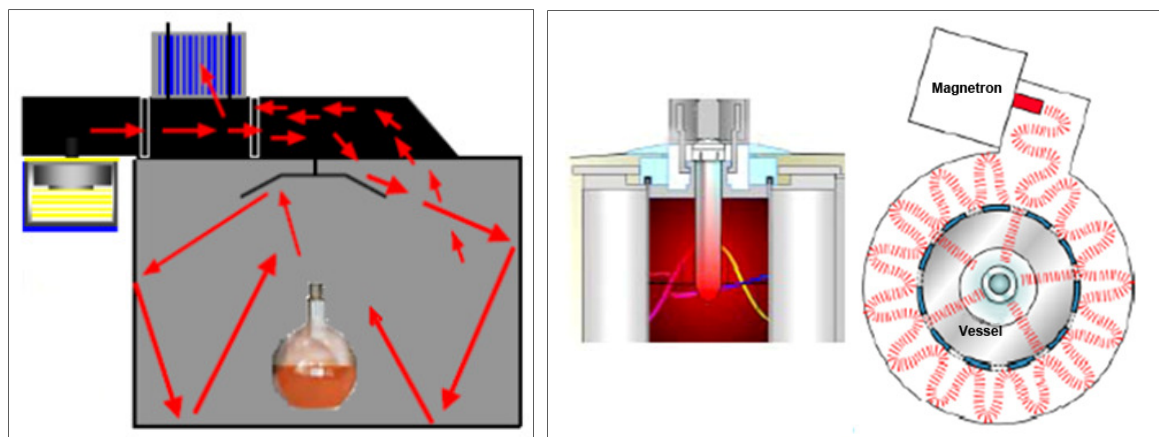
Figure 6. Multimode microwave (l) and single mode microwave (r) [9]

3. Heterogeneous reactions for hydrogen production

There are many sources of hydrogen and many different technologies of its production, e.g. ammonia cracking, alcohols steam reforming or water gas shift reaction. The common feature for all of these systems is that they belong to one group of reactions called heterogeneous catalysis. The purpose of this study is to investigate the microwave effect on gas phase heterogeneous catalytic systems. Therefore in this chapter an overview on the specifics of ethanol steam reforming, methanol steam reforming, water gas shift reaction and deployment of them for hydrogen production for fuel cell application is provided. Literature covering the microwave influence on heterogeneous reactions is consulted to provide reference for the experimental findings in this research.

3.1 Water gas shift reaction

The water gas shift reaction is a mildly exothermic reaction of carbon monoxide and water to form carbon dioxide and hydrogen:

$$CO + H_2O \leftrightarrows CO_2 + H_2 \qquad \Delta H^0_{298} = \text{-41.2 kJ mol}^{-1} \qquad \textbf{(3.1)}$$

Since this is an exothermic reaction, from a thermodynamic point of view low reaction temperatures favor the conversion of this reaction. However the kinetic is favored at higher temperatures. Due to the favored kinetics at higher temperature, an industrial process conducting the water gas shift reaction often consist of a high temperature step ($350 - 600^{o}C$) followed by a low temperature step ($180 - 250^{o}C$). Commonly copper based catalysts are used for the low temperature conversion step. One of the most common catalysts of this kind is composed of CuO and ZnO on an Al_2O_3 support. The maximum operating temperature of this catalyst is around $250^{o}C$, because at higher temperatures the catalyst is sensitive to deactivation by sintering. For the activation of this catalyst, the CuO needs to be reduced to Cu^0, which is usually done at temperatures around $220 - 230^{o}C$; using higher temperatures may again cause sintering. The zinc oxide of this catalyst does not provide an active site for the water gas shift reaction. It does however have two main functions; to protect the copper from sulfur poisoning, and to act as support for the copper [16].

For the purpose of producing hydrogen for automotive applications, the water gas shift reaction may not provide the best system. The hydrogen content in the combination CO/H_2O is very low; for one mole of converted CO only one mole of H_2 is produced. Moreover CO has a low solubility in water (0.0028 g/100 ml at $20^{o}C$) [17], making the storage of the fuel challenging as much as the storage of H_2 itself. Even more important, CO is a highly toxic gas, making the handling of the fuel a hazardous undertaking.
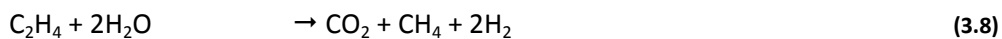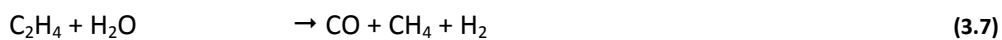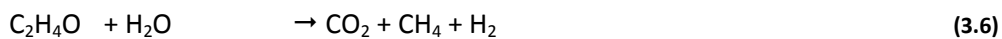
3.2 Steam reforming of ethanol
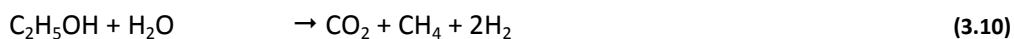
3.2.1 Reaction mechanism

The steam reforming of ethanol is an attractive option for the production of hydrogen. Ethanol can easily be obtained from renewable sources, and has high hydrogen content. The reaction is endothermic and has a theoretical hydrogen yield of six moles of H_2 per mole of C_2H_5OH. However it is more complicated than the water gas shift reaction. The overall steam reforming reaction of ethanol suggests a simple reaction system:

$$C_2H_5OH + 3H_2O \rightarrow 2CO_2 + 6H_2 \qquad \Delta H^0_{298} = 347.4 \text{ kJ mol}^{-1} \text{ [18]} \qquad \textbf{(3.2)}$$

However behind this overall reaction the reforming comprises a more complicated reaction system. Several reactions occur, which add up to the overall steam reforming reaction. However side reactions occur simultaneously and usually the product distribution comprises not only CO_2 and H_2, but CO and traces of CH_4 as well. Based on previous studies of ethanol steam reforming the following reaction mechanism is proposed [19]:

$$C_2H_5OH \rightarrow C_2H_4O + H_2 \qquad \textbf{(3.3)}$$

$$C_2H_5OH \rightarrow C_2H_4 + H_2O \qquad \textbf{(3.4)}$$

$$C_2H_4O \rightarrow CO + CH_4 \qquad \textbf{(3.5)}$$

$$C_2H_4O + H_2O \rightarrow CO_2 + CH_4 + H_2 \qquad \textbf{(3.6)}$$

$$C_2H_4 + H_2O \rightarrow CO + CH_4 + H_2 \qquad \textbf{(3.7)}$$

$$C_2H_4 + 2H_2O \rightarrow CO_2 + CH_4 + 2H_2 \qquad \textbf{(3.8)}$$

This reaction system indicates a lot of possible by-products. However the results of the practical study of M. Verónica suggest that reactions (3.5) and (3.6) are much faster than reaction (3.3), so no acetaldehyde is present in the product mixture. The same goes for the ethylene consumption; reactions (3.7) and (3.8) are as fast as reaction (3.4). Therefore, the reaction system is better represented as:

$$C_2H_5OH \rightarrow CO + CH_4 + H_2 \qquad \textbf{(3.9)}$$

$$C_2H_5OH + H_2O \rightarrow CO_2 + CH_4 + 2H_2 \qquad \textbf{(3.10)}$$

$$CH_4 + H_2O \leftrightarrows CO + 3H_2 \qquad \textbf{(3.11)}$$

$$CH_4 + 2H_2O \leftrightarrows CO_2 + 4H_2 \qquad \textbf{(3.12)}$$

To decrease the amount of CH_4 in the product gas inerts can be added, which shift the equilibrium of reactions (3.11) and (3.12). These equilibrium reactions determine the final composition of the product gas. In case only traces of methane are detected in the product gas, this system can be represented by:

$$C_2H_5OH + H_2O \rightarrow 2CO + 4H_2 \qquad \textbf{(3.13)}$$

$$C_2H_5OH + 3H_2O \rightarrow 2CO_2 + 6H_2 \qquad \textbf{(3.14)}$$

However for many ethanol steam reforming systems, the amount of methane often cannot be neglected. Generally, at low temperatures ethanol dehydrogenation takes place, while the reforming reactions occur at the higher temperatures [20]. Therefore at relatively low temperatures high conversion of ethanol can be observed. However at these low temperatures the produced methane often remains unconverted. This depends mostly on used catalyst.

3.2.2 Catalysts

For the steam reforming of ethanol there are different combinations of active material and support. The most common catalysts have active sites based on group VIII metals like nickel, rhodium, platinum or ruthenium, on metal oxide supports. A rhodium based catalyst promotes steam reforming of ethanol in the low temperature range, reaching full conversion around 300°C, with a high hydrogen yield (~60%) [21]. For the low temperature steam reforming nickel based catalysts are used as well. Conversions up to 80% can be reached at temperatures as low as 250°C, and at 300°C a conversion of 96% was reached in case when the nickel was supported by La_2O_3. However the hydrogen yield was slightly lower (~50%) than for the Rh catalyst [22,23]. For both Rh and Ni based catalysts at lower temperatures the selectivity for CO increases, with CO yield values depending on the support material. Regarding the production of methane the nickel based catalysts generally have a higher yield than the rhodium based catalysts. Carbon monoxide being a poison for most hydrogen fuel cells, and the formation of methane decreasing the hydrogen yield, the potential of this reaction system is not very high at low temperature.
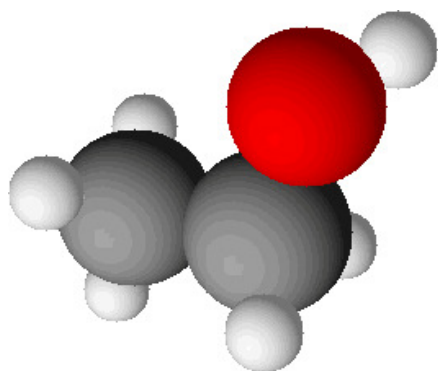

The use of ethanol as an indirect fuel for hydrogen fuel cells fits in the search for renewable fuels for automotive applications. Ethanol can be obtained from energy crops, like corn, maize and wheat crops, from trees and grasses. Ethanol is biodegradable and has low toxicity, therefore the impact on the environment is minimal when spilled [24]. However for the steam reforming reaction of ethanol a lot of energy is needed to break the C-C bond which is present in the molecule (see figure 7). Moreover the trade-off between high temperature and low temperature steam reforming with high CO and CH_4 selectivities induce difficulties in adoption of ethanol in mobile applications.

Figure 7. Ethanol molecule

3.3 Steam reforming of methanol

3.3.1 Reforming mechanism

Methanol, as well as ethanol, is seen as a potential source of hydrogen for hydrogen fuel cell applications. High hydrogen content and the liquid state of the fuel at standard temperature and pressure facilitate easy storage and handling. Moreover methanol can be produced from a variety of renewable sources, including wood waste, methane gas from animal waste and landfills, sugar beet pulp and glycerol [25]. Methanol has some significant advantages over ethanol, like high hydrogen content per carbon, 4/1 for methanol as opposed to 3/1 for ethanol. Due to the absence of the C-C bond methanol can be successfully converted at temperature range between 150°C and 300°C, as is illustrated in figure 8 [26]. Low reforming temperature is a major advantage since it boosts CO consumption by the water gas shift reaction. Another advantage of the absence of the C-C bond is

lower by-product formation than in the steam reforming of ethanol. However the main drawback of methanol is its toxicity [27]; ingestion of small amounts can cause permanent blindness or even death. A more important problem in the application of methanol in fuel systems is that metals are sensitive to corrosion by methanol. Therefore special consideration must be given to the choice of material for the methanol fuel system. Similar problems to those that methanol poses as a fuel have already been solved for other fuels, like LPG and gasoline, making methanol a very competitive candidate for application in the automotive industry.
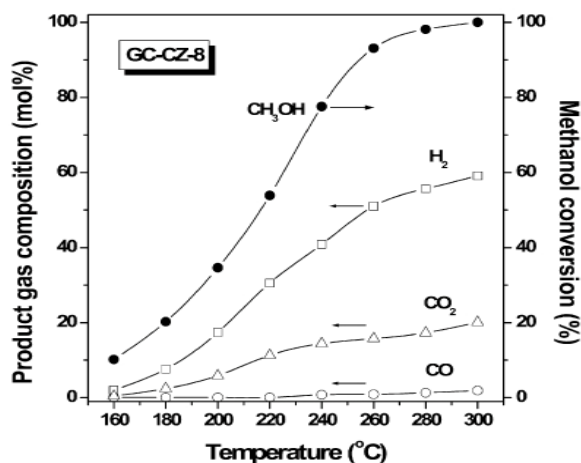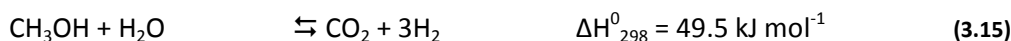

Figure 8. Product gas composition and methanol conversion vs. reaction temperature during steam reforming of methanol over a Cu/ZnO catalyst [26]

Just like the reforming of ethanol, the methanol steam reforming is a reversible endothermic reaction. The hydrogen yield in this case is 3 moles hydrogen per mole of methanol:

$$CH_3OH + H_2O \quad \leftrightarrows CO_2 + 3H_2 \qquad \Delta H^0_{298} = 49.5 \text{ kJ mol}^{-1} \qquad \textbf{(3.15)}$$

The steam reforming of methanol, similar to the steam reforming of ethanol, follows a reaction mechanism more complicated than this overall reaction. Although agreement exists that the mechanism of the steam reforming is simpler than that of ethanol steam reforming, controversies about the actual reaction pathway have not yet been resolved [28]. Traditionally it was believed that methanol steam reforming was the combination of methanol decomposition (3.16), followed by the water gas shift reaction (3.1), regardless of what catalyst is used.

$$CH_3OH \quad \leftrightarrows CO + 2H_2 \qquad \Delta H^0_{298} = 90.70 \text{ kJ mol}^{-1} \qquad \textbf{(3.16)}$$

Over copper based catalysts this theory is supported by the fact that at higher temperatures the conversion of methanol is higher, which is due to the endothermicity of the decomposition reaction. Moreover the production of CO is higher as well, which can be explained by the fact that the CO mitigation follows an exothermic reaction, hence is slowed down at higher temperature. However other mechanisms, which do not involve the production of CO are proposed as well [28]. Iwasa et al. [29] report a steam reforming mechanism over copper catalysts with a formic acid intermediate:

$$CH_3OH \quad \rightarrow HCHO + H_2 \qquad \textbf{(3.17)}$$

$$HCHO + H_2O \quad \rightarrow HCOOH + H_2 \qquad \textbf{(3.18)}$$

$$HCOOH \quad \rightarrow CO_2 + H_2 \qquad \textbf{(3.19)}$$

Research on another type of catalyst, based on group VIII metals, provides much evidence that the steam reforming reaction follows a mechanism via a formaldehyde intermediate. Depending on the catalyst, two reaction pathways are proposed, both of which start with reaction 3.17. In one pathway the formaldehyde decomposes into CO and hydrogen, followed by the water gas shift reaction (3.20 – 3.21).

$$HCHO \qquad\qquad \rightarrow CO + H_2 \tag{3.20}$$

$$CO + H_2O \qquad\qquad \rightarrow CO_2 + H_2 \tag{3.21}$$

In the other pathway the formaldehyde reacts with water to form formic acid, which is then decomposed into CO_2 and hydrogen (3.18 – 3.19), a pathway similar to that of the copper catalyst [29, 30].

Although both pathways seem similar, there is a difference of major importance; the first mechanism is CO-based, while the second is not. Therefore catalysts promoting the second reaction mechanism will be favored over the catalysts promoting the first.

3.3.2 Catalysts

Since the mechanism and product distribution of methanol steam reforming depends greatly on the catalyst, much attention has been focused on the development of active catalysts for this reaction. For the steam reforming reaction it is of major importance that an active catalyst is present. If this is not the case, low temperatures and long residence times give rise to the production of methane instead of hydrogen [28]. Catalyst development focuses mostly on two types of active material; copper and metals of group VIII.

Copper catalyst

Originally a copper catalyst was widely used as methanol synthesis catalyst. Methanol can be produced by the conversion of syngas over a Cu/ZnO catalyst under high temperature (250 – 300°C) and pressure (50 – 100 bar) via reaction 3.22 [31].

$$CO_2 + 3H_2 \qquad\qquad \leftrightarrows CH_3OH + H_2O \tag{3.22}$$

Since the reaction can be seen as the inverse to methanol steam reforming, development of copper catalysts has been investigated. A composition of $CuO/ZnO/Al_2O_3$ is known to be very active in the formation and steam reforming of methanol. The activity of this catalyst is related to the oxidation state of the copper; the combination of Cu^0 and Cu^I sites determine largely the activity and selectivity of the catalyst [28]. Even though the $CuO/ZnO/Al_2O_3$ catalyst is very active for methanol steam reforming and has a low selectivity for CO, it is very sensitive to deactivation due to sintering. Temperatures above 300°C are high enough to trigger sintering and significantly decrease the activity of catalyst [32]. A high degree of dispersion of copper crystallites prevents the sintering to some extent. For this reason to the most copper based catalysts a metal oxide is added. On the $CuO/ZnO/Al_2O_3$ catalyst both the alumina support and the ZnO increase the dispersion of the copper crystallites, improving the thermal stability of the catalyst [32]. Apart from the increased thermal stability, the presence of ZnO also decreases deactivation by sulfur poisoning. Sulfur is a strong poison for copper catalysts, and can be present in low concentrations in the form of H_2S. ZnO can react with H_2S to form zinc sulfide, a reaction which is thermodynamically favored over the formation of Cu_2S on the active copper sites [32]. Nevertheless it is necessary to keep the concentrations of sulfur below 1 ppm.

Research has been conducted to other supports for the copper catalyst. A lot of attention has been given to ceria (CeO_2), which is said to yield higher activity and stability to the copper catalyst than alumina. These effects are believed to be caused by the higher degree of dispersion of the copper,

and by the stronger copper-support bonding. Also the addition of yttrium to a Cu/Al_2O_3 catalyst was investigated. The activity of this catalyst was much higher than that of the pure Cu/Al_2O_3, which was most likely caused by the increased number of Cu^I sites on the catalyst, which are believed to be more active than Cu^0 sites [33].

Group VIII catalyst

Because of the deactivation issues of the copper catalysts, other metals are investigated for use as methanol reforming catalyst. Group VIII metals are known to be active for the conversion of methanol, however they have rather low selectivity towards the steam reforming reaction [28]. Steam reforming of methanol over a palladium catalyst, for example, follows the reaction pathway of reactions 3.20 – 3.21. However the catalyst does not promote the water gas shift reaction, so large amounts of CO are produced [29]. Another option for using the group VIII metals as catalyst is by using them in alloys with other materials. A Pd/ZnO catalyst has been shown to form a PdZn alloy during reduction at temperatures >300°C [29]. This alloy was very selective towards methanol steam reforming, following the path of reactions 3.18 – 3.19. Since this pathway does not involve CO, the use of group VIII metals in alloys provides a good alternative for the copper catalyst.

4. Application of microwaves to heterogeneous catalyzed reactions

This study is focused on the microwave effect on methanol steam reforming. Microwave effects on different heterogeneous reactions are nowadays widely investigated mostly due to the potential benefits coming from providing energy to the reaction zone in a different way. In conductively heated heterogeneous reactions, the temperature of the active sites is usually lower or equal to the bulk temperature, because the active sites are heated by the bulk. In microwave-assisted catalysis the active sites of the catalyst are heated very rapidly, because of effective coupling of microwave energy with nano-size metallic particles. This rapid heating creates perfect conditions at which the active sites could have a higher temperature than the bulk. Since the temperature at the active sites of the catalyst determines the reaction rate, this means that reaction rates can be increased when microwave heating is applied. The difference in heating can also lead to different products. Most conductively heated reactions are kinetically controlled, because the heat is provided in small amounts at a time. Due to the slow heating the thermodynamic activation energy is not applied before the reactants have taken the kinetic route. During microwave heated reactions, a large amount of heat can be provided instantly, and thermodynamic control of the reaction is possible yielding products with lower energy than the kinetically controlled reaction [9], which is illustrated in figure 9.
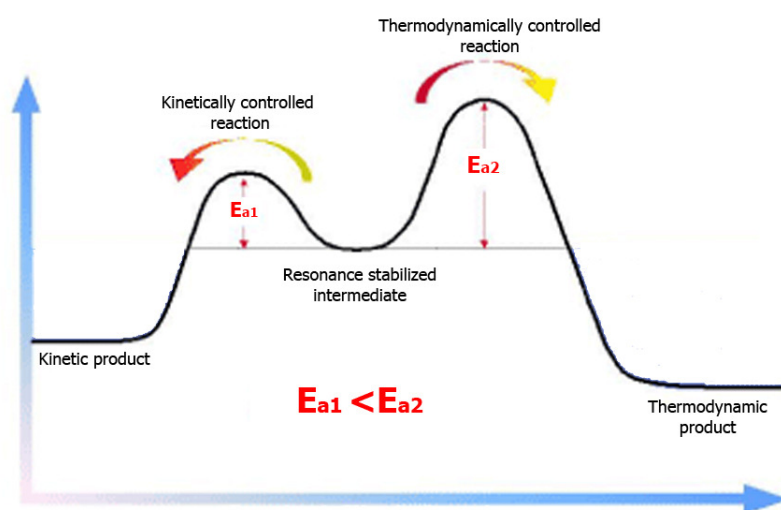

Figure 9. Activation energy for kinetically controlled reactions and thermodynamically controlled reactions [12]

4.1 The microwave effect

A huge effort has been taken to establish a mechanism of the microwave enhancement of reactions. The main question raised in this research is whether the effect is purely thermal, or molecular interaction with the microwaves or equilibrium shifts, better known as 'the microwave effect' are responsible for the enhancement of reactions. To confirm or exclude the presence of non-thermal phenomena an accurate temperature measurement inside the reactor is essential. In the past, various research groups [34, 35] observed an increased selectivity and/or yield in microwave-assisted

21

reaction. As an explanation of observed enhancement the presence of specific microwave effect has been claimed since no thermal effects were observed. However this might be due to the local nature of the temperature effects in combination with inaccurate temperature measurement which has been proven by Jahngen et al. [36]. By comparing a kinetic study in conventional conditions with accurate temperature measurement in microwave conditions, Jahngen et al. predicted the results of the previous study using the kinetic model.

The local nature of the thermal effects can be explained by the fact that microwaves couple directly with the molecules of the heated material. There are several thermal effects that can contribute to increased reaction rates and selectivity of heterogeneous reactions under microwave conditions. These effects can be roughly divided into two types; increased heating rate and temperature gradients on both the macro and micro scale.

The fast heating rates are achieved under microwave irradiation for materials with specific dielectric properties. However inverse temperature gradients to those of conductive heating are present, as illustrated in figure 10 [37]. In homogeneous catalyzed reactions under microwave conditions this macro gradient is not observed. This may be due to the fact that in most homogeneous reactions mixing is applied for even distribution of the heat.

Figure 10. Inverse temperature gradients on the macro scale between (a) microwave and (b) conductive heating [38]

The increased heating rate is one of the main reasons for applying microwave heating to chemical reaction systems. Beside the fact that it can lead to higher reaction rates, different control regimes as well as increased selectivity were observed [39].

In most cases a single-mode microwave is used for the application of microwave heating in heterogeneous catalysis [9]. From figure 6 (r) it can be seen that all waves are directed to the centre of the cavity, yielding a high energy density. On locations further away from the centre the energy density becomes lower, which gives rise to the macro gradients visible in figure 10 [37]. These macro gradients can already be of significant importance to the conversion and selectivity of reactions. Although there is no clear evidence on the existence of micro gradients, it is believed that micro gradients are caused by selective heating of certain materials in combination with poor heat transfer [11].

Selective heating is a process in which a certain material has far better coupling characteristics than its surroundings, and thus heats much faster. This can lead to very high temperature gradients when heat transport from the material to the surroundings is slow. In heterogeneous catalysis the catalyst is often composed of two different materials which differ significantly in ability to absorb microwave energy, e.g. Al_2O_3 support, which is a poor microwave absorber and Cu, Rh or another metallic particles dispersed as active material. To provide a high active surface area the metallic particles have dimensions in the range of micrometers or even nanometers. Metal particles of this size have excellent microwave characteristics and heat faster. This leads to high temperature gradients between catalyst and bulk [40]. The temperature difference can range from 100 - 200°C [41].
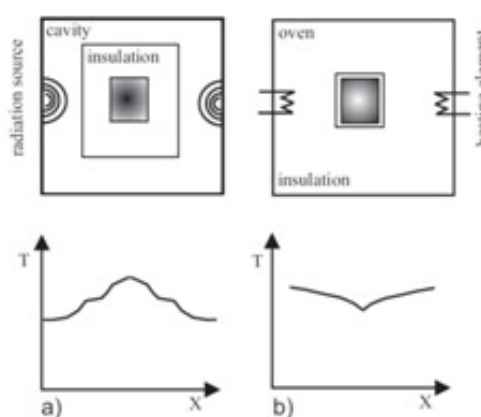
Recently Chen et al. [42] proposed a thermal effect similar to that of selective heating. The effect is called 'microwave double absorption', because both catalyst and feed mixture absorb microwaves very well and are thus heated rapidly, resulting in higher conversion. However no proof was provided in terms of temperature measurement.

When no thermal effect is detected, even though precise and accurate temperature measurement techniques are used, the occurrence of non-thermal effects may be discussed. Non-thermal microwave effects are rarely believed to occur. However Zhang et al. [43] have claimed that in preparation of the catalyst for the reaction, modification of the microstructure can occur, yielding a catalyst with higher activity.

4.2 Temperature measurement

The presence of temperature gradients can be detected by accurate temperature measurement. However under microwave conditions not all measurement techniques can be used. The most frequently applied temperature measurement techniques in experiments using conventional heating are thermocouples, infrared pyrometry and fiber optic thermometry. These measurement techniques have all been applied in experiments under microwave irradiation, however the reliability of the results differs between the techniques due to the features of the measurement techniques and the conditions of the experiments [44].

Conventional thermocouples, for example cannot be used. Consisting of metal, they suffer from interference with the microwaves, which induces self-heating leading to serious temperature measurement errors, and can even lead to electrical discharge [45]. Even though electrical discharge can be prevented by shielding and grounding of the thermocouple [44], inaccurate measurement cannot be entirely avoided [46].

IR thermometry has been proposed to be a more reliable method than using thermocouples, in part because the measurement device does not need to be placed inside the microwave cavity. However due to the fact that IR thermometers measure just the temperature at the surface of a body, they can only be applied for thin samples. When applied for measuring bulk temperatures, like the in-built IR sensors in microwave ovens, the measurement error can be significant [44]. Moreover recalibration is often necessary due to fact that the indicated temperature is dependent on the vessel material as well as on ambient conditions.

Another temperature measurement technique suitable for microwave reactions is based on fiber-optic sensors. The temperature measurement of fiber-optic sensors is not dependent on ambient conditions, hence frequent recalibration is not necessary. Moreover fiber optic sensors can be placed inside the reactor in any position, providing the ability to determine the temperature inside microwave irradiated reactors more accurately. It is generally agreed that fiber-optic temperature sensors provide a reliable means of measuring temperature under microwave conditions. However attention must be paid to the positioning of the probes. Durka et al. [11] showed the necessity of this by changing the vertical location of the fiber optic probe inside a glass vial containing a Rh/CeO$_2$-ZrO$_2$ catalyst, under inert conditions, illustrated in figure 11.
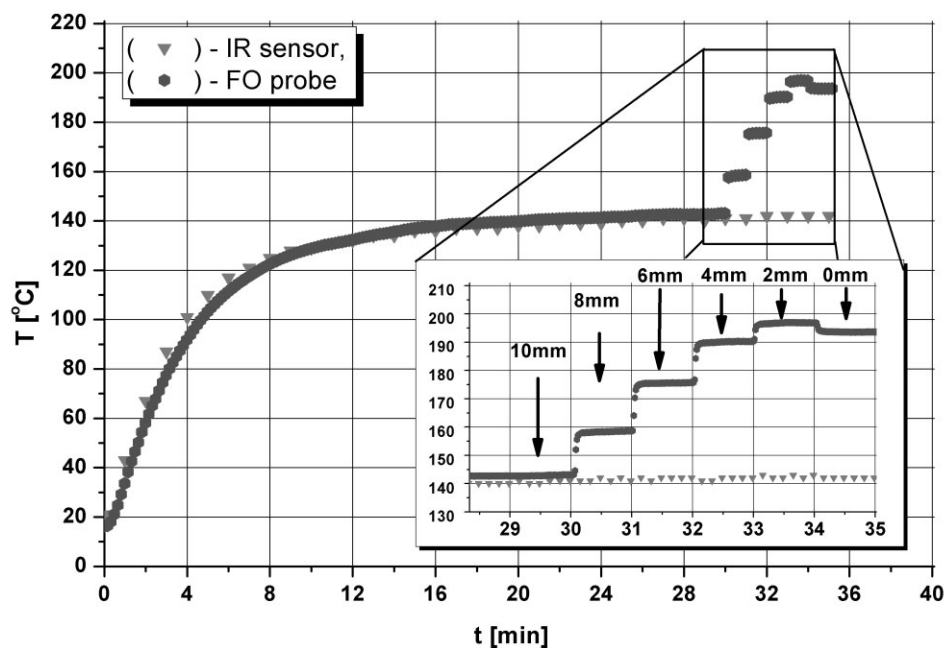
.

Figure 11. Vertical temperature profile inside a catalytic bed of Rh/CeO$_2$-ZrO$_2$. The fiber optic sensor was moved in a downward direction [11]

Another option for temperature measurement of samples in microwave fields, which is not dependent on positioning of the sensor, is making use of a thermovision camera. Bogdal et al. [47] used both fiber-optic sensors and a thermovision camera to determine the temperature inside the reactor. The thermovision camera revealed the existence of hot-spots, which were not detected by the fiber optic sensors due to the fact that the sensors measure only local temperatures, while the thermovision camera was able to detect temperature gradients over the surface of the material.

4.3 Previous results of microwave heating on heterogeneous reactions

In the past years microwave enhancement of heterogeneous reactions has been subject to many studies. A selection of results will be discussed in order to illustrate the type and extent of enhancements on heterogeneous reactions.

Hot-spot formation has been given as cause for many reaction enhancements. Bi and coworkers [48] in their study on methane oxidation over a 10% Co/ZrO$_2$ catalyst observed that higher selectivities for hydrogen and carbon monoxide were obtained in the microwave-assisted reaction for the same temperature as with conventional heating. Moreover comparable methane conversion levels (78%) were reached under reduced temperature of the catalyst bed (approximately 50K). In the study an infrared pyrometer was used to determine the temperature of the catalytic bed in the center of the reactor. To assure comparable temperature measurement in both heating methods the temperature reading from the infrared pyrometer was compared with the readout of the thermocouple. These effects were merited to microwave hot-spots on the oxygen vacancies of the catalyst, which were seen as the active centers for the reaction.

Zhang et al. [49] investigated the endothermic decomposition of H_2S under microwave conditions and observed an increase in conversion compared to that of the conventionally heated experiment. The conversion profiles of H_2S under microwave and conventional heating, as well as the equilibrium data can be seen in figure 12. The conversion profile of the conventional heating experiments follows the theoretical profile very closely, while the conversion profile of the microwave experiments has much higher values than theoretically

Figure 12. Conversion of hydrogen sulfide as function of temperature [49]

possible at the given temperatures. The increase is explained by the formation of hot-spots on the catalyst surface, yielding a much higher reaction temperature and thus a higher conversion, although the applied temperature measurement technique (optical fiber thermometer) precludes detection of the hot-spots due to the local nature of the effect [49]. However, in the study of catalyst morphology a high temperature phase change of the catalytic support (γ-Al_2O_3 to α-Al_2O_3) was observed, when microwave-assisted experiments were performed. This suggested that the temperature of the system was approximately 150K higher than this which was measured. This shows that the catalyst had a higher temperature than the average reaction temperature, which is in accordance with the hot-spot theory. This effect has also been observed by Sinev and coworkers [50] in the oxidative dehydrogenation of ethane, where mixed oxides of the V/Mo were observed to undergo a phase change, leading to different catalytic performance. Beckers et al. [51] in research on propane oxidation under microwave conditions yielded similar conversions in microwave experiments as those obtained with conventional heating at 200°C higher temperatures. Similar to the study of Zhang et al., fibre optic temperature measurement was implemented to determine the average temperature of the catalytic bed, which caused the acclaimed hot-spot formation to be invisible. It may be noted that this was one of the few heterogeneous catalyzed reactions which was performed in a multimode microwave. In HCN synthesis [52], higher selectivity towards the product was observed in microwave experiments. This was claimed to be caused by selective heating of the catalyst material, creating a micro gradient of temperature between the catalyst and the bulk.
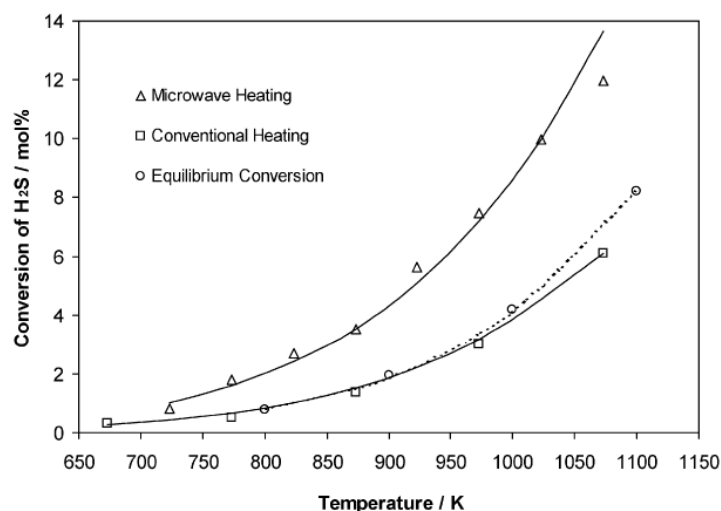
It is stated that these hot-spots do not only induce a change of reaction rate, but also change of apparent shift in the equilibrium constant. It has to be noted that it is not claimed that the equilibrium constant of the reaction itself has changed.

The group of Zhang [49] also investigated the microwave effect on the exothermal reaction of hydrodesulfurization (HDS) of thiophene. The exothermic nature of the reaction gave the possibility to investigate the effect of microwave heating on the equilibrium itself. For lower than optimal temperatures, hot-spot formation would increase the reaction rate of the exothermic reaction. At temperatures higher than optimal, hot-spot formation on the catalyst should give rise to an early decline of the conversion. Both effects were observed in the study, supporting the hot-spot theory.

The other thermal effects gain less attention. However Ioffe et al. [53] have claimed that the increase in selectivity to acetylene in the conversion of methane could be attributed to macro as well as micro gradients of temperature that can occur inside the reactor and on the catalyst surface, when larger catalyst particles are used.

Beside thermal effects of microwave heating, the group of Xin-Rong Zhang [43]claims that microwave irradiation (3 – 10 minutes) of the oxide precursor of the $Cu/ZnO/Al_2O_3$ catalyst, used for the steam reforming of methanol, has an effect on the structural modification of the catalyst surface. It was shown that the catalysts with modified surface characteristics displayed an enhanced performance in the conversion for steam reforming of methanol. This was acclaimed to be due to the creation of highly strained copper nanocrystals. It was observed that the specific copper surface area decreased for increased duration of microwave treatment, however the conversion increased significantly and showed an optimum at 8 minutes of treatment. Further investigation of the catalyst showed that the conversion was directly proportional to the measured microstrain of the copper crystals.

A recent publication by Chen et al. [42] concerns as well the investigation of methanol steam reforming over $Cu/ZnO/Al_2O_3$ catalysts. In this study steam reforming of methanol was performed only under microwave conditions and the results were compared with experimental results from conventional experiments performed by other research groups using different catalysts and different conditions. The microwave effect on the steam reforming reaction over the used catalyst is claimed to be two-fold; both the reactants, water and methanol, and the CuO from the catalyst are good microwave absorbers. According to the authors it was verified that steam reforming of methanol under microwave conditions is superior to that under conventional conditions. However for the temperature measurement a shielded thermocouple was used, which may be influenced by the microwave field itself. Incorrect temperature measurement could influence the

Figure 13. Three dimensional profile of (a) experimental and (b) thermodynamic methanol conversion with respect to temperature and S/C ratio [42]

comparison. Even though an increase of conversion under microwave conditions is observed, unexpected effects were noted as well. According to Le Châtelier's principle, when the S/C ratio is increased, the conversion of methanol should be positively affected. However, in the performed experiments decay in methanol conversion was observed for increasing S/C ratio, as illustrated in figure 13. This effect was contributed to the fact that more microwave energy would be absorbed heating the water, than would be used for the reaction.
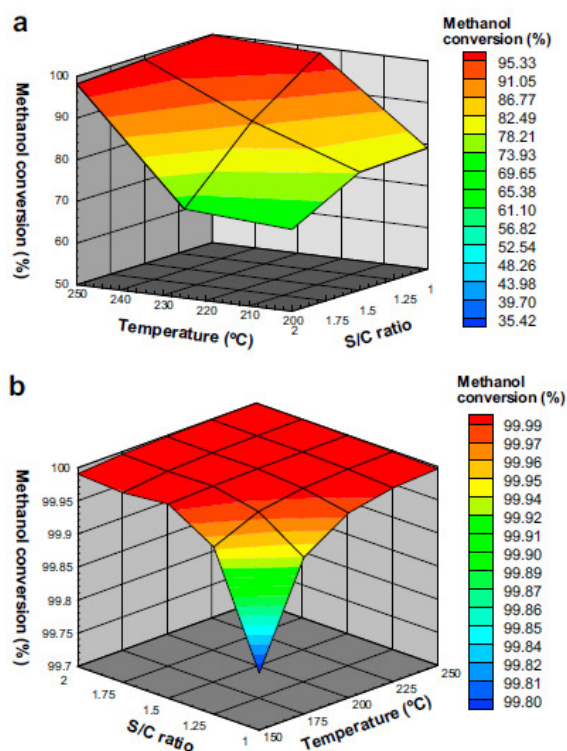
5. Experimental part

The study is focused on comparison of methanol conversion, product distribution and hydrogen selectivity over a range of operating conditions under two heating modes: electric and microwave. In the following paragraphs the experimental setup and experimental procedures used during reaction are explained. Furthermore the set of performed reactions is discussed.

5.1 Setup

The steam reforming of methanol was performed in a reaction system, of which a schematic view is presented in figure 14. This setup can be divided into 3 parts;

- the feed section, including the evaporation of the reaction mixture
- the reaction section, consisting of a reactor suitable for both microwave and conductive heating applications
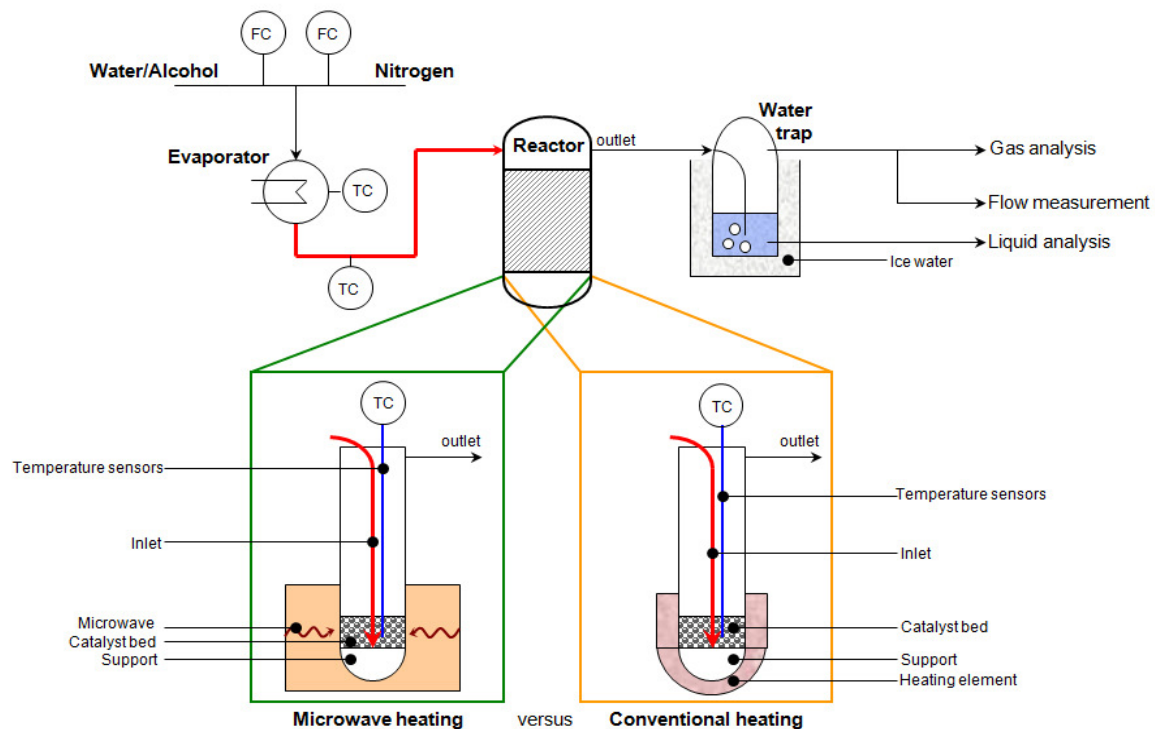- the product section, with effluent treatment and analysis

Figure 14. Schematic view of the reaction system

5.1.1 Feed section

A mixture of water and methanol is stored in a feed vessel, to which stirring is applied to maintain a homogeneous mixture. The mixture is fed to an evaporator at constant mass flow rate, where it is mixed with a carrier gas (nitrogen) to ensure stable and homogeneous flow of reactants. The evaporator temperature was set to $140^{o}C$ in order to ensure that the entire feed stream is in the vapor phase. Finally, the vapor stream from evaporator is sent to the reactor through a heated line.

5.1.2 Reaction section

A more detailed model of the reactor is shown in figure 15. The reactor, 23 mm in diameter and approximately 170 mm long, is made of quartz glass, which is known as almost perfect microwave transparent material. The top of the reactor is closed by a plastic cap with Teflon sealing inside. The temperature sensors and thermocouple are introduced into the reactor through tiny openings in the plastic cap, without compromising the sealing. The catalyst is placed at the lower part of the reactor and is supported by a glass porous disk. The feed enters the reactor from the top in a bended glass tube which crosses the catalytic bed right at the center; the reactants exit the tube below the catalytic bed and then flow upwards through the catalytic bed after they have been radially distributed by the porous glass disk. Finally, the exhaust gas is released from the top-right part of the reactor. The temperature of the catalytic bed is monitored by two fiber optic temperature sensors (FISO); one is located in the center of the reactor while the second is placed next to the reactor wall. Both sensors were introduced into the reactor and thus into the catalytic bed by glass capillaries, what enables to change the location of the sensors in vertical direction on demand without risking the damage to the sensors. This enables the possibility to determine the temperature profiles along the height of the catalytic bed in the center and at the wall of the reactor.
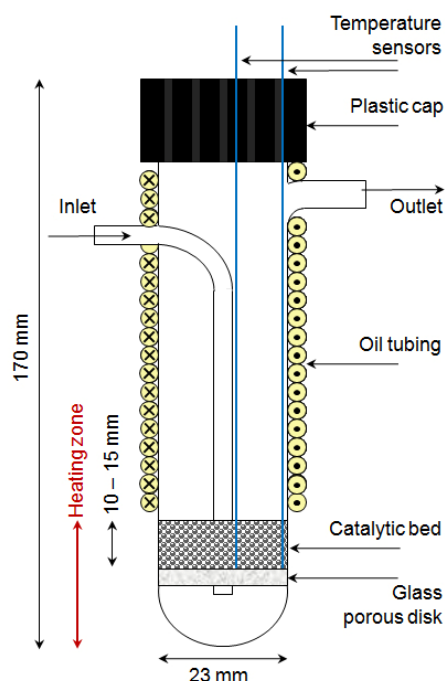

Figure 15. Schematic view of the reactor

In case of reactions performed with conventional, conductive heating the desired temperature of catalytic bed is controlled by a spiral, electric heating element placed around the reactor in the heating zone in combination with a thermocouple (see figure 16 (r)), which is placed at the center of the reactor. In case of a reaction under microwave heating, a monomode microwave (CEM Discover) is applied (see figure 16 (l)). The temperature is controlled manually by changing the power of the magnetron according to the temperature reading from the fiber optic sensor placed in the center of the reactor and thus the middle of the catalytic bed.

Since the vertical range of the microwaves is limited to only few centimeters, and the cavity of the microwave is relatively deep (see figure 6 (r)), the height of the reactor is much larger than the height of the catalytic bed. Therefore the outgoing water and methanol are in danger of condensing in the top. If condensation takes place, droplets fall down to the catalytic bed under influence of gravity, and a large temperature drop can occur. In order to prevent unexpected temperature fluctuations condensation is prevented by heating the reactor by silicon oil (150°C) flowing through silicon tubing around the reactor. The electric heating element, on the contrary, is capable of heating the entire length of the reactor, up to the in and outlet near the top. Nevertheless the oil tubing is used with the conductive heating experiments as well in order to prevent any differences in the experimental set-up other than the heating method of the catalytic bed.

Figure 16. Microwave (l) and conventional (r) setup, each with the heated feed line on the left, temperature sensors coming out the top and the outlet on the right. Around the reactor, the oil tubing is visible.

A part of this study is focused on the temperature mapping inside the catalytic bed. Ideally, application of microwaves yields isothermal conditions. By heating the entire catalyst bed instantaneously, it eliminates the temperature gradients present with conductive heating. However, for both heating methods temperature mapping is necessary because temperature gradients exists along the radius and the height of the catalytic bed. In case the conventional heating method is applied temperature profiles are expected to exist along the radius of the reactor, because the heat transfer relies on conduction. The heating being applied outside the wall of the reactor causes the temperature to be high on the wall, but lower in the center of the reactor, as is illustrated in figure 17. In case the monomode microwave is used, most energy is transferred in the center of the reactor. For increasing radius, the density of the microwaves decreases, yielding an inverse temperature profile along the radius of the reactor (see figure 17), hence no isothermal conditions are reached. In order to assess the microwave effect on the reaction an average temperature of the catalytic bed needs to be computed, to prevent unexpected temperature differences in the comparison.
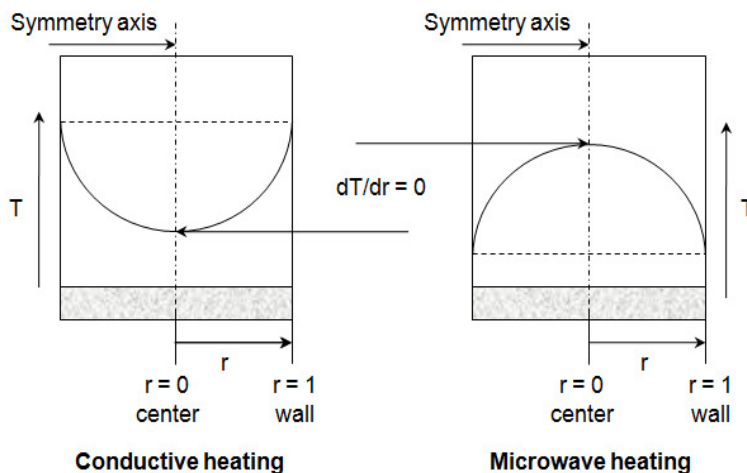

Figure 17. Assumption of radial temperature profile inside the catalytic bed

In order to map temperature inside the catalytic bed the sensors location was changing in a range from 0 mm to 12 mm above the bottom of catalytic bed with increments of 3 mm. As a reference reaction temperature, the temperature at bottom location in the center of the catalytic bed has been controlled. The obtained temperature profiles are used in determination of an average reaction temperature inside the reactor, of which the calculations can be found in appendix A. The average temperature of the catalytic bed is determined as an average of radial temperature profiles along the height of the catalytic bed. Since for the given height of the catalytic bed the temperature was measured only at two locations, in the center of the reactor and near its wall, only a linear profile can be delivered, which is most likely is not occurring. Therefore, based on general knowledge about heat transfer, an assumption of symmetry of temperature profile in the radial direction is made (see figure 17). By assuming symmetry of the radial temperature profile a unique parabolic function can be obtained at each measurement level of catalytic bed (see table 2). By analytical integration of the 2nd order function representing radial temperature profiles, a set of data points creating an average axial temperature profile is obtained (see figure 18). This temperature profile can be described as a 4th order polynomial. Analytical integration allows determining the average temperature of the catalytic bed (table 2).

Table 2. Calculation of radial average temperatures, integrated to yield an average temperature of the catalytic bed

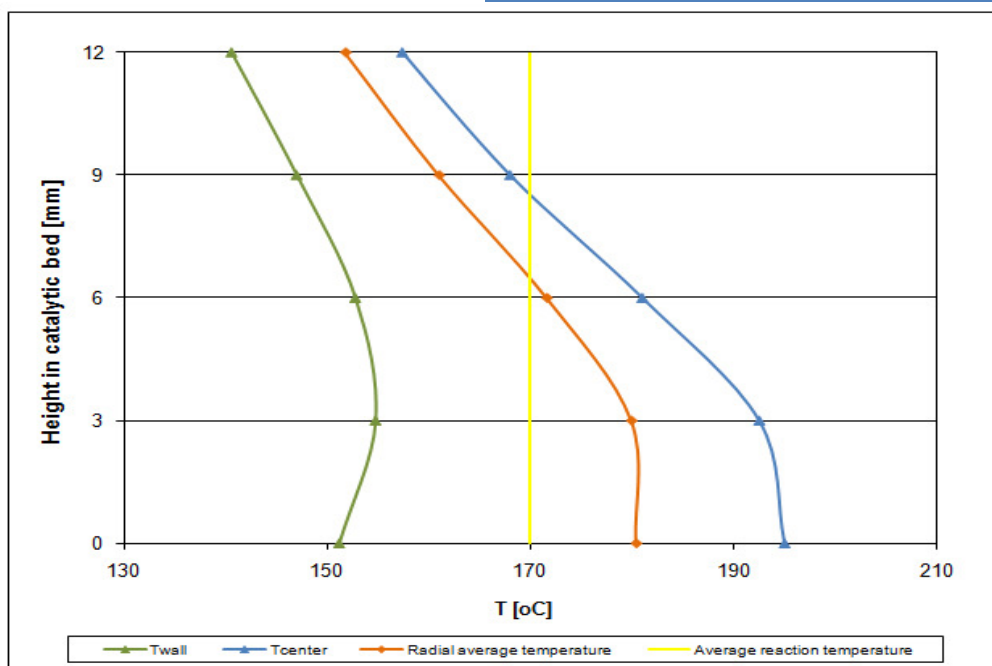| Height	Temperature data		$y = ax^2 + c$		Radial average
[mm]	Twall [^{o}C]	Tcenter [^{o}C]	a	c	
0	151.2	195	-43.8	195	180.4
3	154.8	192.5	-37.7	192.5	179.9
6	152.8	181	-28.2	181	171.6
9	147	168	-21	168	161
12	140.55	157.4	-16.85	157.4	151.78
			Average temperature of the bed		**169.94**

Figure 18. Axial temperature profiles along the height of the reactor in a microwave reaction (S/C = 1.5, GHSV = 65,000 h^{-1}, T = 190°C)

5.1.3 Product section

After reaction has taken place, the products of the reaction and the unconverted reactants flow upwards to the outlet of the reactor. The effluent gas together with unreacted remains is directed to a water-trap, kept at -10°C, in order to condensate the unconverted methanol/water mixture and to separate it from the gas product stream. The composition of the remaining gas is analyzed by an online gas chromatograph (Varian CP-4900), which also measures the remaining methanol vapor. The volume flow is measured using a bubble flow meter. An offline GC (Varian 3900) and a density meter (Anton Paar DMA 5000) are used to analyze the concentration of methanol in the collected liquid from the water-trap. The data obtained by the gas- and liquids analysis are used in a mass balance, from which conversion, yields and selectivities are calculated.

5.2 Reaction procedure

For each reaction the same procedure is used, from the application of the catalyst until the analysis of the effluent. Keeping the same procedure for each reaction is important, because different procedures may lead to unexpected differences in obtained results. The total reaction procedure can be divided into 3 parts, namely the preparation, the reaction, and the shutdown and analysis. All three parts are discussed below.

5.2.1 Preparation

For each reaction fresh catalyst is used in order to prevent different reaction rates due to deactivation. The catalyst is a commercial water gas shift catalyst (HiFUEL W220, Alfa Aesar), and comes in the form of cylindrical pellets. The pellets contain 52.5% Cu as CuO, and 30.2% Zn as ZnO. The cylinders are 3.4 mm long and have a density of 1.40 kg/L [54]. Approximately 4 g of catalyst is applied to the reactor. Although the bed of the catalyst is random packed, before each experiment reactor is manually shaken to make the packing as compact possible. Activation of the catalyst is performed in situ at a temperature of 220°C. A H_2/N_2 gas mixture (9%vol.) with a flow rate of 275 cm^3/min is applied for 1.5 hours. Regardless of the heating method of the reaction, reduction is carried out with conductive heating. When the reduction is finished, the catalytic bed remains at 120°C under 100% N_2 flow until the reaction commences.

5.2.2 Reaction

When the catalyst is reduced, the proper heating method is applied and the desired temperature is set. In case of conductive heating, the electric heating element remains in place, in case of microwave heating, the electric heating element is replaced by the microwave oven and the thermocouple is extracted from the reactor. Before experiment starts the feed tank with reaction mixture and the empty water-trap are weighed. The evaporator is set to 140°C, and the heating line to 150°C. The nitrogen flow is set to the desired value, which depends on the desired temperature and GHSV of the reaction, and measured using the bubble flow meter. When all parameters are set, feed flow is introduced, after which the online micro-GC is started to monitor concentrations of hydrogen and CO_2 in the gas. The liquid flow rate is related to the nitrogen flow rate, maintaining a molar ratio of liquid flow/N_2 flow around 1.4. When steady state is reached, which takes approximately 20 minutes, a temperature map is made to determine the average temperature in the reactor. The first measurement of products distribution and other process conditions starts 30 minutes after the start of the liquid flow. The volume flow of the effluent gas is determined using the

bubble flow meter, and the composition of the gas is analyzed by the GC. Every hour henceforth this procedure is repeated, until the reaction is finished.

5.2.3 Aftermath

Each reaction runs for 4 – 4.5 hours. At the end of the reaction, the liquid flow is terminated, and again the online GC is used to monitor the composition profile of the product gas. When the concentrations of hydrogen and CO_2 have dropped below 1%, the reactor is purged with nitrogen, so no reactants or products remain inside. The feed tank with reaction mixture and the water-trap, which now contains an unconverted water/methanol mixture, are weighed again. The system is cooled down and the catalyst is removed from the reactor. The collected liquid from the water-trap is analyzed to determine concentration of methanol. All results from the experiments are combined in a mass balance to determine the performance of the reactions. The calculations are presented in appendix B.

5.3 Variation of parameters

There are various heterogeneous reactions for the production of hydrogen. Three of the more common reactions are the steam reforming of ethanol, the steam reforming of methanol and the water gas shift reaction. All three reaction systems were considered for the study. For these reactions different catalysts can be used, each promoting different reactions (see figure 19).
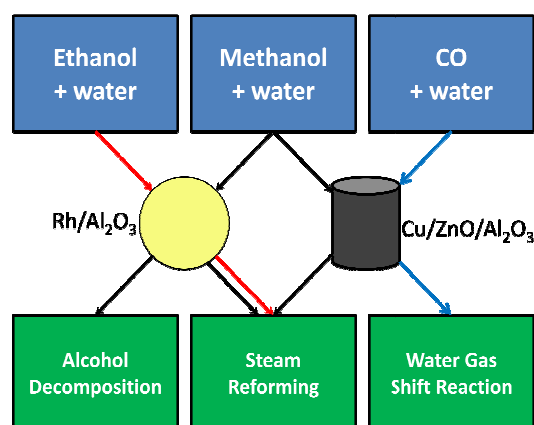

Figure 19. Scheme of reactions on different catalysts

The steam reforming of ethanol over the rhodium catalyst starts at approximately 600°C [55]. This temperature is too high for the FISO temperature sensors, which have a temperature range up to 250°C. However the ethanol steam reforming reaction over a nickel based catalyst shows significant ethanol conversion at temperatures as low as 250°C [34], however the high production of CO in the lower temperature range makes low temperature steam reforming of ethanol not suitable for the application in automotive industry, since CO is a poison for most hydrogen fuel cells. Furthermore the high production of methane means that a valuable amount of hydrogen is lost. Therefore this study is not focused on this reaction system. Due to the absence of a C-C bond in both CO and methanol, the water gas shift reaction and the steam reforming of methanol can be performed at lower temperatures, making these reactions more suitable for this study. Moreover less byproducts are expected in these reaction systems. Since the produced hydrogen is to be used in automotive applications, liquid fuels are desired. Therefore methanol steam reforming is the primary subject of this study.

The potential benefits coming up from application of microwave irradiation to the methanol steam reforming reaction are investigated over a range of operating conditions:

- Steam-carbon (S/C) ratio (1:1, 1.5:1 and 2:1)

- Temperature (130°C-210°C)

- Gas hourly space velocity (GHSV) (37,000 – 120,000 [h^{-1}]).

The study is focused on comparison of methanol conversion, product distribution and hydrogen yield and selectivity.

6.   Results and Discussion

In this study several reactions were performed to determine the effect of microwaves on the heterogeneously catalyzed production of hydrogen, with the abovementioned system (see section 5.3). Different catalysts were tested, as well as different reactants, in order to determine the most suitable system for this comparative study. Through these explorative experiments, it was found that the methanol steam reforming reaction over a Cu/ZnO/Al$_2$O$_3$ catalyst is the best system for this study. The results of these experiments are discussed in this chapter. The results of the temperature mapping during these reactions, which may explain different results between microwave and conductive heating, are presented as well. Since some experiments showed a mass consumption of >3%, while there was no evidence of any leaks, it was investigated whether coke formation had taken place on the catalyst, using a Scanning Electron Microscope (SEM) with element analysis.

6.1 Reaction systems

The first experiments comprised of methanol and ethanol steam reforming over a 1% Rh/Al$_2$O$_3$ catalyst under conductive heating conditions. The composition of the effluent gas is a good indication of the reaction specifics. In figures 20 and 21 the temporal concentration profiles of the effluent gas from steam reforming reactions of ethanol and methanol over the rhodium catalyst are presented respectively. A qualitative inspection shows that in ethanol steam reforming, even at high temperatures, a significant amount of methane is formed, while in methanol steam reforming the concentration of the methane was hardly detected. The high concentration of methane in the product mixture of the ethanol steam reforming reaction suggests that the reaction follows the pathway proposed by M. Verónica (equations 3.9 − 3.12) via the dehydrogenation of ethanol and subsequent reforming of methane into CO and CO$_2$.
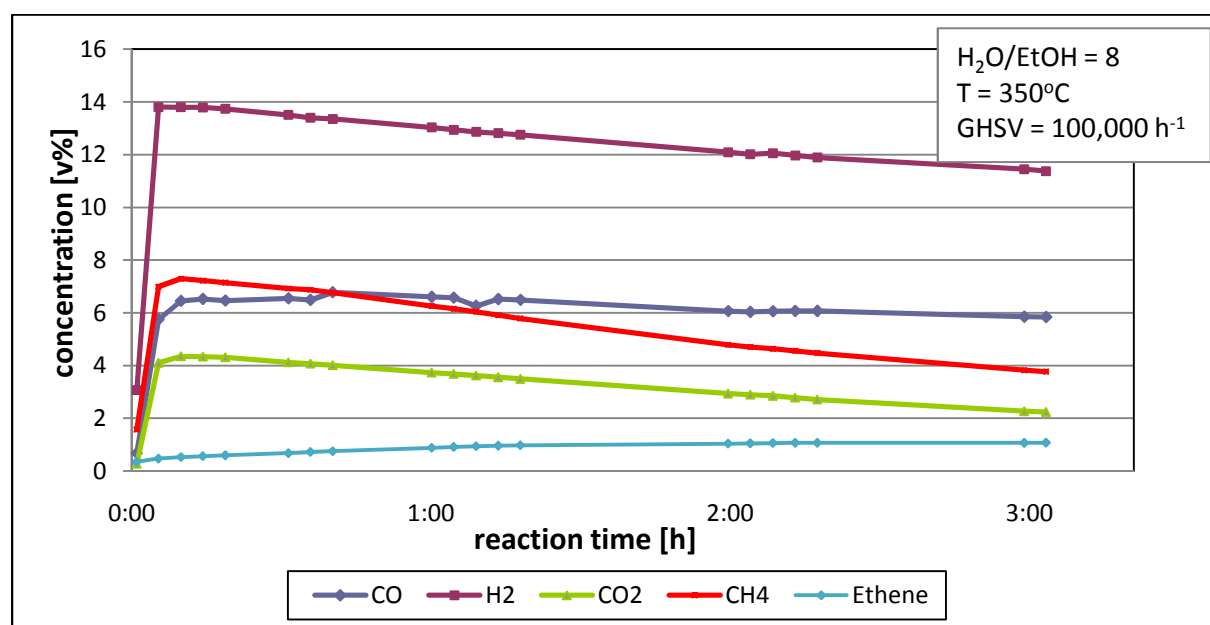

Figure 20. Temporal concentration profile of an ethanol steam reforming reaction over 2 grams of 1% Rh/Al$_2$O$_3$ under conductive heating conditions

However not all methane is consumed, which results in low production of the desired compounds. The same effect is observed in an ethanol reforming reaction at lower temperature. These results are consistent with the suggestion of Diagne et al. [21], that the rhodium catalyst facilitates dehydrogenation at lower temperatures, but production of methane is still present. Moreover with ethanol steam reforming a small concentration of ethylene was observed in the effluent. This means that under the reaction conditions used, the consumption reactions of ethylene (3.7 and 3.8) is not propagating fast enough to be neglected. Another difference between ethanol and methanol steam reforming over the rhodium catalyst is that all effluent concentrations decrease over time in case of ethanol steam reforming, whereas the concentrations assume a more or less constant value in methanol steam reforming. This can be an indication of deactivation taking place during ethanol steam reforming.
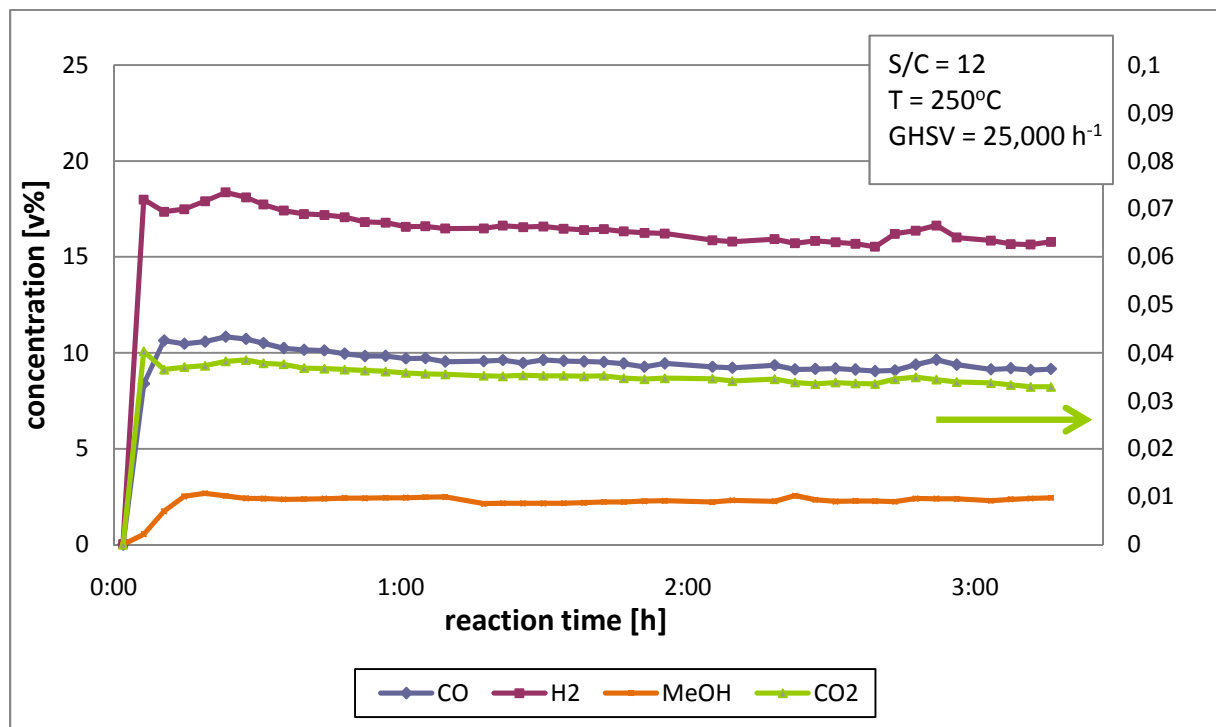

Figure 21. Temporal concentration profile of a methanol steam reforming reaction over 2 grams of Rh/Al$_2$O$_3$ under conductive heating conditions

Even though the effluent gas gives a good indication of processes taking place during the reaction, other parameters, like conversion, product yields and selectivity are important as well in determining the performance of the reaction system. In table 3 different reaction conditions are presented, which can illustrate the performance of the catalyst. In the first column the results of a high temperature ethanol steam reforming reaction over the rhodium catalyst are given. The conversion at 350°C is high, however the product yields are very far from their ideal values in column 3. The calculations of conversion of alcohols and yields of products are given in equations (6.1) and (6.2) respectively:

$$X_{alcohol} = \frac{mol\ alcohol\ in - mol\ alcohol\ out}{mol\ alcohol\ in} \cdot 100\%$$

(6.1)

$$Y_{product} = \frac{mol\ product\ formed}{mol\ alcohol\ in\ - mol\ alcohol\ out}$$

(6.2)

The low H_2 and CO_2 yields can be attributed to the production of methane and ethene, which both contain relatively large amounts of H_2 and CO_2. The second column provides a steam reforming reaction of ethanol as well, but at a temperature 100°C lower. The result is a significant decrease in conversion. Moreover the yields stay farther from the ideal case and a much higher selectivity towards CO is observed. Since 250°C is the upper limit for the temperature sensors needed for the microwave experiments, ethanol steam reforming over the rhodium catalyst is rejected for this study.

Instead methanol is used as reactant over the rhodium catalyst in the fourth column. In this experiment the conversion of methanol is low in comparison to that of ethanol, given the facts that a lower GHSV is maintained, and that methanol steam reforming is theoretically a process that takes place at lower temperatures. The fact that the yields of H_2 and CO_2 are closer to the theoretical level in column 6 can be attributed to the fact that only small amounts of methane by-product are formed. Because in the ethanol steam reforming experiments evidence of deactivation was observed in the form of a decrease in effluent concentrations, a high S/C ratio was used in this experiment. An excess steam was added to prevent deactivation of the catalyst. P.V. Mathure [56] found that a water/ethanol ratio of 12 gave a high conversion for ethanol steam reforming and low carbon deposition on the catalyst. This number was used for methanol as well. Another reason for adding more steam is because Le Châtelier's principle suggests that a higher S/C ratio improves the alcohol conversion.

Table 3. Reaction results over 1% Rh/Al_2O_3 catalyst. Y_{H2} is the production of hydrogen over the consumption of the alcohol. Methanol* is the reaction of methanol over a $Cu/ZnO/Al_2O_3$ catalyst.

Reactant	Ethanol		Ideal	Methanol	Methanol*	Ideal
T_{set} [°C]	350	250		250	250	
S/C	4	4		12	2	
GHSV [h^{-1}]	104,000	90,000		25,000	70,000	
$X_{alcohol}$ [%]	90	40		32	77	
Y_{H2}	1.33	0.78	6	1.3	2,64	3
Y_{CO}	0.66	0.82	0	0.66	0.02	0
Y_{CO2}	0.34	0.014	2	0.018	1.03	1
Y_{CH4}	0.65	0.77	0	0	0	0
CO/CO_2	2	58	0	37	0,019	0

The fact that the results from this reaction were still far from literature values led to a change of catalyst. In the fifth column presented in table 3 a $Cu/ZnO/Al_2O_3$ catalyst is used, depicted by Methanol*. Originally this catalyst is used for the water gas shift reaction, but is known to be active for methanol steam reforming, and has been developed for this purpose as well. The S/C ratio has been decreased to 2 for this catalyst, since deactivation of this catalyst is expected to be caused by thermal sintering, more than by coke formation. The high temperatures at which this would happen were not expected to be reached. The steam reforming of methanol over this catalyst has much higher conversion at the same temperature as the reforming over the rhodium catalyst, while the GHSV is much higher. Moreover the product yields are very close to the ideal values. No methane production is observed at all and the selectivity towards CO is very small.

Even though the methanol steam reforming has a small selectivity towards CO, it is not negligible. Since in literature it is suggested that the reaction pathway of methanol steam reforming often comprises the water gas shift reaction, this reaction was performed as well. The $Cu/ZnO/Al_2O_3$ catalyst being foremost a water gas shift catalyst, the influence of the S/C ratio on this reaction was investigated. This was done by varying both the water and the CO flow rates. In figure 22 the conversion is plotted versus the S/C ratio. It is evident that a higher S/C ratio increases the CO conversion, however this reaches a maximum value around a molar ratio of 3.
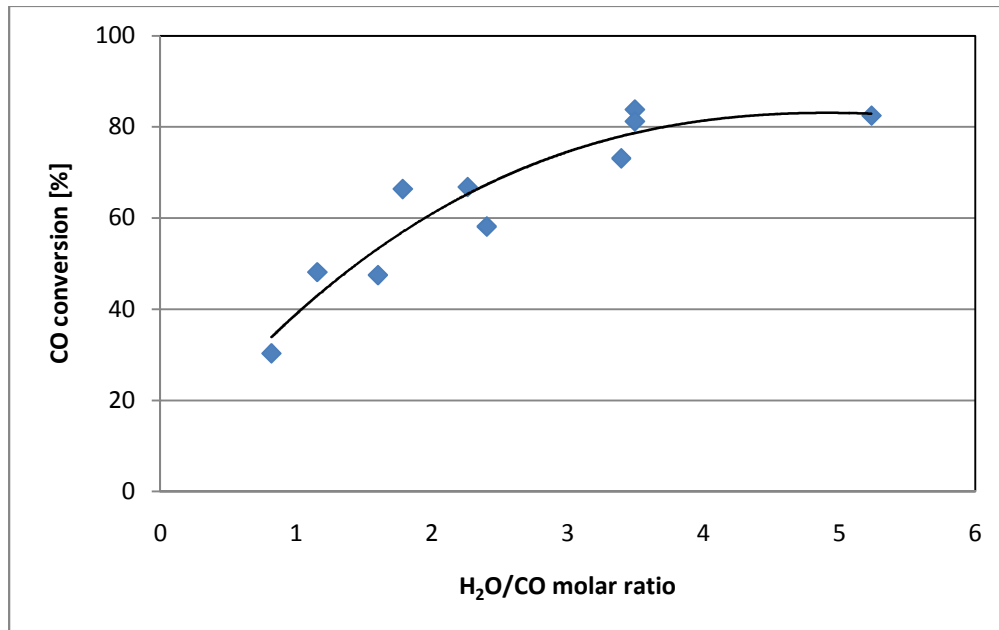

Figure 22. Conversion of CO in the water gas shift reaction as function of the H_2O/CO molar ratio in the feed

Figure 22 gives clear evidence of Le Châtelier's principle on the water gas shift reaction. For this equilibrium reaction it means that when more water is added to the feed, the equilibrium shifts towards the product side, increasing the conversion of CO. For all flow rates of CO, increased water flow yielded a higher conversion. Also for all flow rates of water it was observed that a lower CO flow rate yielded higher CO conversion, indicating that a higher H_2O/CO ratio indeed increases conversion of CO. The maximum conversion however, is approximately 80% at the reaction conditions. This means there is still a significant amount of CO in the effluent gas, yielding a poor hydrogen production per converted mol of CO. Therefore the water gas shift reaction is not investigated further.

Because of the many by-products formed in ethanol steam reforming and the incomplete conversion of CO in the water gas shift reaction the research is focused on the steam reforming of methanol over the $Cu/ZnO/Al_2O_3$ catalyst. The trend observed with the water gas shift data in figure 22 suggests that in case methanol steam reforming follows a reaction path in which CO is formed and subsequently mitigated by the water gas shift reaction, a higher S/C ratio should decrease the outlet concentration of CO. However for a Steam/CO ratio higher than 3 this effect is diminished.

6.2 Temperature control

The temperatures corresponding to the reaction results given in table 3 are the set-points for the temperature control. However, these set-point temperatures are different from the average temperature in the reactor, since the reactor used in this study was not isothermal. To determine an average reaction temperature the temperature of the catalytic bed was measured both in the center and on the wall of the reactor at a few different heights of the catalytic bed, and averaged according to the procedure described in section 5.1. For both heating methods the temperature measurement inside the reactor was done with FISO temperature sensors. The set-point for temperature control was measured at the bottom of the catalytic bed in the center of the reactor. This set-point temperature was linearly related to the average temperature of the catalytic bed, as illustrated in figure 23.
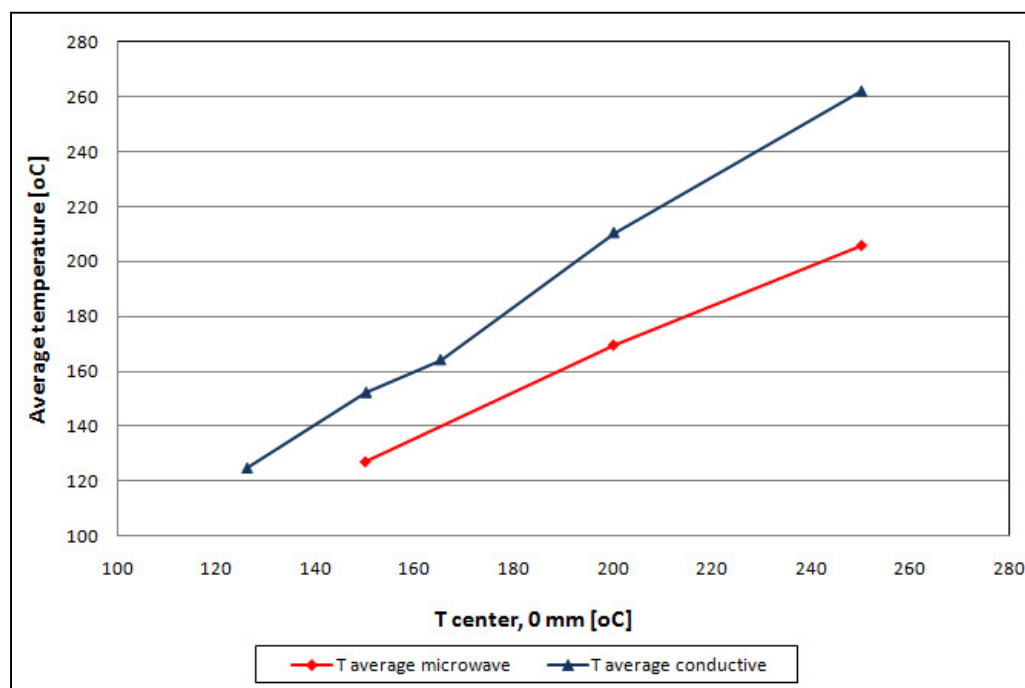

Figure 23. Average temperature inside the reactor related to the temperature at the center bottom of the catalyst bed

For microwave experiments the resulting average temperature is lower for a given set-point than for equivalent experiments conducted with electric heating element. This can be explained by the fact that the radial temperature gradients are the inverse in both cases, as can be seen by comparing figures 24 and 25, and that the microwave field is focused in the center of the reactor while surrounding is heated less efficient. Nevertheless, in both cases, when microwave and conductive heating is applied, the axial temperature gradients are enormous and significantly influence the overall reaction performance.
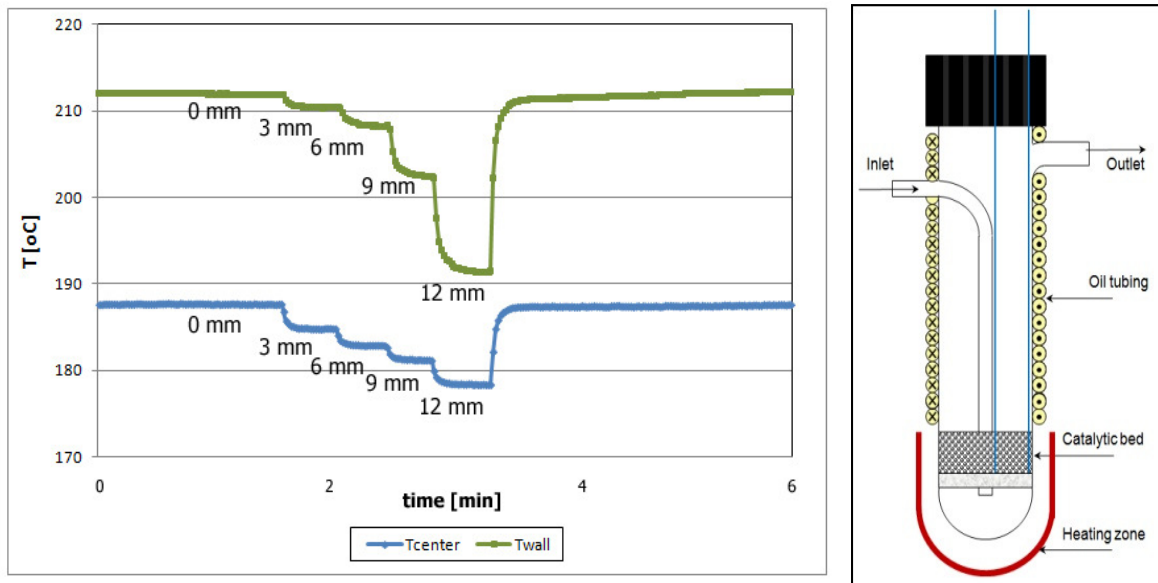
Figure 24. Temperature gradients along wall (green) and center (blue) of the reactor for conventional reaction. 0mm is on the bottom of the reactor (T_{ave} = 190°C, GHSV = 65,000 h^{-1}, S/C = 1.5)
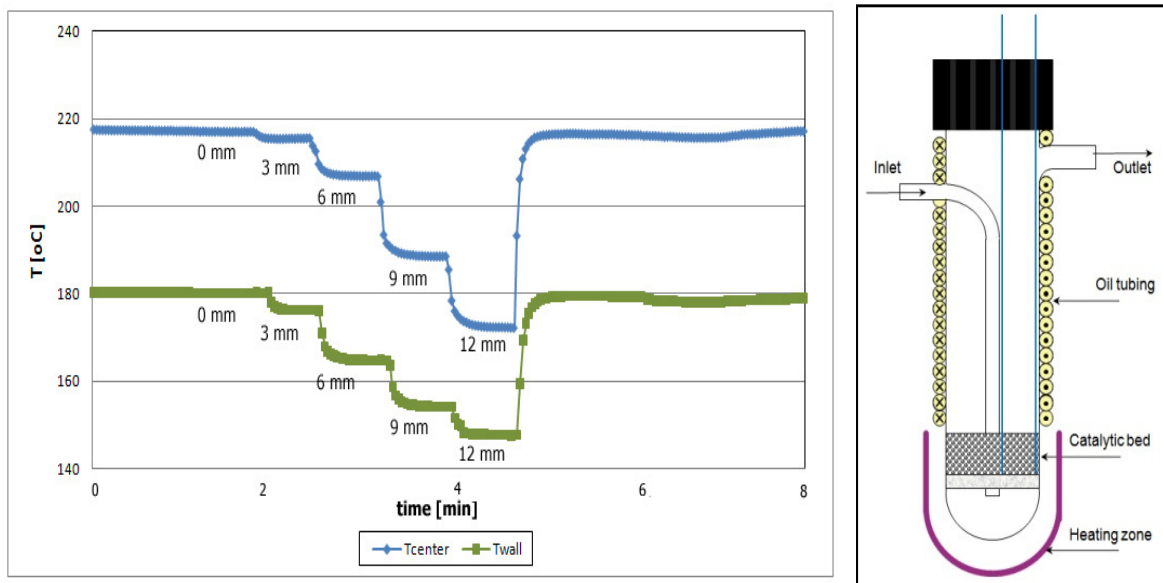

Figure 25. Temperature gradients along wall (green) and center (blue) of the reactor for a microwave reaction. 0 mm is on the bottom of the reactor (T_{ave} = 190°C, GHSV = 65,000 h^{-1}, S/C = 1.5)

This observation is consistent with the findings of Durka et al. [11]. Next to the axial temperature profiles, radial temperature profiles are observed, meaning that the temperature on the wall differs from the temperature in the center of the reactor. It can be seen (figures 24 and 25) that in microwave experiments the center has a higher temperature than the wall, while in conductive experiments this gradient is inverted. The calculation of the temperature gradients from the data of the temperature maps can be found in appendix A.

6.3 Steam reforming of methanol

6.3.1 Reduction

Before each reaction the catalyst is activated by reduction. For this purpose a 9% H_2 in N_2 mixture was used at a temperature of approximately 220°C. When the temperature of the reduction reached the set-point, the outlet concentration of hydrogen, and thus the consumption of hydrogen, changed accordingly (figure 26). The highest consumption rate of hydrogen corresponds to a temperature between 220°C and 230°C. During reduction the top of the reactor is kept at a temperature around 90°C in order to remove water which is formed from the reaction of hydrogen with the oxygen on the catalyst surface.
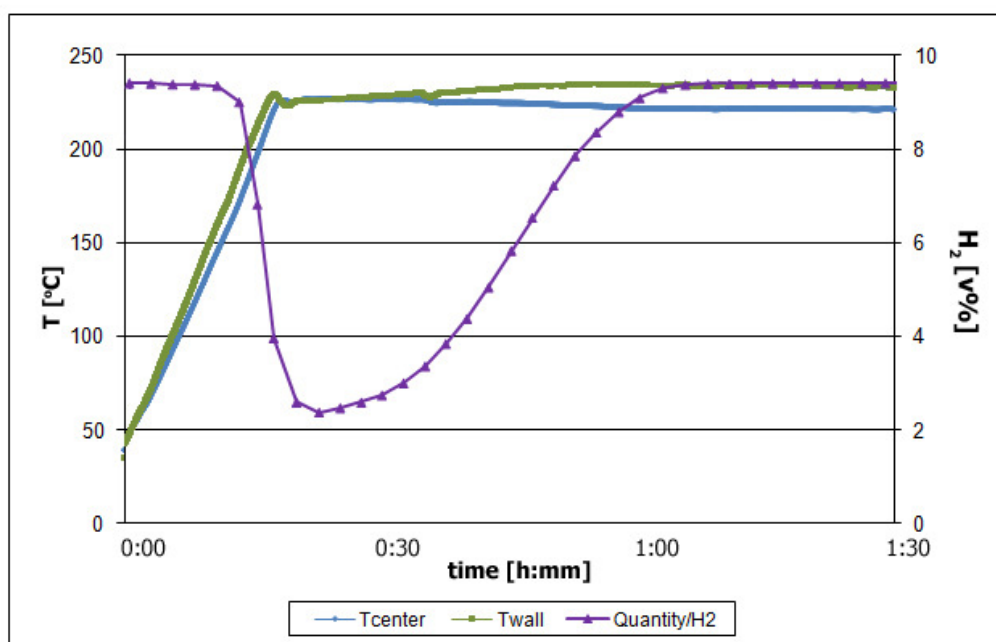

Figure 26. Temperature dependence of reduction efficiency.

6.3.2 Assessment of microwave influence

This study is focused on comparison of methanol conversion, product distribution and hydrogen yield and selectivity between microwave and conductive heating. The varied parameters were temperature, GHSV and S/C ratio. The temperature dependence of these parameters for experiments with intermediate GHSV (GHSV = 65,000 h^{-1}) and S/C ratio (S/C = 1.5) are presented in figures 27 and 28. The comparison of temperature dependence in reactions with higher S/C and lower GHSV can be found in appendix C1.

It is observed that reactions under microwave conditions have higher conversion and generally higher product yields than reactions under conductive heating. It may be noticed that the methanol conversion profile over reaction temperature of the microwave experiments has an irregular shape, which can be attributed to the fact that the graph is constructed of results from single experiments. During the study one of the experiments was repeated for a few times and showed that deviations of 5% are possible. Nevertheless, considering that all reactions can show this deviation, the difference between the conversion profiles for comparable heating modes has no consequence for the conclusions of this research.
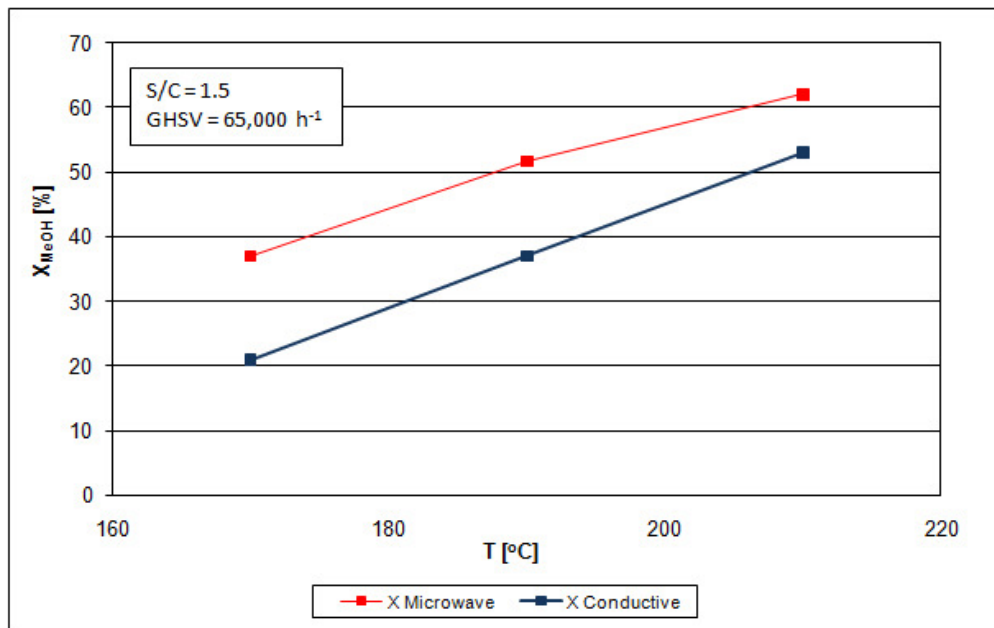
Figure 27. Conversion of methanol versus reaction temperature for microwave (red) and conductive (blue) heating (S/C = 1.5, GHSV = 65,000 h^{-1})

The combination of the conversion and product yield data supports the theory that a heterogeneously catalyzed reaction has higher performance under microwave irradiation due to temperature gradients on the micro scale, however the existence of the micro gradients has not been proven. The evidence arises mostly from the combination of methanol conversion and CO production, because both are temperature sensitive. Under microwave conditions the methanol conversion is consistently higher than with conductive heating. The same trend is observed for CO production. The water gas shift reaction, which consumes CO, is a mildly exothermic reaction, hence it will proceed at lower temperatures. This means that at lower temperatures the conversion of CO can be completed, while at higher temperatures it will decrease. The fact that both methanol conversion and CO production are higher under microwave conditions suggests that this is caused by a thermal effect. However since the macro temperature gradients are accounted for in the average temperature, it is likely that the thermal effect has a micro scale character which cannot be detected by the applied method.

Although conversion and product yields are higher in microwave conditions, the product yields also show a downside to operation in microwave conditions. in figure 28 the production of H_2 and CO_2 increases with increasing temperature, until they reach their maxima near 190°C. The CO production however, increases with temperature as well. In case of conductive heating only trace amounts of CO are produced below 210°C. Since the hydrogen and CO_2 yields are maxed out at 190°C, a high H_2 yield is not necessarily compromised by the production of CO. Under microwave conditions the H_2 and CO_2 yields find their maximum values around 190°C as well. However the CO production commences already at lower temperatures, yielding a trade-off between high H_2 yield and CO formation. For the application of the reforming reaction to produce hydrogen for fuel cells the production of CO is a major drawback, since it is a poison for most fuel cells. Therefore a separation step will be needed in the application when CO is produced. However it must be noticed that at 190°C the methanol conversion is only 37% under conductive heating, which suggests that in an application a reflux might be necessary to ensure all fuel is consumed.
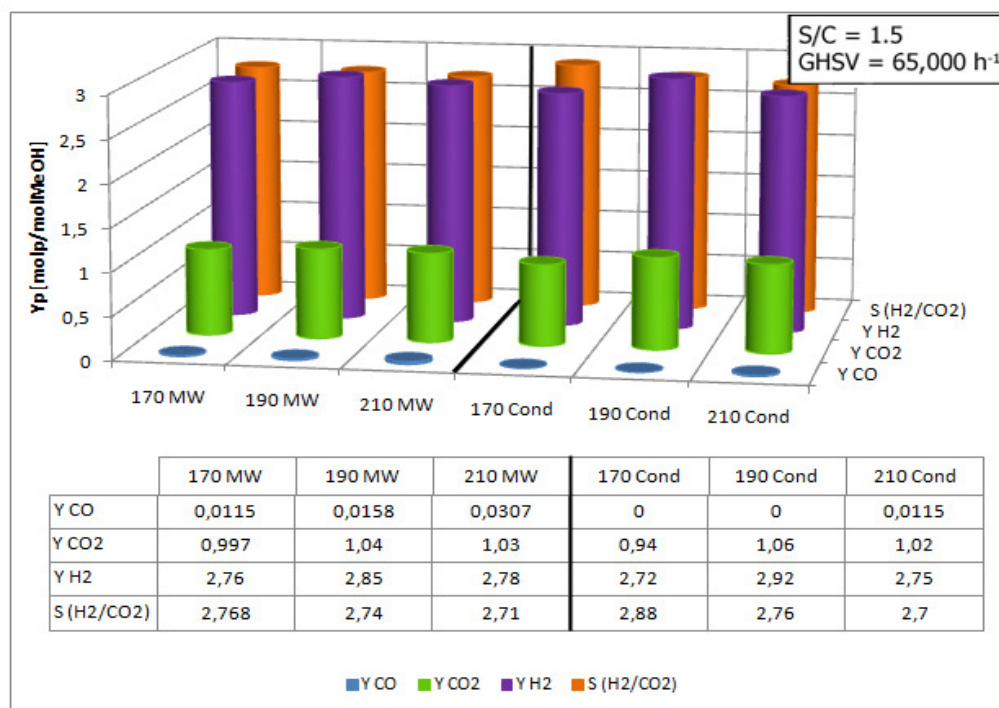
	170 MW	190 MW	210 MW	170 Cond	190 Cond	210 Cond
Y CO	0,0115	0,0158	0,0307	0	0	0,0115
Y CO2	0,997	1,04	1,03	0,94	1,06	1,02
Y H2	2,76	2,85	2,78	2,72	2,92	2,75
S (H2/CO2)	2,768	2,74	2,71	2,88	2,76	2,7

Figure 28. H$_2$ (purple), CO$_2$ (green) and CO (blue) yields and H$_2$ selectivity (orange) dependence on temperature for microwave (l) and conductive (r) heating (S/C = 1.5, GHSV = 65,000 h^{-1})

From Figure 28 it follows that neither in microwave nor conductive experiments the theoretical maximum hydrogen yield of 3 molH$_2$/molMeOH was reached. The figure also shows that the theoretically ideal values for CO and CO$_2$ of 0 and 1 respectively, have been reached. The selectivity of hydrogen over carbon dioxide (S (H$_2$/CO$_2$)) in the theoretical ideal case has a value of 3. At lower temperatures the observed selectivity is higher than this theoretical value. This is most likely caused by a carbon loss to the catalyst. At higher temperatures the deficiency of hydrogen is more profound, which shows from a decreasing selectivity. The fact that the effluent at regular temperatures was short only of hydrogen was a major point of concern. This hydrogen deficiency has been apparent from the very first experiments. Although the setup has been developed to ensure that hydrogen cannot escape via connections from the setup and despite of using a gas detector and soap water to proof leak tightness of the setup during experiments, the problem with hydrogen loss was not solved.

Chen et al. [42] found similar maximum values for the hydrogen yield. They attribute this to the fact that the water gas shift reaction is taking place, which reduces the hydrogen concentration. However in our experiments the decrease of hydrogen yield cannot be explained by this theory, because it was also found to be low in experiments where no CO formation was observed. Moreover the production of CO in all experiments was not high enough to account for the corresponding hydrogen loss. A possible explanation is that the Cu^0/Cu^I active sites have been found to change in oxidation state, resulting in undesired changes in selectivity [28]. Support for this theory was found in the temporal yield profiles. In the mass balance (appendix B) for each hourly measurement the conversion, yields and selectivities were determined. For each reaction it was evident that the CO$_2$ and H$_2$ yields decreased over time, as is illustrated in Figure 29. It is visible that the yields after 30 minutes are higher in conductive heating, but after 1 hour the microwave shows higher product yields constantly. This can be the result of the temperature overshoot in the startup of conductive heating. The

temperature overshoot is due to the slow response intrinsic to conductive heating. The overshoot is avoided in microwave heating due to the fast response of the system and manual temperature control in this setup. The temperature overshoot is directly visible in the composition of the effluent gas, which is shown in Appendix C2.
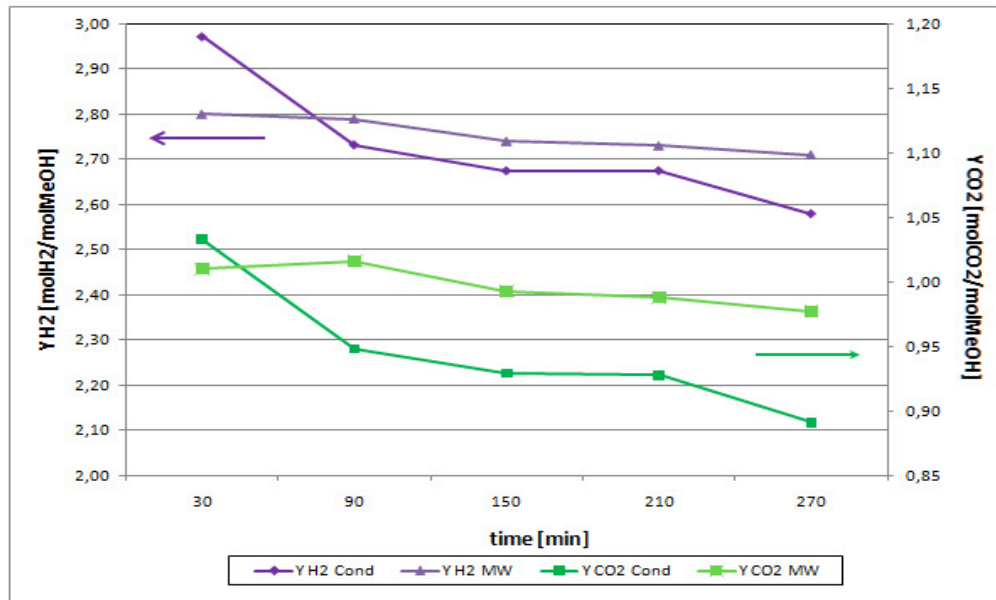

Figure 29. Temporal yield profiles of H_2 (purple, axis 1) and CO_2 (green, axis 2) in microwave and conductive heating (S/C = 1.5, T = 170°C, GHSV = 65,000 h[1])

The influence of GHSV on the reaction specifics is illustrated in figures 30 and 31. For increased GHSV the conversion decreases, what is in agreement with the theoretically expected result. Due to a lower residence time, the reaction cannot proceed until full conversion is reached. The same effect is observed for the H_2 and CO_2 yields, however the CO yield is not structurally affected. The selectivity of hydrogen over carbon dioxide increases for increasing GHSV in microwave conditions, however in conductive conditions no structural effect is observed.
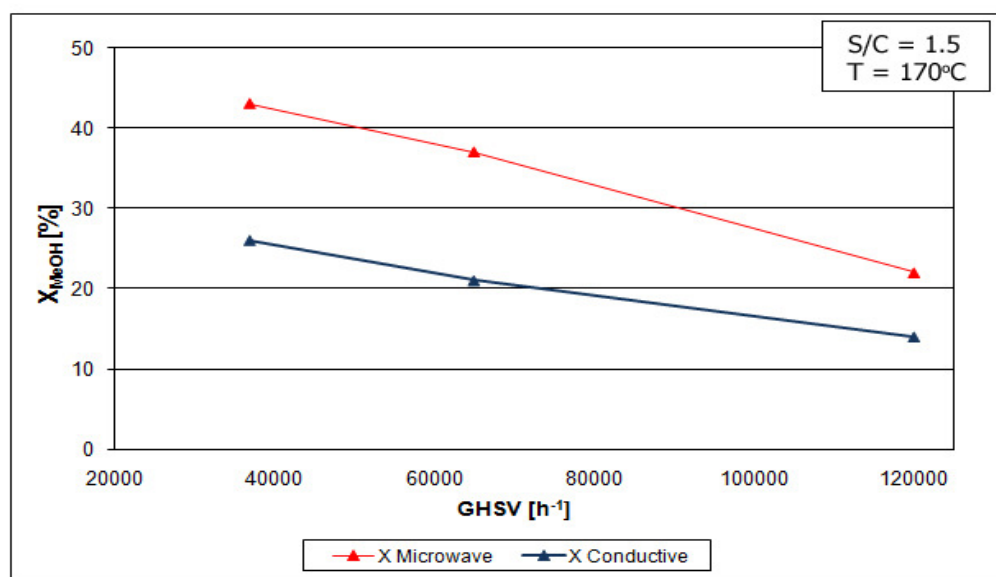

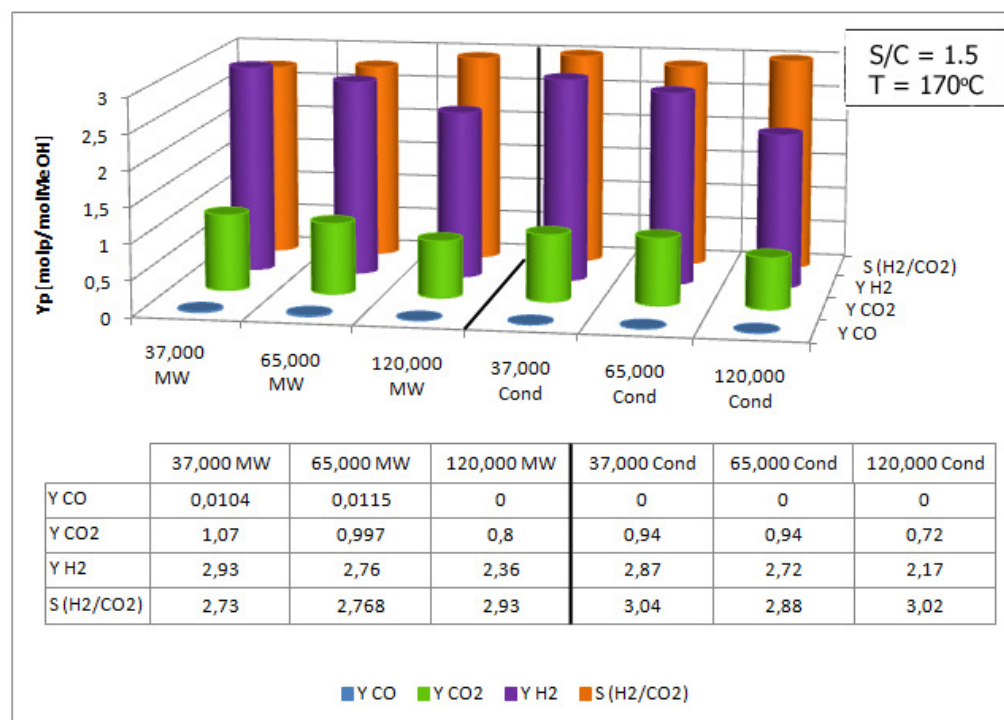**Figure 30. Conversion of methanol versus GHSV for microwave (red) and conductive (blue) heating (S/C = 1.5, T = 170°C)**

	37,000 MW	65,000 MW	120,000 MW	37,000 Cond	65,000 Cond	120,000 Cond
Y CO	0,0104	0,0115	0	0	0	0
Y CO2	1,07	0,997	0,8	0,94	0,94	0,72
Y H2	2,93	2,76	2,36	2,87	2,72	2,17
S (H2/CO2)	2,73	2,768	2,93	3,04	2,88	3,02

Figure 31. H$_2$ (purple), CO$_2$ (green) and CO (blue) yields and H$_2$ selectivity (orange) dependence on GHSV for microwave (l) and conductive (r) heating (S/C = 1.5, T = 170°C)

The influence of the steam-to-carbon ratio on the conversion of methanol was investigated as well. Usually the microwave heated experiments showed similar trends to the conductive heated experiments, in this case the rule is not obeyed (figure 32). For the experiments with conductive heating conversion of methanol decreases for increasing S/C ratio, while it increases for experiments under microwave heating. Both Le Châtelier's principle and the thermodynamic profile presented by Chen et al. [42] suggest that the methanol conversion should increase for increasing S/C ratio. However figure 32 clearly shows a minor decline of methanol conversion for the conductive heating experiments. This effect is opposite to the results of Chen, who also investigated influence of microwaves on the methanol steam reforming and reported a decrease of conversion for higher S/C ratio under microwave radiation instead of under conductive conditions. The authors suggest that the inverted conversion profile is caused by the fact that water is a good microwave absorber, which results in the fact that the microwave energy is not used for the reaction, but for the heating of water instead. However since the inverse profile in this study appears in conductive experiments, this explanation is not valid.

The difference in conversion was only a few percent, which suggests that the observed effect can be caused by the fact that only single experiments were performed, and that the conversion can differ up to a few percents in a reproduced result. However the same trend is observed in experiments at lower GHSV (37,000 h^{-1}), where the effect is even more significant (figure 33). This means that the chance of measurement error being responsible for the negative trend is very small.
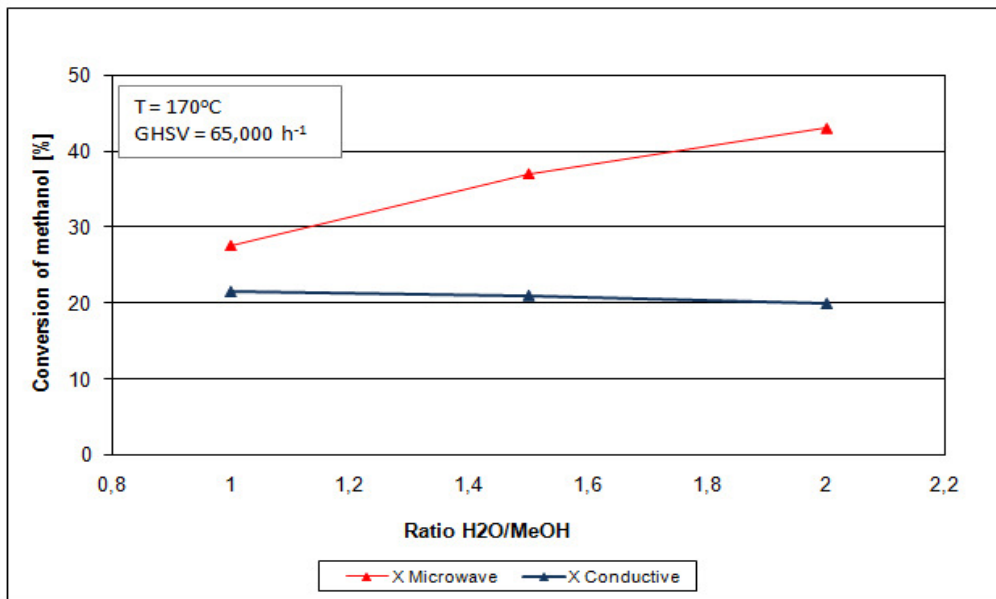
Figure 32. Conversion of methanol versus S/C ratio for microwave (red) and conductive (blue) heating (T = 170°C, GHSV = 65,000 h⁻¹)
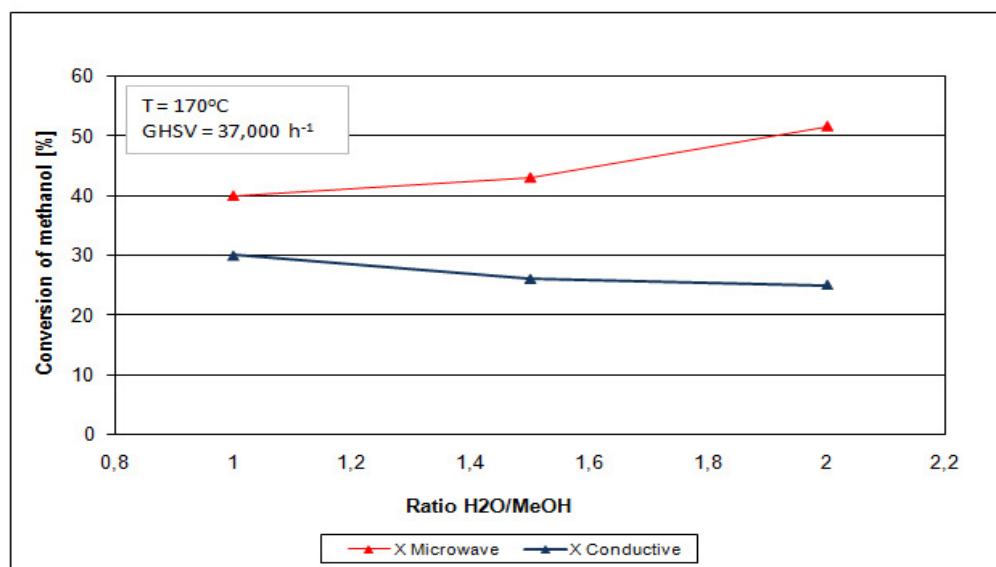

Figure 33. Conversion of methanol versus S/C ratio for microwave (red) and conductive (blue) heating (T = 170°C, GHSV = 37,000 h⁻¹)

The influence of S/C ratio on the products yields for both heating modes is also not negligible. In case of experiments performed with microwave heating a change of S/C ratio from 1 to 1.5 results in a slight increase of hydrogen yield, while if the S/C ratio is changed from 1.5 to 2 it decreases as it is illustrated in figure 34. The same hydrogen yield profile was observed in experiments performed with an external heating element, however the effect between 1 and 1.5 is more profound. The CO_2 yield in conductive experiments shows this profile as well, but in microwave experiments the CO_2 yield is almost unaffected. The effect of S/C ratio has a significant effect on the CO yield. This decreases for increasing ratio over the entire range of ratios, which is expected from Le Châtelier's principle which states that water drives the conversion of CO into hydrogen and CO_2.
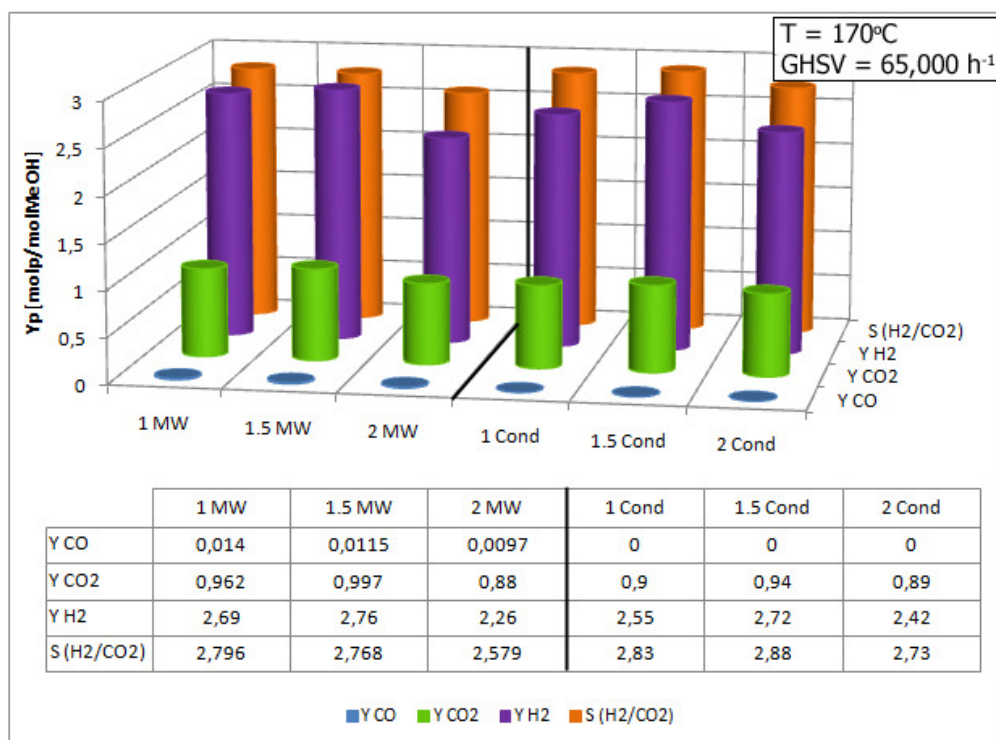
Figure 34. H$_2$ (purple), CO$_2$ (green) and CO (blue) yields and H$_2$ selectivity (orange) dependence on S/C ratio for microwave (l) and conductive (r) heating (T = 170°C , GHSV = 65,000 h^{-1})

	1 MW	1.5 MW	2 MW	1 Cond	1.5 Cond	2 Cond
Y CO	0,014	0,0115	0,0097	0	0	0
Y CO2	0,962	0,997	0,88	0,9	0,94	0,89
Y H2	2,69	2,76	2,26	2,55	2,72	2,42
S (H2/CO2)	2,796	2,768	2,579	2,83	2,88	2,73

6.3.3 Catalyst analysis

Some reactions showed a mass consumption of >3%, therefore the catalyst was analyzed to investigate whether coke formation was taking place. The analysis was performed by a SEM with element analysis. Results of fresh catalyst and of catalysts after reaction are compared by visual inspection (see figure 35). For the fresh catalyst and a catalyst used in a reaction (Microwave, T = 230°C, GHSV = 140,000 h^{-1}, S/C = 2) elemental analysis was performed. More detailed results of the element analysis can be found in appendix D. From the atom% numbers for the metal species in combination with the theoretical oxygen load per atom of the oxidized form, a theoretical number of oxygen atoms could be derived (see table 4).

Table 4. Atom percentage of components on the catalyst surface. 'Exp. Fresh' and 'Exp. Reacted' stand for the oxygen percentages expected on the fresh catalyst and the used catalyst respectively, '+/-' gives the difference between the real value and the expected.

Atom%	After reaction		Fresh catalyst	
	Point 2	Point 3	Point 1	Point 4
C	9.84	8.75	6.16	5.03
Al	13.34	14.97	11.18	11.75
Cu	21.49	19.58	17.95	19.38
Zn	16.78	16.58	16.36	15.36
O	38.54	40.14	48.35	48.47
Exp. Fresh			51.08	52.37
Exp. Reacted	36.79	39.04		
+/- [%]	4.76	2.83	-5.65	-8.04

The comparison of the expected values with the measured atom% of oxygen provided evidence that during reduction only the Cu sites are reduced, and that the ZnO and Al_2O_3 remain intact. According to the numbers not all copper sites are reduced (approximately 7% of the copper sites are not reduced) however, it is considered as re-oxidation of catalyst which occurred between reduction process and analysis.

The fresh catalyst contains a small amount of carbon as well, which is evident from table 1. The atom% numbers of carbon on the fresh and spent catalyst samples suggest that there is a small increase in carbon load due to reaction. However these numbers represent very local surface compositions, hence they cannot be used in order to determine whether coke formation has taken place. The assessment of carbon deposition was therefore done by visible inspection of the SEM pictures, of which an example is given in figure 35.
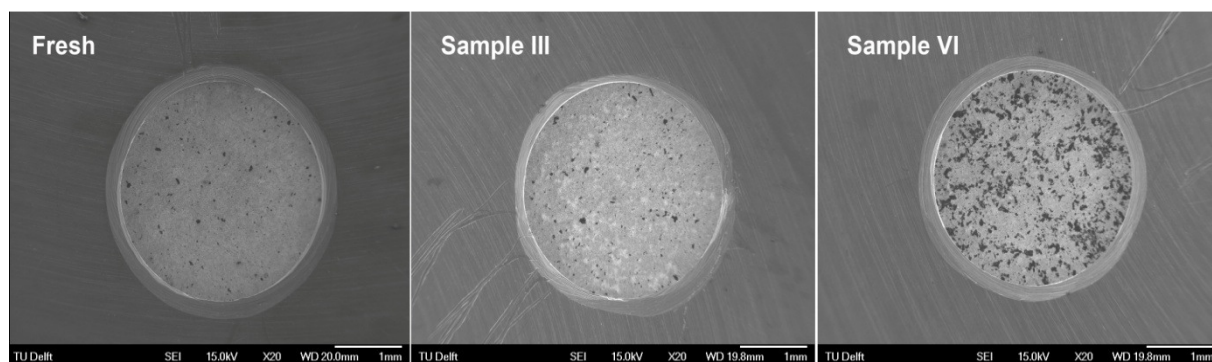

Figure 35. SEM pictures of catalyst particles with magnification x20. Sample III is taken after a reaction under microwave conditions (T = 170°C, GHSV = 37,000 h⁻¹), Sample VI is taken after a reaction under conductive heating (T = 125°C, GHSV = 33,000 h⁻¹)

The black spots on the catalyst surfaces are composed of carbon, which was determined by an elemental analysis of one of these spots. Details of this analysis can be found in appendix D. A comparison of the number density of these spots could therefore be used to assess whether any significant carbon deposition has taken place.

As it can be seen on figure 35 the fresh catalyst already contain small amount of carbon what in fact is due to its composition. A comparison of the three samples shows that in the reaction under microwave conditions (T = 170°C, GHSV = 37,000 h⁻¹, S/C = 2) the carbon deposition during reaction can be neglected, but that during the conductive experiment at T = 125°C (GHSV = 33,000 h⁻¹, S/C = 2) a lot of carbon was deposited on the catalyst. It cannot be stated however, that microwave irradiation cuts back carbon deposition. Even though the GHSVs of these experiments are relatively similar, the temperature in the microwave experiment is much higher than that in the conductive experiment. In other pictures from reactions at high temperatures no significant carbon deposition is observed, regardless of the heating method. This suggests that it is purely the low temperature which is the cause of the carbon deposition.

This theory is consistent with the theory that methanol steam reforming follows a reaction pathway with CO as intermediate product. Disproportionation of CO can take place forming CO_2 and carbon black, according to the Boudouard reaction [57]:

$$2\,CO \rightleftarrows CO_2 + C \qquad \Delta H^0_{298} = -173 \text{ kJ mol}^{-1} \qquad \textbf{(6.3)}$$

On the catalyst surface the CO concentration is high due to the decomposition reaction of methanol. At the active sites the Boudouard reaction (6.3) competes with the water gas shift reaction (3.1). Because the water gas shift reaction is only mildly exothermic, it will prevail over the Boudouard reaction at higher temperatures, but at lower temperatures the highly exothermic Boudouard reaction will gain the upper hand, resulting in carbon deposition and deactivation of the catalyst. Figure 36 (r) presents a close-up of a carbon particle on the catalyst surface.
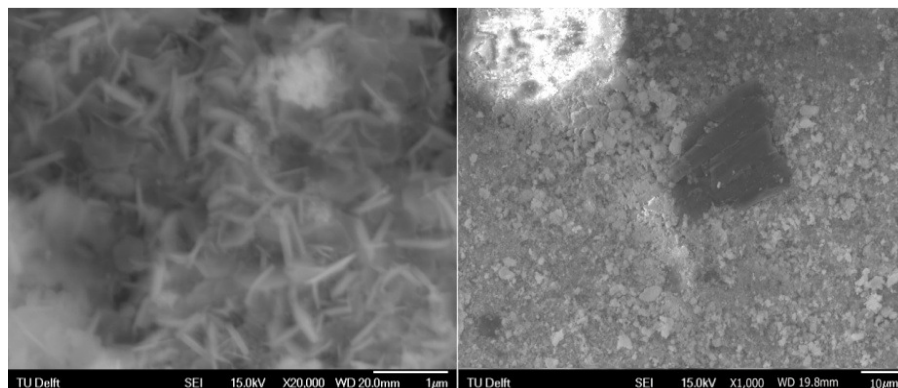

Figure 36. Close-up pictures of the catalyst surface. On the left the porous structure of the catalyst is visible with a magnification of x20,000. On the right the black spot is a carbon particle, and the white spot is nearly pure alumina with only little active sites (see appendix D)

In figure 36 two close-ups of the catalyst surface are presented. No specifics are given about the catalysts of these pictures, because the structures of both pictures were present on all catalysts. On the left side, the magnification is x20,000, which shows that the structure of the catalyst is very porous, yielding a high specific surface area. The needles that are visible on this size were determined to contain both support and catalytically active material. On the right side the magnification is x1,000. Apart from the general surface of the catalyst, two significantly different locations can be seen. The black location is a carbon particle deposited on the surface, and the white spot is nearly pure alumina with only small amounts of catalytically active material. These compositions were determined by elemental analysis (see appendix D).

6.4 Application potential

The potential for the application of microwave assisted steam reforming for hydrogen production depends on various properties; the fuel is preferable a liquid, to provide easy storage and handling and the conversion and hydrogen yield should be high using low energy input, while keeping the CO production at a minimum. Therefore the methanol steam reforming is a suitable reaction. Methanol and water are very well miscible, providing a liquid fuel. Moreover the hydrogen content in this system is high and full conversion can be reached at relatively low temperatures. The production of CO, which is a poison for most hydrogen fuel cells, is restricted to trace amounts.

The application of microwave heating for the methanol steam reforming reaction has several advantages. The conversion and the product yields are higher at the same bulk temperatures like in conventionally heated reaction. However the CO production is not limited to trace amounts under microwave heating. Therefore the choice must be made whether a conductive heating system is used, with a reflux to ensure full use of the fuel, or a microwave heating system is used, in which case a separation step is needed after the reformer.

Another important issue is the low energy requirement of the system. Although the study was not focused on the energy consumption issue and no specific calculations have been made, it was observed that for most of the microwave-assisted reactions the microwave power applied to the cavity was in a range of 7-11W. However, this low power input does not reflect the overall energy consumption which in this case was even 15 times higher. Therefore, as long as microwave generators have low energy efficiency the application of microwave assisted methanol steam reforming is not economically feasible. Moreover safety and control systems may be more complicated for microwave ovens than for conventional heating methods, resulting in further implications. This means that even though microwave heating enhances the reaction, a lot more research, not only on reaction engineering or chemistry, is needed before the microwave system will be suitable for automotive applications.

7. Conclusions

The aim of this study was to investigate the microwave effect on heterogeneous reactions, specifically on the methanol steam reforming reaction for the production of hydrogen for automotive application. The experimental results were compared in terms of the methanol conversion and the product yields. The performances of reactions carried out under conductive heating and microwave heating are compared, with the variation of the following parameters: steam-carbon (S/C) ratio (1:1, 1:1.5 and 1:2), temperature (130°C-210°C), and gas hourly space velocity (GHSV) (37,000 – 120,000 [h^{-1}]).

The reactions carried out under microwave heating out-performed the reactions carried out under conductive heating in terms of methanol conversion and hydrogen yield. However the CO yield was higher under microwave conditions, which is undesirable since the CO is a poison for most hydrogen fuel cells. The higher CO formation suggests that temperature gradients on the micro scale are the cause for the higher conversion and hydrogen yields, since the macro temperature gradients are taken into consideration. However the existence of these micro temperature gradients was not positively confirmed, due to the local, nano-scale nature of the phenomena.

During the investigation of the microwave effect on the reforming reaction more reaction specifics and operation challenges were encountered. During reactions under microwave irradiation the top of the reactor had to be heated with silicon oil, flowing in silicon tubes around the reactor, in order to prevent condensation of unconverted reactants. This problem was caused by the fact that the microwave cavity was relatively high compared to the limited microwave heating zone. It was found that $Cu/ZnO/Al_2O_3$ is indeed a good catalyst for both the steam reforming of methanol and the water gas shift reaction at low temperatures. The formation of CO at higher temperatures was evidence for the fact that the pathway of methanol steam reforming over this copper catalyst proceeds via a CO intermediate, which is consumed by the water gas shift reaction. The theory of CO formation was supported by the fact that at low temperatures carbon deposition was observed on the catalyst, which may be the result of the Boudouard reaction.

Special consideration was paid to the temperature mapping inside the catalytic bed. High radial and axial temperature gradients were observed over the catalyst bed for both heating methods, however the radial gradients being the opposite of each other. From these temperature gradients an average reaction temperature was constructed to aid the comparison of the heating methods.

The dependence of conversion on the varied parameters is found to be similar for both microwave and conductive heating modes, with the microwave heating obtaining higher results. For increasing temperatures the conversion increases, aiding, yet not confirming the theory of the existence of micro temperature gradients. An increase in GHSV yields a decrease in conversion, as the reaction has less time to achieve completion. An increase in S/C ratio provided higher conversion in microwave conditions, which is in accordance with Le Châtelier's principle. However for conductive experiments the conversion has been shown to decrease. The cause of this is unknown at the present time.

The product yields were differently related to the varied parameters. Both CO_2 and H_2 yields increased for increasing temperature and decreasing GHSV. The S/C ratio had no direct relation with the H_2 and CO_2 yields. The CO yield increased with increasing temperature, as the water gas shift reaction is a slightly exothermic reaction. The influence of the GHSV and the S/C ratio on the yield of CO could not be established with certainty, because the concentrations were either below or very close to the detection limit of the analytical equipment.

For the most part the H_2 yield did not reach the theoretically ideal value, whereas the CO_2 and CO yields did. In literature similar trends were observed and no valid explanation has been found. The suggestion that the reversed water gas shift reaction would decrease the production of hydrogen was dismissed since the amount of CO produced in such case was far too low to be of significant influence on the hydrogen concentration.

Furthermore the implementation of a microwave enhanced methanol steam reformer for hydrogen production in automotive applications depends on the energy requirement of the entire system. Whereas the conversion in microwave assisted reactions was significantly higher than that in conductive reactions, the total energy requirement may yet be higher. The heat input is assumed to be lower in case of microwave heating, however the safety and control systems can be more complicated and energy consuming. As usually, a trade-off between using conductive or microwave heating has to be found; in reactions carried out under conductive heating conditions the hydrogen yield can reach its maximum while no CO is produced, but at the cost of low conversion. This means a methanol reflux would have to be added to the system. In the microwave assisted reaction the conversion is higher, but CO formation is not avoided, which gives rise to the need of a separation step.

8.   Recommendations

Although the research findings positively answer to the aim of the study, more work is to be done to finalize the reaction results and to obtain a real understanding of the microwave effect on the steam reforming of methanol.

The experimental setup was not ideally optimized. Use of silicon oil in order to prevent condensation of unconverted reactants by keeping the top of the reactor warm, results in a more complicated catalyst exchanging procedure and startup of the system. Moreover the temperature gradients were very large over the catalytic bed. Therefore it is advised that a setup is designed specifically for this reaction, with the aim of reducing the risk of condensation and temperature gradients inside the reactor. It is encouraged to apply a different or additional temperature measurement technique which allows for detection of possible temperature gradients on the micro scale.

The decreasing conversion at higher S/C ratio in conductive experiments is inconsistent with theory, therefore the cause of this effect should be investigated. Moreover it is advised to perform an extra set of reactions at higher temperatures, to determine at what temperatures 100% conversion can be reached. Special attention for the yield of CO versus the yield of H_2 may help in determining the extent to which the drawback of higher CO production is significant. Moreover for the most part the hydrogen yield has been shown to be lower than expected. No explanation has yet been given which accounts for the magnitude of the hydrogen losses. It is encouraged to determine the cause of the hydrogen deficiency.

When implementing a system using methanol steam reforming for hydrogen supply it must be determined whether a reflux of methanol is preferred over a separation step, before the choice is made for a system with or without microwave enhancement. However beside the trade-off between CO production and methanol conversion the energy requirement of the system is of influence as well. Therefore it is advised that the energy input into the reactor necessary to achieve the desired reaction results is investigated for both heating methods. Also an investigation into the energy requirements of the safety and control systems of both optimized systems is advised, in order to gain a better knowledge of the actual energy efficiency of microwave and conductive heating.

Bibliography

[1] Kreith, F., and West, R. E., 2003, ''Gauging Efficiency, Well to Wheel,'' *Mechanical Engineering Power* 2003, supplement to Mechanical Engineering magazine

[2] Heffernan, V. 2002, "Storing Hydrogen Safely," *NICKEL*, Vol. 18, no. 1, October 2002

[3] Wang, Y, et al., 2002, "Methane and Methanol steam reforming to produce hydrogen using catalytic microchannel reactors," *Fuel Chemistry Division Preprints* 2002, 47(1), 115

[4] Chemat-Djenni, Z., Hamada, B., and Chemat, F., 2007, "*Atmospheric* Pressure Microwave Assisted Heterogeneous Catalytic reactions," *Molecules* 2007, 12, 1399-1409

[5] Buchenhorst, D., Kopinke, F.D., Roland, U., 2006, "Radiowellenerwärmung von Adsorbenzien und Katalysatoren – Teil 2: Untersuchungen zur selectiven Erwärmung von Katalysatoren," *Chemie Ingenieur Technik* 2006, 78, no. 5

[6] Zhang, X., Hayward, D.O., 2006, "Applications of microwave dielectric heating in environment-related heterogeneous gas-phase catalytic systems," *Inorganica Chimica Acta* 359 (2006), 3421-3433

[7] Sparkmuseum, "The Discovery of Radio Waves – 1888", *Sparkmuseum*, http://www.sparkmuseum.com/BOOK_HERTZ.HTM, Last visited; April 22nd, 2010

[8] Encyclopedia Brittanica, "Hertz: Radio-wave experiments", *eb.com*, http://www.brittanica.com/EBchecked/topic/1262240/radio-technology/25129/Hertz-radio-wave-experiments, last visited; April 28th, 2010

[9] Hayes, B.L., "Microwave Synthesis: Chemistry at the Speed of Light*", CEM Publishing*, Matthews, NC 2002

[10] Bobolicu, G., 2008, "History of the Microwave Oven, The evolution of an alternative way of cooking", *Softpedia*, 11 October 2008, http://gadgets.softpedia.com/news/History-of-the-Microwave-Oven-042-01.html, last visited; April 28th, 2010

[11] Durka, T., van Gerven, T., Stankiewicz, A.I., "Microwaves in Hetererogeneous Gas-Phase Catalysis: Experimental and Numerical Approaches", *Chem. Eng. Technol.* (2009) No. 9, 1301-1312

[12] CEM, 2009, "Microwave Chemistry: How it all Works", *CEM Publishing,* 2009, http://www.cem.com, last visited; April 27th, 2010

[13] Blattenberger, K., "Dielectric Constant, Strength & Loss Tangent, *RF Cafe,* 1989*,* http://www.rfcafe.com/references/electrical/dielectric-constants-strengths.htm, last visited; April 22nd, 2010

[14] Speight, J.G., 2003, in "Perry's standard tables and formulas for chemical engineers", *The McGraw-Hill Professional,* April 1st, 2003

[15] Manoj Gupta and Eugene Wong Wai Leong, 2007, in "Microwaves and Metals", *John Wiley & Sons,* New York, Nov 2nd, 2007

[16] Callaghan, C.A., 2006, "Kinetics and Catalysis of the Water-Gas-Shift Reaction: A Microkinetic and Graph Theoretic Approach*", Worcester Polytechnic Institute*, Department of Chemical Engineering, March 31, 2006

[17] Perry, R.H., Green, D., 1984, "Perry's Chemical Engineers' Handbook*", McGraw-Hill Book Company*, 6th edition, 1984, Table 3-120, page 3-98

[18] Bi, J., 2007, "Novel zirconia-supported catalysts for low-temperature oxidative steam reforming of ethanol", *Catalysis Today*, 129 (2007) 322-329

[19] Verónica, M. et al., 2008, "Ethanol steam reforming using Ni(II)-Al(III) layered double hydroxide as catalyst precursor – Kinetic Study", *Chemical Engineering Journal*, 138 (2008) 602-607

[20] Torres, J.A., 2007, "Steam reforming of ethanol at moderate temperature: Multifactorial design analysis of Ni/La_2O_3-Al_2O_3, and Fe- and Mn-promoted Co/AnO catalysts", *Journal of Power Sources*, 169 (2007) 158-166

[21] Diagne, C., Idriss, H., Pearson, K., Gómez-García, M.A., Kiennemann, A., 2004, "Efficient hydrogen production by ethanol reforming over Rh catalysts. Effect of addition of Zr on CeO_2 for the oxidation of CO to CO_2", *C.R. Chimi* 7, 2004, 617-622

[22] Sun, J., Qiu, X.P., Wu, F., and Zhu, W.T., 2005, "H_2 from steam reforming of ethanol at low temperature over Ni/Y_2O_3, Ni/La_2O_3 and Ni/Al_2O_3 catalysts for fuel-cell application", *International Journal of Hydrogen Energy* Vol. 30, Issue 4, March 2005, 437 - 445

[23] Zhang, L., 2009, "Ethanol steam reforming reactions over $Al_2O_3 \cdot SiO_2$-supported Ni-La catalysts", *Fuel*, 88 (2009) 511-518

[24] Energy Systems Research Unit (ESRU), "What is Bioethanol?", *University of Strathclyde,* UK. http://www.esru.strath.ac.uk/EandE/Web_sites/02-03/biofuels/what_bioethanol.htm, Last visited; April 22nd, 2010

[25] Kirkbride McElroy, A., 2008, "Is biomethanol in biodiesel's future?," *Biodiesel magazine* April 2008

[26] Wang, L.C., et al., 2007, "Production of hydrogen by steam reforming of methanol over Cu/ZnO catalysts prepared via a practical soft reactive grinding route based on dry oxalate-precursor synthesis", *Journal of Catalysis* 246 (2007), 193 – 204

[27] Terra Nitrogen Corporation, 2001, "MSDS for Methanol", *Terra Nitrogen Corporation,* MSDS Number 2016, Sioux City, Iowa, April 1st, 2001

[28] Palo, D. R., and Holladay, J. D., 2007, "Methanol Steam Reforming for Hydrogen Production", *Chem. Rev.* 2007, 107, 3992 – 4021

[29] Iwasa, N., and Takezawa, N., 2003, "New supported Pd and Pt alloy catalysts for steam reforming and dehydrogenation of methanol, *Topics in Catalysis* Vol. 22, Nos. 3-4, April 2003

[30] Takezawa, N., and Iwasa, N., 1997, "Steam reforming and dehydrogenation of methanol: Difference in the catalytic functions of copper and group VIII metals", *Catalysis Today* 36 (1997), 45 - 56

[31] Tsubaki, N., Zeng, J., Yoneyama, Y., and Fujimoto, K., 2001, "Continuous synthesis prodcess of methanol at low temperature from syngas using alcohol promoters", *Catal. Comm.* Vol 2, Issues 6-7, September 2001, 213-217

[32] Twigg, M.V., Spencer, M.S., 2003, Deactivation of Copper Metal Catalysts for Methanol Decomposition, Methanol Steam Reforming and Methanol Synthesis, *Top. Catal.* Vol. 22, Nos. 3-4, April 2003, 191 - 203

[33]Cheng, W.H., Chen, I., Liou, J.S., Lin, S.S., 2003, "Supported Cu catalysts with yttria-doped ceria for steam reforming of methanol", *Topics in Catalysis* Vol. 22, Nos. 3-4, April 2003

[34]Sun, W.C., Guy, P.M., Jahngen, J.H., Rossomando, E.F., and Jahngen, E.G.E., 1988, "Microwave-Induced Hydrolysis of Phospho Anhydride Bonds in Nucleotide Triphosphates", *J. Org. Chem.* 1988, 53, 4414-4416

[35]Sanders, A.P., Joines, W.T., Allis, J.W., 1985, "Effects of continuous-wave, pulsed, and sinusoidal-amplitude-modulated microwaves on brain energy metabolism", *Bioelectromagnetics* 1985, 6(1), 89-97

[36]Jahngen, E.G.E., Lentz, R.R., Pesheck, P.S., Sackett, P.H., 1990, "Hydrolysis of Adenosine Triphosphate by Conventional or Microwave Heating", *J. Org. Chem.* 1990, 55, 3406 – 3409

[37]Will, H., Scholz, P., and Ondruschka, B., 2004, "Microwave-Assisted Heterogeneous Gas-Phase Catalysis", *Chem. Eng. Technol.*2004, 27, 2

[38]Will, H., Scholz, P., and Ondruschka, B., 2004, "Heterogeneous gas-phase catalysis under microwave irradiation – a new multi-mode microwave applicator", *Topics in Catalysis* Vol. 29, Nos. 3 – 4, June 2004, 175 - 182

[39]Stuerga, D., Gonon, K., and Lallemant, M., 1993, "Microwave heating as a new way to induce selectivity between competitive reactions. Application to isomeric ratio control in sulfonation of naphthalene", *Tetrahedron* Vol. 49, Issue 28, 9 July 1993, 6229-6234

[40]Roussy, G., Thiebout, J.M., Souiri, M., Marchal, E., Kiennemann, A., Maire, G., 1994, "Controlled oxidation of methane doped catalysts irradiated by microwaves", *Catalysis Today* 21 (1994), 349 - 355

[41]Zhang, X., Hayward D.O., Michael, D., and Mingos P., 1999, "Apparent equilibrium shifts and hot-spot formation for catalytic reactions induced by microwave dielectric heating", *Chem. Commun.*, 1999, 975 – 976

[42]Chen, W.H., Lin, B.J., 2009, "Effect of microwave double absorption on hydrogen generation from methanol steam reforming", *International Journal of Hydrogen Energy* 35 (2010), 1987 – 1997

[43]Zhang, X. R., et al., 2005, "A unique microwave effect on the microstructural modification of $Cu/ZnO/Al_2O_3$ catalysts for steam reforming of methanol", *Chem. Comm.* 2005, 4104 – 4106

[44]Durka, T., Stefanidis, G.D., van Gerven, T., and Stankiewicz, A., 2010, "On the accuracy and reproducibility of fiber optic (FO) and infrared (IR) temperature measurements of solid materials in microwave applications", *Meas. Sci. Technol.* 21 (2010) 045108 (8pp)

[45]Pert, E., Carmel, Y., Birnboim, A., Olorunyolemi, T., Gershon, D., Calame, J., Lloyd, I.K., and Wilson, O.C. Jr., 1981, "Temperature Measurements during Microwave Processing: The Significance of Thermocouple Effects", *J. Am. Ceram. Soc.,* 84 [9], 1981 – 86

[46]Gammampila, K., Dunscombe, P.B., Southcott, B.M., and Stacey, A.J., 1981, "Thermocouple thermometry in microwave fields", *Clin. Phys. Physiol. Meas.,* 1981, Vol. 2, No.4, 285-292

[47]Bogdal, D., Bednarz, S., and Lukasiewicz, M., 2006, "Microwave induced thermal gradients in solventless reaction systems", *Tetrahedron* 62 (2006), 9440 – 9445

[48]Bi, X. J., et al., 1999, "Microwave effect on partial oxidation of methane to syngas", *React. Kinet. Catal. Lett.* Vol 66, No. 2, 381-386 (1999)

[49] Zhang, X., Hayward, D.O., Michael, D., and Mingos, P., 2003, "Effects of microwave dielectric heating on heterogeneous catalysis", *Cat. Lett.* Vol. 88, Nos. 1-2, May 2003

[50] Sinev, Il, Kardasch, T., Kramareva, N., Sinev, M., Tkachenko, O., Kucherov, A., Kustov, L.M., 2009, "Interaction of vanadium containing catalysts with microwaves and their activation in oxidative dehydrogenation of ethane", *Catalysis Today* 141, 2009, 300 – 305

[51] Beckers, J., van der Zande, L.M., and Rothenberg, G., 2006, "Clean Diesel Power via Microwave Susceptible Oxidation Catalysts", *Chem. Phys. Chem* 2006, 7, 747 – 755

[52] Koch, T. A., Krause, K. R., Mehdizadeh, M., 1997, "Improved safety through distributed manufacturing of hazardous chemicals", *Process Safety Progress* Vol. 16, Issue 1 , Pages 23 - 24

[53] Ioffe, M.S., Pollington, S.D., Wan, J.K.S., 1995, "High-Power Pulsed Radio-Frequency and Microwave Catalytic Processes: Selective Production of Acetylene from the Reaction of Methane over Carbon", *Journal of Catalysis* 151, 1995, 349-355

[54] Alfa Aesar, Certificate of Analysis: Copper based low temperature water gas shift catalyst, HiFUEL^{TM} W220, Stock Number 45466, Lot Number B11T010, *Alfa Aesar*

[55] Liguras, D.K., Kondarides, D.I., and Verykios, X.E., 2003, "Production of hydrogen for fuel cells by steam reforming of ethanol over supported noble metal catalysts", *Applied Catalysis B: Environmental* Vol. 43, Issue 4, 25 July 2003, 345 - 354

[56] Mathure, P.V., 2007, "Steam Reforming of Ethanol Using a Commercial Nickel-Based Catalyst", *Ind. Eng. Chem. Res.* 2007, 46, 8471-8479

[57] Moulijn, J.A., Makkee, M., van Diepen, A., 2001, in Chemical Process Technology, "chapter 5: Production of Synthesis Gas", *John Wiley & Sons, Ltd.,* page 133

Microwave-assisted low temperature steam reforming of methanol for hydrogen production

Master Thesis

Appendices

Appendix A. Temperature profiles

In the steam reforming reaction of methanol over a $Cu/ZnO/Al_2O_3$ catalyst under microwave or conductive heating the catalyst bed suffers from large radial and axial temperature gradients. The axial temperature gradients are mapped in the center and at the wall of the reactor. From these temperature maps an average temperature is computed. Based on general knowledge about heat transfer, an assumption of symmetry of temperature profile in the radial direction is made (see figure A1). This assumption delivers the third boundary condition for the description of the radial average temperature by a 2nd order polynomial.
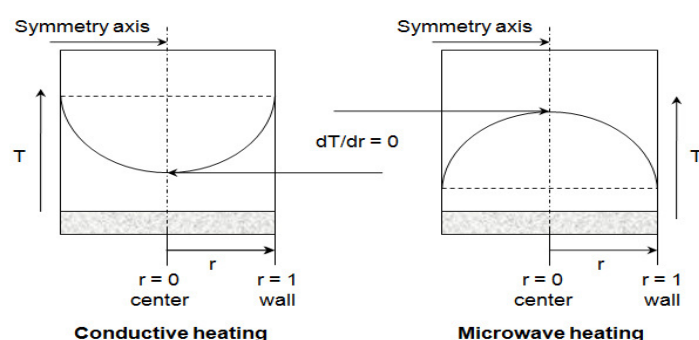

Figure A1. Assumption of radial temperature profiles over the catalyst bed for conductive heating (l) and microwave heating (r)

In figure A2 examples are presented of the measured axial temperature profiles (green = T_{wall}, blue = T_{center}), the computed radial average temperature profile (orange), and the computed average reaction temperature (yellow). The average reaction temperature for these reactions is the same (190°C), as are the reaction conditions (GHSV and S/C ratio). It is clear that the radial temperature profiles are the inverse of each other. The axial temperature profile on the other hand, are similar in shape. However the temperature profiles, both axial and radial, are less profound for conductive heating than for microwave heating.
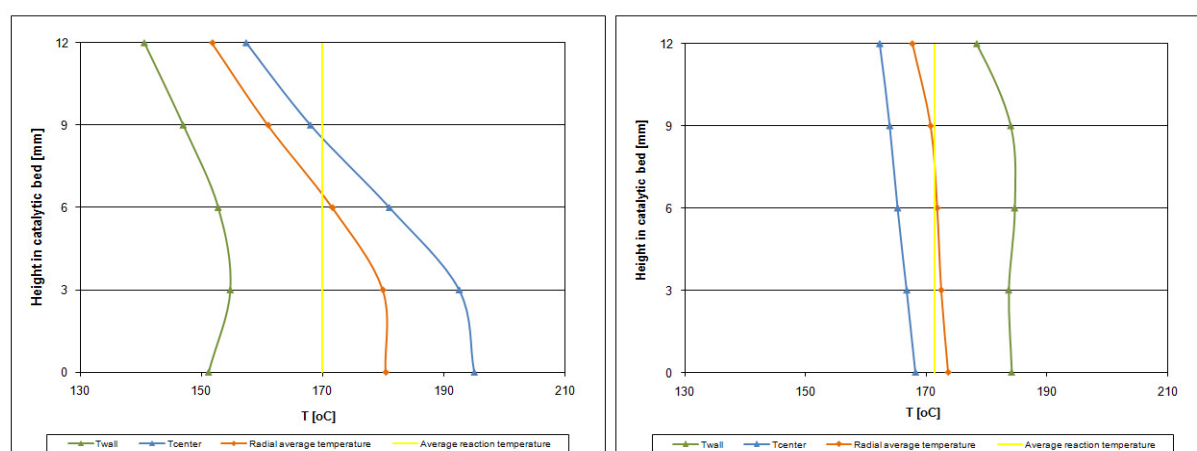

Figure A2. Measured axial temperature profiles over the catalyst bed for microwave heating (l) and conductive heating (r) (S/C = 1.5, GHSV = 65,000 h^{-1}, T = 170°C). The orange line is the radial average temperature, the yellow line represents the axial average temperature thereof, and thus the average temperature of the catalytic bed.

The radial and reaction average temperature profiles are computed from the measured axial temperature profiles in the center and on the wall of the reactor. In table A1 a numerical example is given of the average temperature calculation of the microwave experiment in figure A2.

Table A1. Computation of average reaction temperature from temperature mapping data of the microwave experiment

Height [mm]	Temperature data		$y = ax^2 + c$		Radial average	4th degree polynomial	
	Twall [$^{\circ}$C]	Tcenter [$^{\circ}$C]	a	c			
0	151.2	195	-43.8	195	180.4	a	-0.001
3	154.8	192.5	-37.7	192.5	179.9	b	0.053
6	152.8	181	-28.2	181	171.6	c	-0.847
9	147	168	-21	168	161	d	1.940
12	140.55	157.4	-16.85	157.4	151.78	e	180.4
				Average temperature of the bed		**169.94**	

The radial average temperature at each vertical location in the reactor is calculated from the two data points at the wall and in the center. The symmetry axis provides the third constraint for the second order polynomial of which the shape is used. Due to the fact that only two data points are used, the second order polynomial takes the form:

$$y = ax^2 + c \tag{A1}$$

From which a and c are calculated using the data points:

$$a = T_{wall} - T_{center} \tag{A2}$$

$$c = T_{center} \tag{A3}$$

The average temperature at the specific height is then calculated by integration of the polynomial:

$$T_{Rad} = \int_0^1 ax^2 + c = \left[\frac{1}{3}ax^3 + cx\right]_0^1 = \frac{1}{3}a + c = \frac{1}{3}(T_{wall} - T_{center}) + T_{center} \tag{A4}$$

The average reaction temperature can be computed by integrating the polynomial that describes the radial average temperature profile. Since there are five data points, a 4th order polynomial can be determined which describes the profile accurately:

$$y = ax^4 + bx^3 + cx^2 + dx + e \tag{A5}$$

In which y represents the temperature and x the height of the reactor. The constants a – e can be determined from the data points and were found to follow the functions:

$$a = \frac{1}{1944} \cdot T_0 - \frac{1}{486} \cdot T_3 + \frac{1}{324} \cdot T_6 - \frac{1}{486} \cdot T_9 + \frac{1}{1944} \cdot T_{12} \tag{A6}$$

$$b = -\frac{5}{324} \cdot T_0 + \frac{1}{18} \cdot T_3 - \frac{2}{27} \cdot T_6 + \frac{7}{162} \cdot T_9 - \frac{1}{108} \cdot T_{12} \tag{A7}$$

$$c = \frac{11}{216} \cdot T_0 - \frac{14}{54} \cdot T_3 + \frac{19}{36} \cdot T_6 - \frac{26}{54} \cdot T_9 + \frac{35}{216} \cdot T_{12} \tag{A8}$$

$$d = -\frac{1}{12} \cdot T_0 + \frac{4}{9} \cdot T_3 - T_6 + \frac{4}{3} \cdot T_9 - \frac{675}{972} \cdot T_{12} \tag{A9}$$

$$e = T_0 \tag{A10}$$

In which T_x is the radial average temperature at height x in the reactor. Integrating the 4th order polynomial over the height of the reactor, using the values of a – e, yields the average reaction temperature:

$$T_{reaction} = \frac{20736}{5} \cdot a + 432 \cdot b + 48 \cdot c + 6 \cdot d + e \qquad \text{(A11)}$$

Appendix B. Mass balance

In order to assess the performance of reactions, the data obtained from experiments are combined in a mass balance calculation. The parameters of interest are:

- S/C ratio of reaction mixture [mol/mol]
- Input and output of the reactor [mol] and [mol/min], per reactant/product
- GHSV [h^{-1}]
- Liquid feed/N_2 ratio [mol/mol]
- Conversion [%]
- Product yields (H_2, CO_2 and CO) [mol product formed/mol methanol reacted]
- Mass balance deviation [%]

The input into the mass balance from which these data are computed are:

- Catalyst weight [g] and density [g/cm^3]
- Ambient temperature [^{o}C] and pressure [mbar]
- Carrier gas flow [cm^3/min]
- Molar concentration of methanol in the reaction mixture and the effluent liquid [mol%]
- Initial and final weight of the vessel with reaction mixture and the water trap [g]
- Start time and end time of the reaction, noted at start and stop of liquid flow
- Every hour: time, effluent gas flow rate [cm^3/min], composition of effluent gas [v%]
- Reaction temperature, from the temperature maps

In the next section the equations for the computation of the assessment parameters are presented.

The S/C ratio of the reactant mixture is calculated from the concentration of methanol (MeOH) in this mixture. The concentration is measured either by an offline GC, or by a density meter. From the molar concentration of methanol (c_{MeOH}), the S/C ratio is calculated by:

$$\frac{S}{C} \left[\frac{mol}{mol} \right] = \frac{100\% - c_{MeOH,in} \, [\%]}{c_{MeOH,in} \, [\%]} \tag{B1}$$

The flow rates of reactants and products in and out of the reactor consist of multiple outputs. The computation of most of these outputs is the same. Therefore only the calculation of different species is presented in case the calculation is different. First the flow rates of the feed components are computed. These include the flow rate of nitrogen, water and methanol.

The ingoing flow rate of nitrogen is measured as volumetric flow rate in [cm^3/min], and is computed to a molar flow rate using the ideal gas law at ambient conditions:

$$F_{N_2} \left[\frac{mol}{s} \right] = \frac{P \, [Pa] \cdot F_{N_2} \left[\frac{cm^3}{s} \right]}{R \left[\frac{J}{mol \cdot K} \right] \cdot T_{amb} [K]} \tag{B2}$$

The ingoing flow rate of water and methanol are computed from the ingoing liquid mass flow rate and the concentration of methanol. The overall liquid flow rate is calculated in [g/h] by the weight change of the vessel with reactants divided by the time:

$$F_{w,tot} = \frac{M_b - M_a \ [g]}{t \ [h]}$$ (B3)

In which M_b is the mass of the vessel with reaction mixture before the reaction, and M_a the mass of this vessel after the reaction. The total liquid flow rate is converted to units of [mol/s] by a number of calculations. The molar S/C ratio from eq. B1 is used to compute the weight ratio of the mixture. Therefore the relative mass is computed first. This is done by assuming that there is 1 mole of methanol, and S/C moles of water. This numerical trick can be used because the result is a ratio. The mass for each species is computed as follows:

$$Mass_i[g] = mol_i \ [mol] \cdot M_i \left[\frac{g}{mol}\right]$$ (B4)

In which M_i is the molar mass of the species. The weight ratio can then be calculated by:

$$W_i \left[\frac{g}{g}\right] = \frac{Mass_i \ [g]}{\sum Mass_i \ [g]}$$ (B5)

Using the density and weight ratio of each species, the density of the mixture can be computed:

$$\rho_{mix} \left[\frac{g}{cm^3}\right] = \sum W_i \cdot \rho_i$$ (B6)

Which can then be used to calculate the total volumetric flow rate:

$$F_{v,tot} \left[\frac{cm^3}{s}\right] = \frac{F_{w,tot}[g/h]}{3600 \cdot \rho_{mix}\left[\frac{g}{cm^3}\right]}$$ (B7)

The volumetric flow rate is then converted to a molar flow rate according to:

$$F_{m,tot} \left[\frac{mol}{s}\right] = \sum F_{v,tot} \left[\frac{cm^3}{s}\right] \cdot W_i \left[\frac{g}{g}\right] \cdot \frac{\rho_i \left[\frac{g}{cm^3}\right]}{M_i \left[\frac{g}{mol}\right]}$$ (B8)

This molar flow rate is then combined with the molar concentration of each species to arrive at the molar flow rate of each species:

$$F_{i,in} \left[\frac{mol}{s}\right] = F_{m,tot} \left[\frac{mol}{s}\right] \cdot \frac{c_{i,in}[\%]}{100 \ [\%]}$$ (B9)

In which i represents methanol or water. The molar concentration of water being:

$$c_{H_2O}[\%] = 100\% - c_{MeOH}[\%]$$ (B10)

The ingoing flow rates being known, the outgoing flow rates of the products can be calculated as well. There are both liquid and gaseous products, both of which are calculated in a different way. The flow rates of the liquid products are calculated from the molar concentration of methanol in the collected liquid and the outgoing mass flow rate of liquid. The outgoing mass flow rate of liquid is calculated from the weight change of the water trap and the time in a similar way as in eq. B3:

$$F_{w,tot}\left[\frac{g}{min}\right] = \frac{M_{wt,a}-M_{wt,b}[g]}{t\,[min]} \tag{B11}$$

In which $M_{wt,a}$ is the mass of the water trap after the reaction, and $M_{wt,b}$ the mass of the water trap before the reaction. Using the molar masses and concentrations of the outgoing water and methanol, the outflow of each species is calculated according to:

$$F_{i,out}\left[\frac{mol}{min}\right] = \frac{F_{w,tot}\left[\frac{g}{min}\right]\cdot c_{i,out}[\%]\cdot M_i\left[\frac{g}{cm^3}\right]}{\sum c_{i,out}[\%]\cdot M_i\left[\frac{g}{cm^3}\right]} \cdot \frac{1}{M_i\left[\frac{g}{cm^3}\right]} \tag{B12}$$

Because nitrogen is an inert, the outgoing flow rate of nitrogen is assumed to be equal to the ingoing flow rate of nitrogen (eq. B2). The calculation of the outgoing flow rate of nitrogen enables the possibility to compare the ingoing flow rate, measured before the reaction commenced, with the outgoing flow rate; the outgoing nitrogen concentration is measured by the GC as well. When the values of in- and outgoing flow rates of nitrogen are similar, the other species' flow rates can be assumed to be correct. The outgoing flow rates of the product gases are calculated from the measured gas flow rate and the composition of this gas, provided by the online GC. The molar flow rate of each species is calculated from the volumetric flow rate of the species, using the ideal gas law with ambient conditions in the same way as the ingoing flow rate of nitrogen was calculated in eq. B2. The volumetric flow rate of each species is calculated by:

$$F_i\left[\frac{cm^3}{min}\right] = \frac{Q_{v,i}[v\%]}{100\%} \cdot F_{v,gas}\left[\frac{cm^3}{min}\right] \tag{B13}$$

In which $Q_{v,I}$ is the quantity of the species in the gas, expressed in volume%, and $F_{v,gas}$ is the measured total flow rate of the effluent gas.

The GHSV can be calculated by the ingoing flow rates of carrier gas and liquids at reaction temperature divided by the interstitial volume:

$$GHSV[h^{-1}] = \frac{\left(F_{N_2}+F_{v,tot}\left[\frac{cm^3}{s}\right]\right)\cdot 3600}{V_R-V_{cat}\,[cm^3]} \tag{B14}$$

In which the V_R is calculated by:

$$V_R[cm^3] = \frac{\pi\cdot\left(\frac{D_1}{2}\right)^2 - \pi\cdot\left(\frac{D_2}{2}\right)^2\cdot L}{1000} \tag{B15}$$

In which D_1 is the inner diameter of the reactor in [mm], D_2 is the outer diameter of the bended glass feeding tube in [mm], and L is the height of the catalytic bed in [mm]. The catalyst volume is calculated from the catalyst mass [g] and density [g/cm³]. For the GHSV the ingoing flow rates have to be calculated at reaction temperature. The flow rate of nitrogen is therefore scaled to the temperature according to:

$$F_{N_2}(@T_r)\left[\frac{cm^3}{s}\right] = F_{N_2}\left[\frac{cm^3}{s}\right] \cdot \frac{T_r[K]}{T_{amb}[K]} \tag{B16}$$

At reaction temperature methanol and water are both in the gas phase. Therefore the ideal gas law is used to calculate the volumetric flow rates of these species:

$$F_{v,tot}\left[\frac{cm^3}{s}\right] = \sum \frac{F_{i,mol}\left[\frac{mol}{s}\right] \cdot R\left[\frac{J}{mol \cdot K}\right] \cdot T_r[K]}{P[Pa]} \cdot 1 \cdot 10^6 \tag{B17}$$

The liquid feed/N_2 ratio can be calculated from the previously calculated molar flow rates of nitrogen (eq. B2) and the liquid feed (eq. B8):

$$\frac{Feed}{N_2}\left[\frac{mol}{mol}\right] = \frac{F_{m,tot}\left[\frac{mol}{s}\right]}{F_{N_2}\left[\frac{mol}{s}\right]} \tag{B18}$$

The calculation of the in- and outgoing flow rates enables the possibility of calculating the conversion of methanol:

$$X_{MeOH}[\%] = \frac{MeOH_{in}[mol] - MeOH_{out}[mol]}{MeOH_{in}[mol]} \cdot 100\% \tag{B19}$$

The molar amounts of methanol are obtained when the molar flow rates (eq. B9) are multiplied by the time over which the conversion is desired. In the mass balance the overall conversion is computed as well as the conversion after each hour. The ingoing methanol is purely liquid. The outgoing methanol however, divides itself over both liquid and gas. Therefore the outgoing methanol is computed as:

$$MeOH_{out}[mol] = \left(F_{MeOH,l}\left[\frac{mol}{min}\right] + F_{MeOH,g}\left[\frac{mol}{min}\right]\right) \cdot t\,[min] \tag{B20}$$

With the liquid effluent flow rate of methanol from eq. B12, and the gaseous effluent flow rate from eq. B13 and the ideal gas law. The product yields of H_2, CO_2 and CO are calculated from the outgoing gas flows and the consumption of methanol:

$$Y_i\left[\frac{mol_i}{mol_{MeOH}}\right] = \frac{mol_{i,out}[mol]}{MeOH_{in}[mol] - MeOH_{out}[mol]} \tag{B21}$$

In which the molar production of the species is calculated by multiplying the molar flow rate by the time over which the yield is desired. The selectivity of one product over another product is calculated from the yields:

$$S_{i,j}\left[\frac{mol_i}{mol_j}\right] = \frac{Y_i}{Y_j} \tag{B22}$$

In order to investigate whether the values for conversion and yields are reliable, an assessment is made of the deviation of the mass balance. This is done in two ways to ensure it is correct, and to enable the possibility to determine what kind of mass is lost or created when the balance is not closed. An overall mass balance is constructed from the in- and outgoing mass of liquid and gas, and an element balance is constructed in which the in- and outgoing masses are divided over their elements. The total mass balance is based on mass values as close to the measurements as possible, using the measured weight changes of the reactants and collection vessels and the measured flow rates:

$$M_{tot,in}[g] = (M_b - M_a)[g] + mol_{N_2,in}\left[\frac{mol}{min}\right] \cdot t_r\,[min] \cdot M_{N_2}\left[\frac{g}{mol}\right] \tag{B23}$$

$$M_{tot,out}[g] = (M_{wt,a} - M_{wt,b})[g] + \left(\sum F_{i,out}\left[\frac{mol}{min}\right] \cdot M_i\left[\frac{g}{mol}\right]\right) \cdot t_r \tag{B24}$$

The mass balance deviation is a percentage calculated by:

$$Mass\ production\ [\%] = \frac{M_{tot,out}[g] - M_{tot,in}[g]}{M_{tot,in}[g]} \cdot 100\% \tag{B25}$$

In case the mass production value excluding inerts is desired the nitrogen contribution is easily subtracted.

The elemental balances are easily constructed from the already computed in- and outgoing molar quantities of the different species. The elemental balances are constructed in molar form, and the molar production of the elemental species is finally converted to a mass production via the atomic/molar mass to arrive at the desired mass balance. The elemental balance is a summation of the product of molar quantity of the molecules and the number of elemental atoms this molecule contains. For example the ingoing hydrogen is calculated by the number of hydrogen atoms in the ingoing water + the number of hydrogen atoms in the ingoing methanol:

$$H_{in}[mol] = 2 \cdot mol_{H_2O,in}[mol] + 4 \cdot mol_{MeOH,in}[mol] \tag{B26}$$

Because water contains 2 hydrogen atoms, and methanol 4. The molar quantities are calculated from eq. B13 and the ideal gas law. The same is done for all in- and outgoing species. Using this technique a hydrogen balance, a carbon balance and an oxygen balance are constructed. Equating the in- and outgoing quantities of the elements, the production of each elemental species can be monitored. The elemental balances are constructed for the overall mass balance only.

Appendix C. Product yields and selectivities

In appendix C1 the performance of microwave assisted reactions is compared to the performance of reactions under conductive heating conditions. The parameters that determine the performance are the conversion, and product yields and selectivities. The variables are temperature, GHSV and S/C ratio. For S/C ratio 2 the temperature dependence of the parameters is investigated for GHSV 37,000 and 65,000 h^{-1}. The results of the high GHSV are compared with results of the same GHSV, but for S/C 1.5. In appendix C2 the temporal concentration profiles of the effluent gas are compared.

C1. Comparison of product yields and selectivities for different reaction conditions

In figures C1 and C2 the temperature dependence of the methanol conversion is presented for different S/C ratios (1.5 and 2 respectively). From these figures it is evident that for higher S/C ratio the conversion is higher in microwave heating, which is in accordance with Le Châtelier's principle. For conductive heating the conversion is approximately the same.
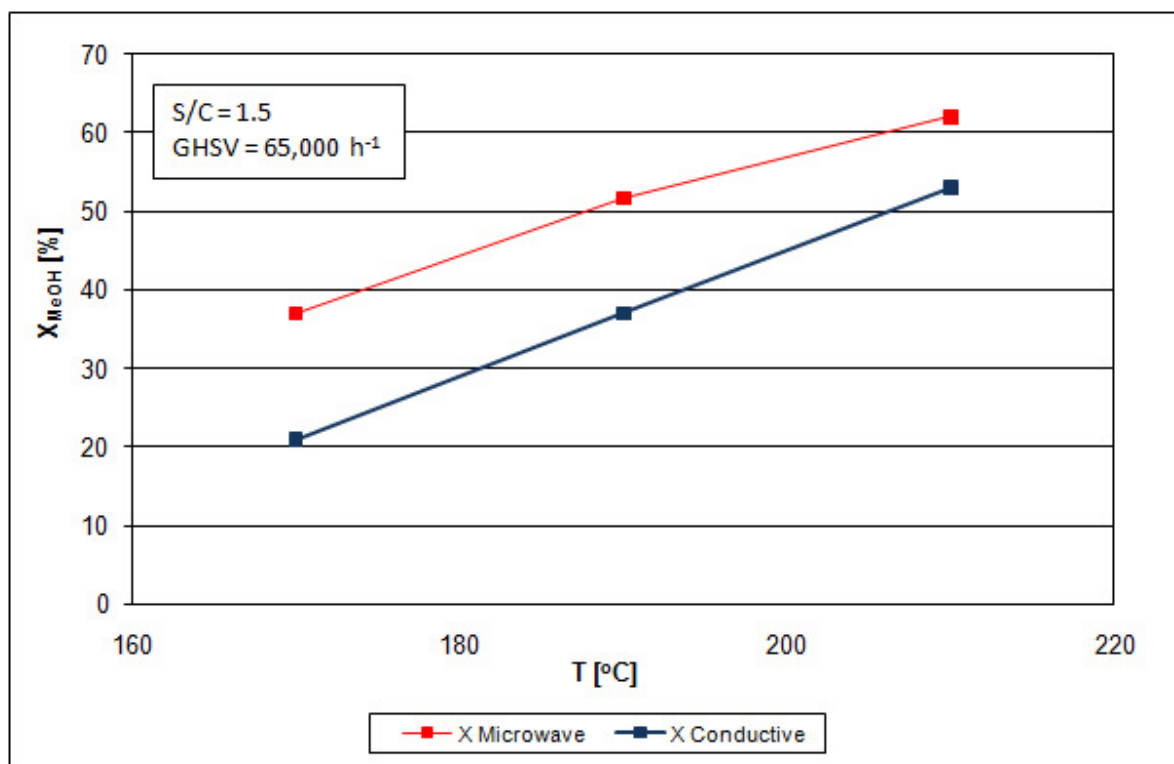

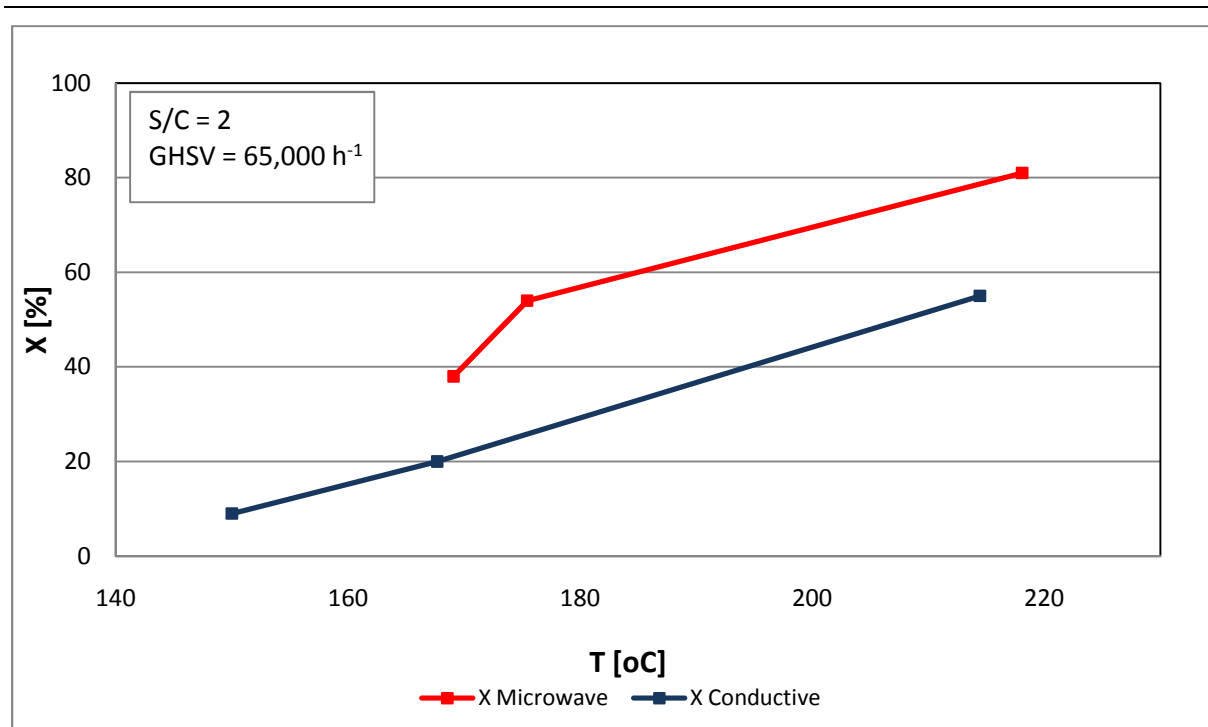**Figure C1. Temperature dependence of methanol conversion at S/C = 1.5 and GHSV = 65,000 h^{-1}**

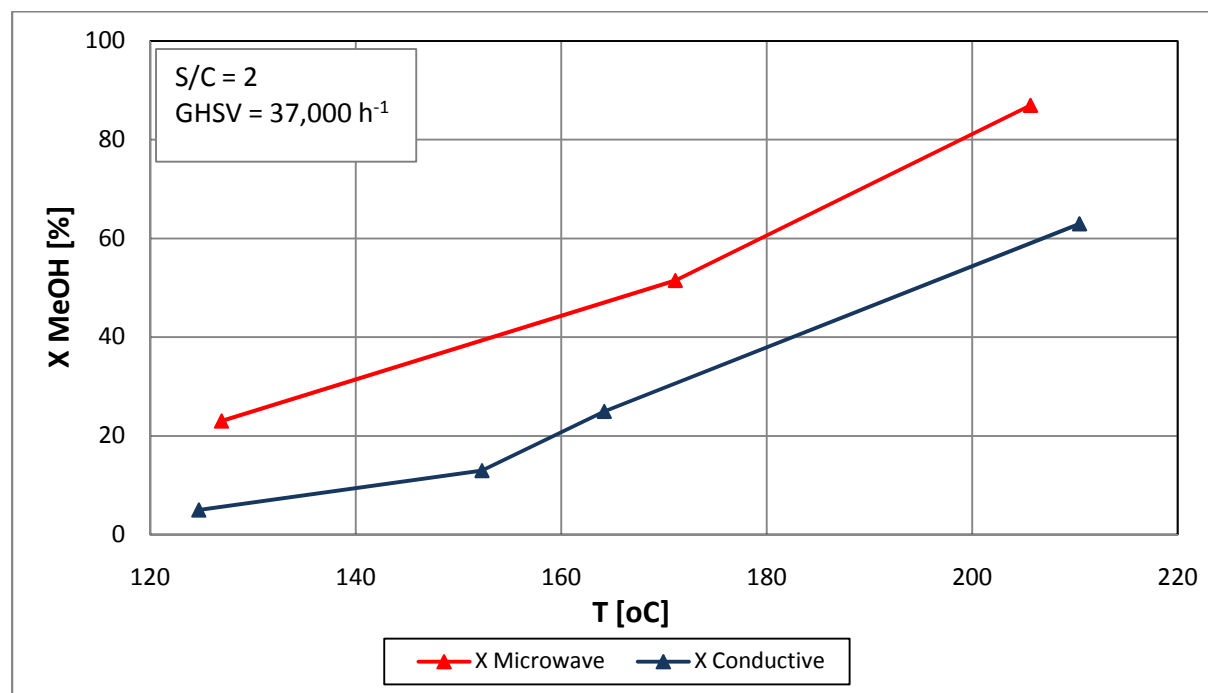**Figure C2. Temperature dependence of methanol conversion at S/C = 2 and GHSV = 65,000 h^{-1}**

Figure C3. Temperature dependence of methanol conversion at S/C = 2 and GHSV = 37,000 h^{-1}

In figure C3 the temperature dependence of the methanol conversion is presented for a lower GHSV. The profile has similar shape to that of figures C1 and C2. In comparison with Figure C2 it is evident that at higher GHSV the conversion is lower. In figures C4 – C6 the product yields and selectivities corresponding to the conversions in Figures C1 – C3 are presented.
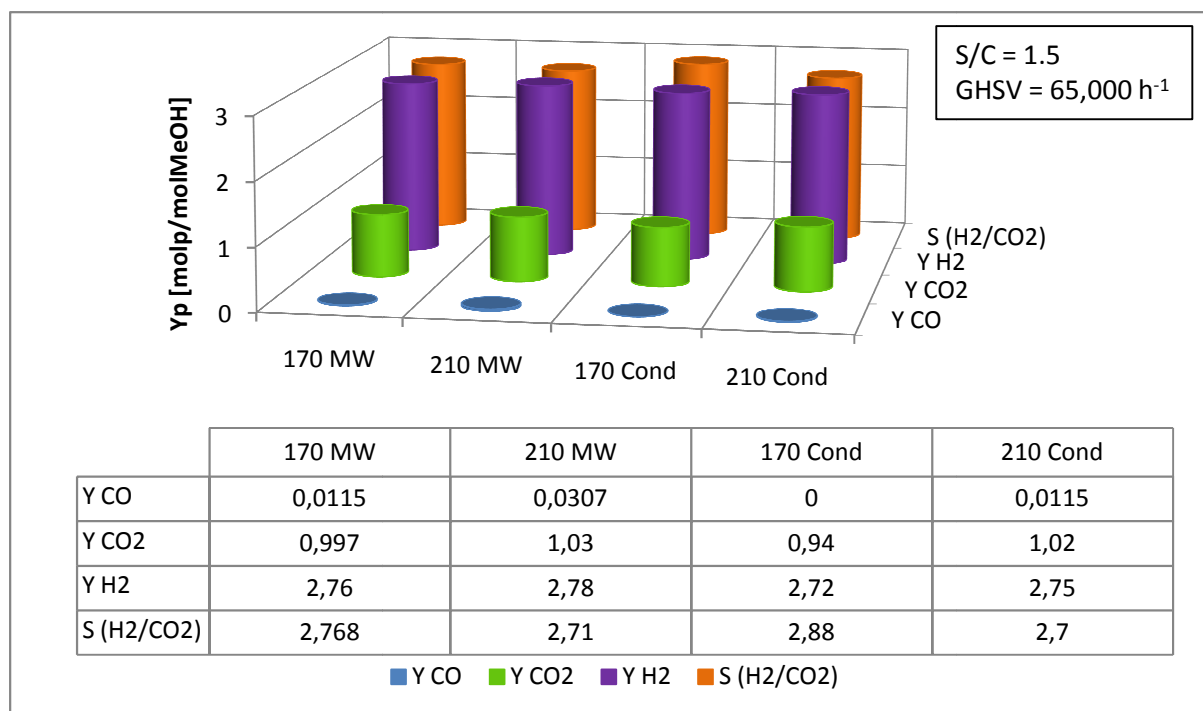
	170 MW	210 MW	170 Cond	210 Cond
Y CO	0,0115	0,0307	0	0,0115
Y CO2	0,997	1,03	0,94	1,02
Y H2	2,76	2,78	2,72	2,75
S (H2/CO2)	2,768	2,71	2,88	2,7

Figure C4. H$_2$ (purple), CO$_2$ (green) and CO (blue) yields and H$_2$ selectivity (orange) dependence on temperature for microwave (l) and conductive (r) heating (S/C = 1.5, GHSV = 65,000 h^{-1})

	170 MW	220 MW	170 Cond	215 Cond
Y CO	0,011	0,08	0	0,004
Y CO2	0,99	1,04	0,93	0,98
Y H2	2,55	2,7	2,52	2,67
S (H2/CO2)	2,576	2,596	2,710	2,724

Figure C5. H$_2$ (purple), CO$_2$ (green) and CO (blue) yields and H$_2$ selectivity (orange) dependence on temperature for microwave (l) and conductive (r) heating (S/C = 2, GHSV = 65,000 h^{-1})
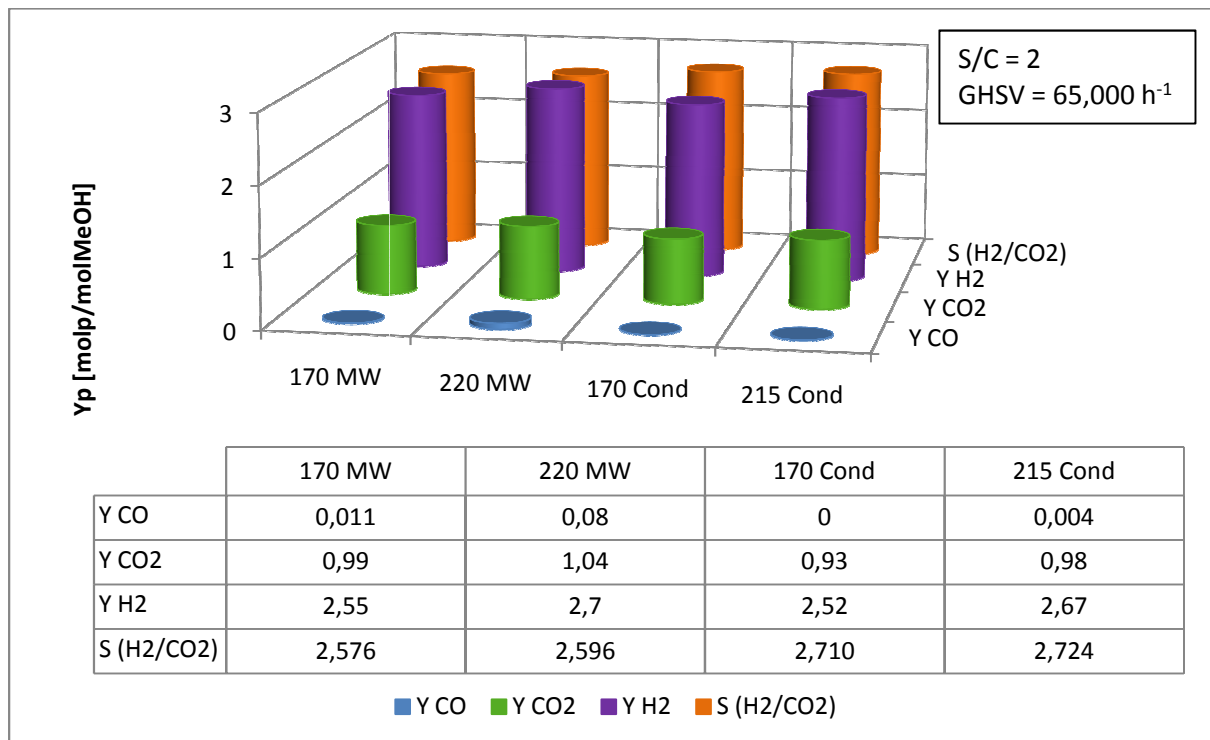
	125 MW	170 MW	205 MW	125 Cond	165 Cond	210 Cond
Y CO	0,0005	0,012	0,07	0	0	0,03
Y CO2	0,76	1,023	1,03	0,06	0,88	0,95
Y H2	2,2	2,8	2,63	0,13	2,51	2,47
S (H2/CO2)	2,895	2,737	2,553	2,167	2,852	2,600

Figure C6. H$_2$ (purple), CO$_2$ (green) and CO (blue) yields and H$_2$ selectivity (orange) dependence on temperature for microwave (l) and conductive (r) heating (S/C = 2, GHSV = 37,000 h^{-1})
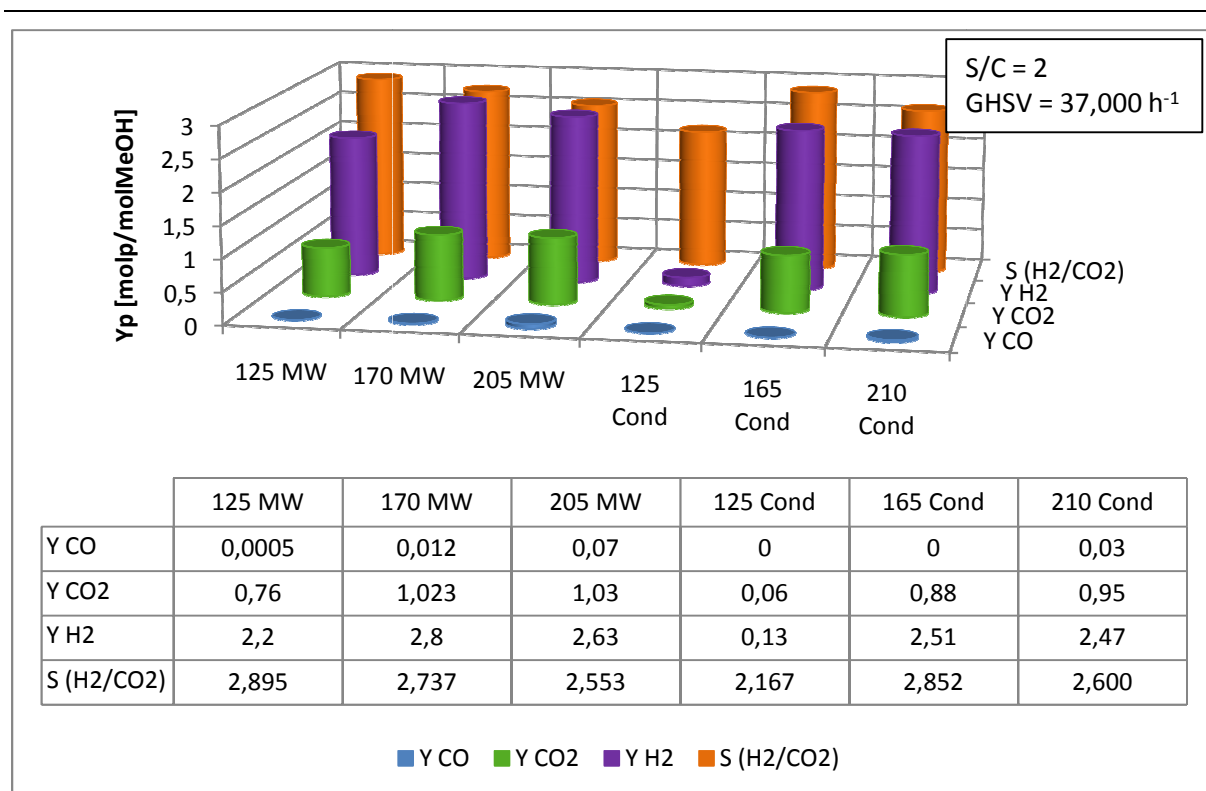
At a GHSV of 65,000 h^{-1} the H$_2$ and CO yields increase for decreasing S/C ratio, which follows from comparison between figures C4 and C5. The S/C has little effect on the yield of CO$_2$, which means that the selectivity of H$_2$ over CO$_2$ increases as well. Comparing figures C5 and C6 the influence of the GHSV can be assessed. This shows that the GHSV has no direct effect on the yields, however the selectivity of H$_2$ over CO$_2$ is higher for lower GHSV. In Figure C6 it shows that at very low temperature (T = 125°C) has significant effect on the yields of the products. In microwave conditions the product yields are relatively low, whereas the selectivity has a high value compared to the experiments at higher temperatures. The high selectivity is most likely caused by the fact that carbon deposition is taking place at these low temperatures. The yields for the conductive reaction at T = 125°C are nearly 0, because the conversion is very small (~5%).

C2. Temporal concentrations in effluent gas

In figures C7 and C8 the temporal concentration profiles of the effluent gas are provided for microwave and conductive heating conditions respectively. The reaction conditions (T, S/C ratio and GHSV) are the same for each reaction. It can be seen that the concentrations of the products are much higher in microwave conditions than in conductive conditions. Another remarkable difference between microwave and conductive heating is the concentration profile during start-up of the reaction. In microwave conditions this profile curves directly towards the steady state value, whereas with conductive heating an overshoot is observed. This overshoot is the cause of the slow response intrinsic to conductive heating. The microwave heating has a very fast response, and provides no overshoot.
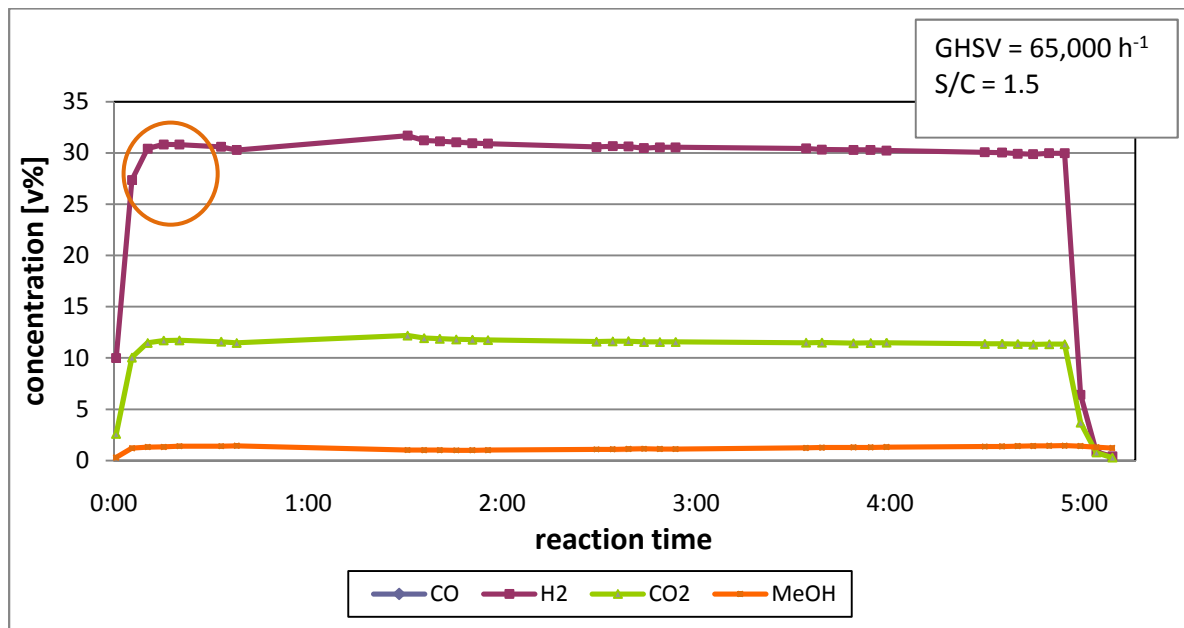

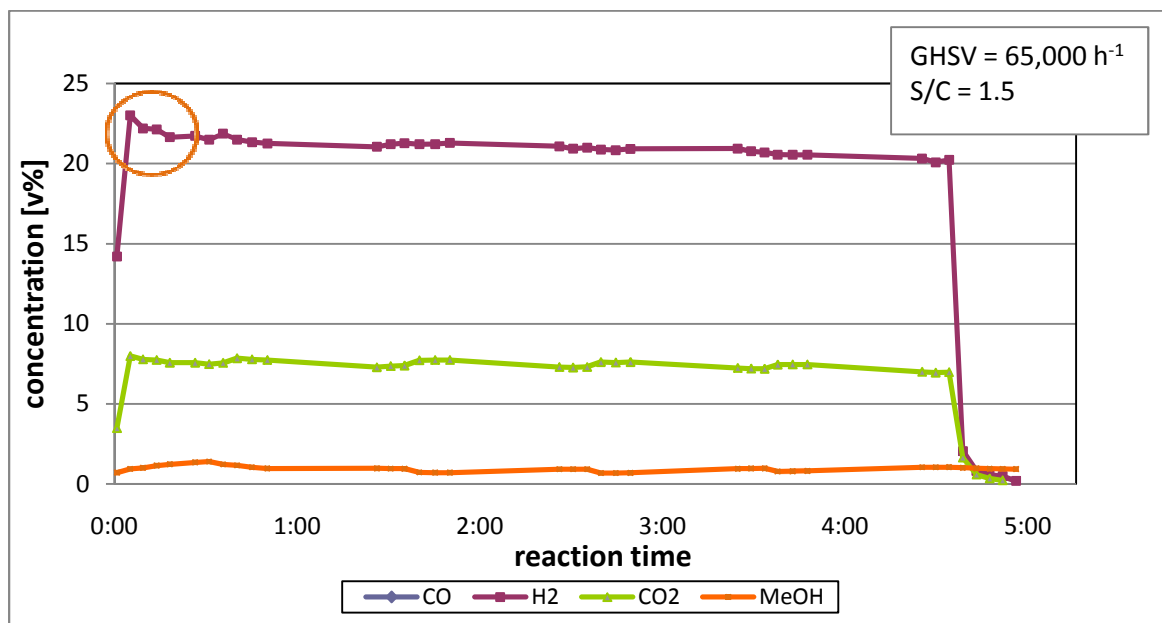**Figure C7. Temporal concentration profile of the effluent gas in a microwave-assisted reaction**

Figure C8. Temporal concentration profile of the effluent gas in a reaction using conductive heating

Appendix D. Catalyst analysis

Samples of Cu/ZnO/Al$_2$O$_3$ catalyst particles, used for steam reforming of methanol, are analyzed using a Scanning Electron Microscope (SEM) with element analysis. The results are compared with the data provided by Alfa Aesar by means of a certificate of analysis, which is presented in figure D1.
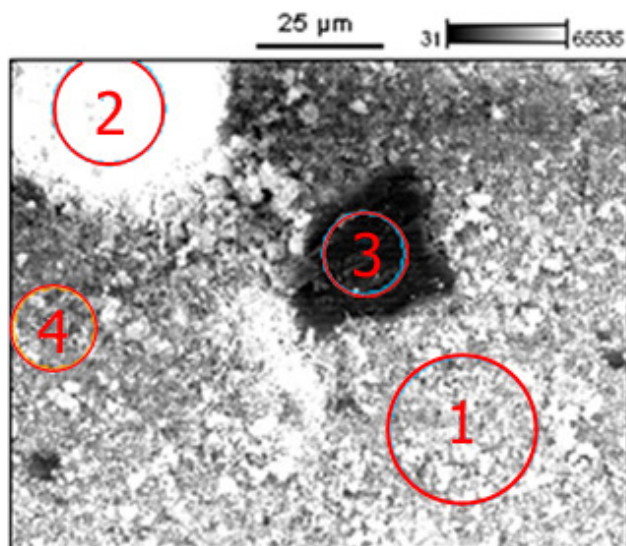
Certificate of Analysis — Alfa Aesar

A Johnson Matthey Company

Copper based low temperature water gas shift catalyst, HiFUEL™ W220

Stock Number: 45466
Lot Number: B11T010

Analysis

Cu as CuO	52.5 %
Zn as ZnO	30.2 %
Al as Al$_2$O$_3$	17.0 %
Na as Na$_2$O	0.01 %
S	0.004 %
Cl	0.0013 %
Fe as Fe$_2$O$_3$	0.02 %
Loss on ignition	6.0 %

Physical Properties

Length	3.4 mm
MVCS	66 kgf
Percent that crush below 20 kgf	< 1 %
Tapped bulk density	1.40 kg/L

Certified by:

Paul V Connolly

Quality Control

Figure D1. Certificate of analysis of the catalyst used in methanol steam reforming experiments

SEM results of catalyst analysis

First a fresh catalyst sample is analyzed, second a catalyst sample used in a methanol steam reforming reaction. The numbered regions in the catalyst surface pictures correspond to the different points of the element analysis.

Fresh catalyst

Accelerating Voltage: 15.0 kV

Magnification: 1000

Figure D2. Fresh catalyst sample with marked regions for element analysis

Of points no. 1, 2 and 4 the elemental analysis is provided. Point 3 was established to consist of carbon. In the spent catalyst sample, of which the results are presented next, the carbon analysis was done. In figure D2 points no. 1 and 4 represent regular catalyst surface. In figure D3 the spectra of the three analysis points is presented, from which it can be seen that in point no. 2 there is much less Cu and Zn as opposed to points 1 and 4. Point no. 2 is the shiny spot on figure D2 and consist nearly purely of support material. The rough counts of the analysis are used for the computation of element concentrations which are presented in table D1. Either the atom% values or the weight% values of Cu, Zn, Al, and O from table D1 can be used for this comparison. The weight percentage of each CuO, ZnO and Al_2O_3 is calculated by dividing the oxygen over the metal species, with 1 oxygen each for copper and zinc, and 1.5 oxygens per aluminium atom. The results of points 1 and 4 are relevant, since these points represent areas that are mostly present over all catalyst samples. For both points the results are similar: the weight% of Al_2O_3 is near 17%, which is close to the value provided by Alfa Aesar. However the CuO and ZnO weight% values are far from those provided by the company. In the element analysis the weight% of CuO is between 40 – 42% as opposed to the theoretical value of 52%, and the weight% of ZnO ranges from 36 – 38% in contrast to 30% as given by the company. Hence less copper is present on the catalyst surface than claimed by Alfa Aesar, which may mean that the catalyst has less active sites.
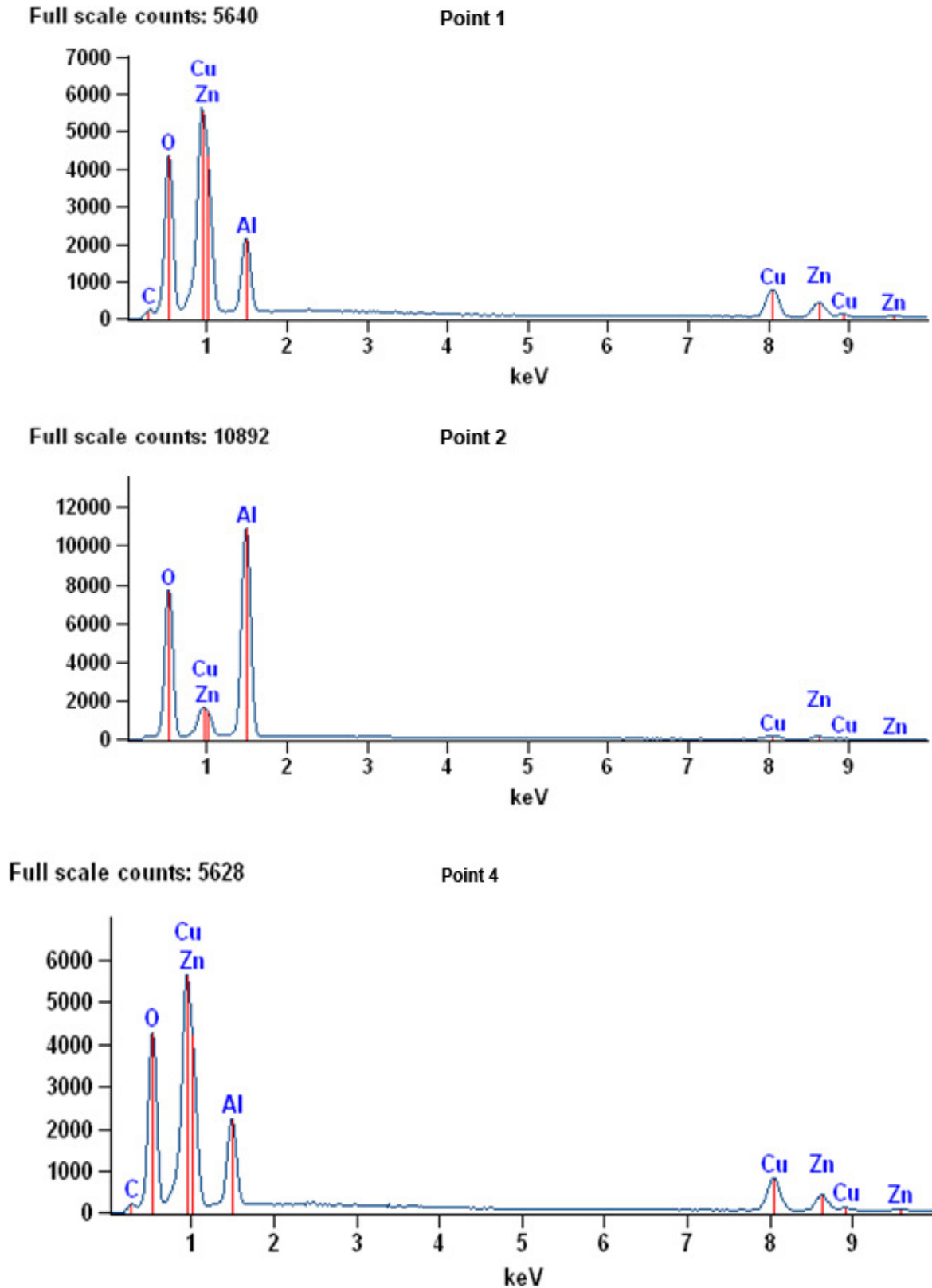
Figure D3. Full scale element counts of the fresh catalyst surface in points 1,2 and 4 of figure D2

Table D1. Numerical results of the element analysis of a fresh catalyst sample

Net Counts

	C-K	O-K	Al-K	Cu-L	Zn-K
Point 1	791	42295	22361	53833	8071
Point 2		71900	124414	18086	2019
Point 4	626	41421	22878	56667	7367

Weight %

	C-K	O-K	Al-K	Cu-L	Zn-K
Point 1	2.20	23.03	8.98	33.95	31.85
Point 2		38.84	38.03	14.22	8.91
Point 4	1.78	22.88	9.36	36.34	29.64

Weight % Error (+/- 1 Sigma)

	C-K	O-K	Al-K	Cu-L	Zn-K
Point 1	+/-0.16	+/-0.15	+/-0.09	+/-1.19	+/-1.03
Point 2		+/-0.19	+/-0.14	+/-0.96	+/-0.64
Point 4	+/-0.15	+/-0.15	+/-0.09	+/-1.19	+/-1.02

Atom %

	C-K	O-K	Al-K	Cu-L	Zn-K
Point 1	6.16	48.35	11.18	17.95	16.36
Point 2		57.84	33.58	5.33	3.25
Point 4	5.03	48.47	11.75	19.38	15.36

Atom % Error (+/- 1 Sigma)

	C-K	O-K	Al-K	Cu-L	Zn-K
Point 1	+/-0.45	+/-0.32	+/-0.11	+/-0.63	+/-0.53
Point 2		+/-0.28	+/-0.13	+/-0.36	+/-0.23
Point 4	+/-0.43	+/-0.32	+/-0.11	+/-0.64	+/-0.53

In figure D4 the regions are mapped of the element analysis of a spent catalyst sample, used in a microwave enhance reaction at high temperature, high gas hourly space velocity and high S/C ratio.
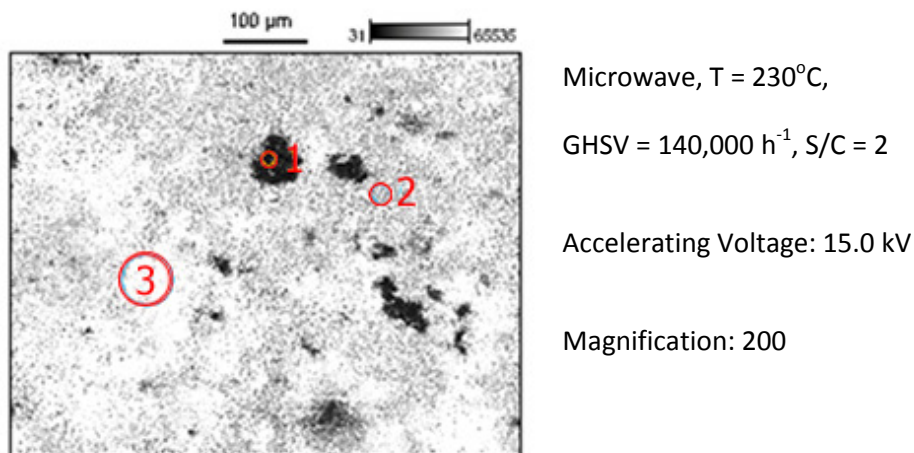

Microwave, T = 230°C,

GHSV = 140,000 h^{-1}, S/C = 2

Accelerating Voltage: 15.0 kV

Magnification: 200

Figure D4. Spent catalyst sample with marked regions for element analysis

The spectra of the three analysis points are depicted in figure D6. From these spectra it can be seen that points nos. 2 and 3 represent regular catalyst surface, while the black spot, no. 1 consists purely out of carbon. Because of the usual strength of the Cu and Zn peaks, and the intensity that is measured on this spot, the SEM operator estimated the thickness of the carbon layer to be approximately 3 μm. The numerical data from table 2 are used to determine the composition of the catalyst surface after reaction. Slightly higher carbon atom% were observed on the spent catalyst, as opposed to the fresh catalyst, although the difference is not large (~6% at the fresh catalyst versus ~9% at the spent catalyst). A larger difference has been observed in the amount of oxygen; whereas it was nearly 50% in the fresh catalyst, it was only 40% in the spent catalyst. This is due to reduction of the catalyst, and through calculation it was found that it was most likely that only CuO was reduced, and that the ZnO remained intact. Furhtermore close-up pictures of the catalyst surface were made (see figure D5), and elemental analysis was performed to determine whether the composition of the surface was different near a carbon particle (point no. 4 in figure D5 (l)), or on the needle-like structure (r) that was encountered on many places of the catalyst surface. The composition near the carbon particle was determined to be very similar to regular catalyst surface, as was the needle-like structure. Both contained roughly the same amounts of Cu, Zn, Al, and O atoms.
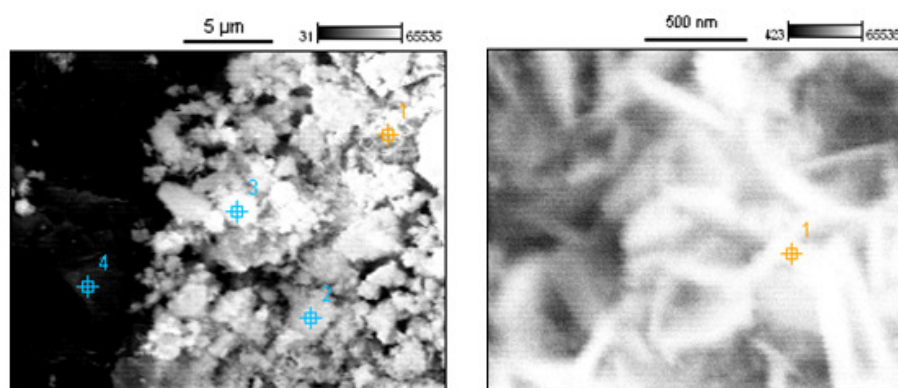

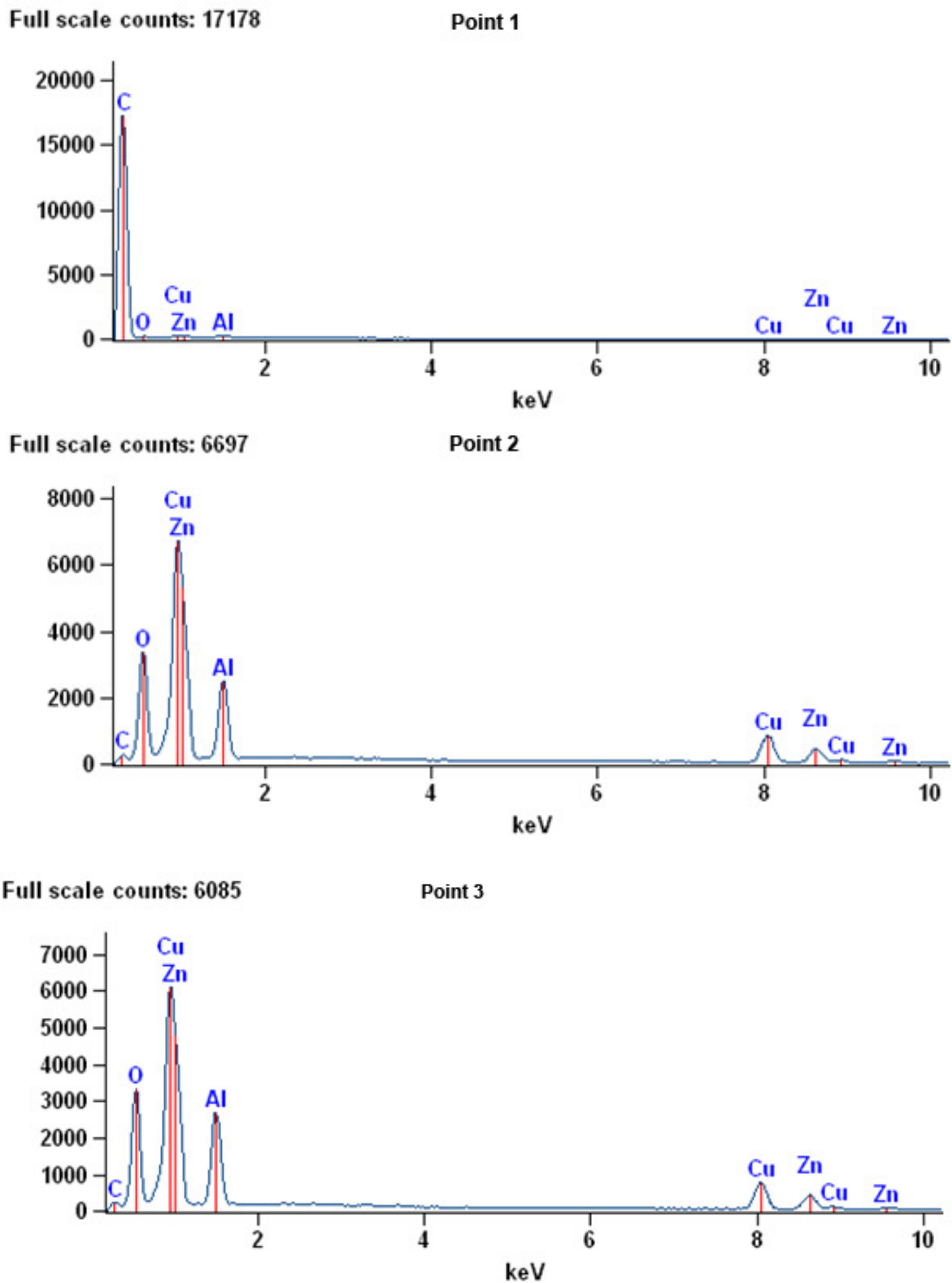**Figure D5. Close up elemental analysis near a carbon particle (l) and of catalyst structure (r)**

Figure D6. Full scale element counts of the spent catalyst surface in points 1 - 3 of figure D4

Table D2. Numerical results of the element analysis of a spent catalyst sample

Net Counts

	C-K	O-K	Al-K	Cu-L	Zn-K
Point 1	147114	0	1606	1459	212
Point 2	1249	32630	26881	69083	8433
Point 3	1045	32548	29107	59255	7902

Weight %

	C-K	O-K	Al-K	Cu-L	Zn-K
Point 1	97.15	0.00	0.44	1.28	1.13
Point 2	3.32	17.33	10.12	38.39	30.84
Point 3	3.02	18.46	11.61	35.77	31.14

Weight % Error (+/- 1 Sigma)

	C-K	O-K	Al-K	Cu-L	Zn-K
Point 1	+/-0.29	+/-0.00	+/-0.03	+/-0.07	+/-0.21
Point 2	+/-0.16	+/-0.14	+/-0.09	+/-1.09	+/-0.98
Point 3	+/-0.16	+/-0.14	+/-0.10	+/-1.14	+/-1.02

Atom %

	C-K	O-K	Al-K	Cu-L	Zn-K
Point 1	99.34	0.00	0.20	0.25	0.21
Point 2	9.84	38.54	13.34	21.49	16.78
Point 3	8.75	40.14	14.97	19.58	16.57

Atom % Error (+/- 1 Sigma)

	C-K	O-K	Al-K	Cu-L	Zn-K
Point 1	+/-0.29	+/-0.00	+/-0.01	+/-0.01	+/-0.04
Point 2	+/-0.46	+/-0.30	+/-0.12	+/-0.61	+/-0.53
Point 3	+/-0.47	+/-0.31	+/-0.12	+/-0.63	+/-0.54